Universidade de Lisboa

Faculdade de Farmácia

Synthesis of Glibenclamide co-crystals through grinding methods

Inês Gonçalves Pêcego

Dissertation supervised by Professor João Almeida Lopes and co-supervised by Doctor Mafalda Cruz Sarraguça.

Master in Pharmaceutical Engineering

2018

Universidade de Lisboa

Faculdade de Farmácia

Synthesis of Glibenclamide co-crystals through grinding methods

Inês Gonçalves Pêcego

Dissertation supervised by Professor João Almeida Lopes and co-supervised by Doctor Mafalda Cruz Sarraguça.

Master in Pharmaceutical Engineering

2018

Abstract

The pharmaceutical industry has been struggling against problems related with drugs with low solubility as this is a very limiting factor in the development of drug products. Co-crystals are solid forms known for a very long time although they have not been fully explored in their potentialities. Co-crystals can be defined as crystalline homogenous structures composed of two or more compounds, held together by noncovalent bonds, usually hydrogen bonds, and solid at room temperature. These structures can change the physicochemical properties of drugs, like solubility, dissolution rate, stability and particle properties, which could be interesting for the drug development process. It is still difficult to identify the optimal co-crystallization method for each situation and typically this process is evaluated on a case-by-case basis. Reported studies show that the most commonly used method is solvent evaporation. However, the main drawback of solvent evaporation is the scale-up difficulty. Therefore, this work explored milling as an alternative method. This method can more easily be scaled-up. This work is based on the co-crystallization of glibenclamide, a sulfonylurea used in the treatment of non-insulin-dependent *diabetes mellitus*. Glibenclamide is categorized as a class II drug (low solubility, high permeability) by the Biopharmaceutical Classification System. The formation of co-crystals was attempted with six different co-formers – adenine (ADE), nicotinamide (NICO), malic acid (MAL), mannitol (MAN), *p*-aminobenzoic acid (PABA) and tromethamine (TRIS). The grinding assisted co-crystallization method was performed on a ball mill. Grinding products were characterized by differential scanning calorimetry and vibrational spectroscopy (near and mid-infrared) and compared with glibenclamide, co-formers and physical mixtures. It was concluded that the most suitable co-formers for the formation of a glibenclamide co-crystals were MAL, PABA (without solvent) and TRIS.

Key-words: pharmaceutical co-crystals; glibenclamide; ball milling; vibrational spectroscopy; differential scanning calorimetry.

Resumo

A indústria farmacêutica tem ao longo do tempo enfrentado problemas relacionados com a fraca biodisponibilidade de muitos fármacos, nomeadamente os integrantes de formas orais. Muitos destes problemas estão relacionados com a baixa solubilidade ou fraca velocidade de dissolução. A abordagem para minimização de problemas relacionados com estes fatores tem sido muito variada, e estão documentadas várias abordagens físicas e químicas. Neste contexto, a produção de co-cristais, ou co-cristalização, é uma técnica de alteração de estado sólido e tem apresentado resultados vantajosos relativamente à melhoria da solubilidade de fármacos. Os co-cristais são formas sólidas homogéneas compostas por duas ou mais moléculas, contidas numa única estrutura cristalina, sendo sólidos à temperatura ambiente. Tais compostos apresentam uma estequiometria bem definida e estão ligados entre si através de ligações não-covalentes, normalmente pontes de hidrogénio. Existem várias metodologias para produção de co-cristais sendo que as mais utilizadas (p.e., evaporação por solvente) têm desvantagens ao nível da transposição de escala e por isso dificuldade de utilização a uma escala de produção. A opção de produção de co-cristais por moagem tem sido documentada ao longo dos últimos anos embora não seja ainda uma técnica muito utilizada e por isso ainda razoavelmente desconhecida em termos do seu potencial, nomeadamente no que respeita à pureza dos co-cristais obtidos assim como o impacto que as condições de fabrico têm nos co-cristais. Esta tese pretende aumentar o conhecimento na área da produção de co-cristais pela técnica de moagem, nomeadamente aferindo a sua capacidade em produzir co-cristais com caraterísticas de pureza adequadas fazendo a ponte com outros métodos como a evaporação de solvente. A glibenclamida foi o fármaco selecionado como caso de estudo. Está categorizado como um fármaco de classe II pelo Sistema de Classificação Biofarmacêutica, isto é, apresenta baixa solubilidade e elevada permeabilidade. Tal fármaco é uma sulfonilureia utilizada para o tratamento da *diabetes mellitus*, sendo esta uma doença do foro metabólico, caracterizada por níveis elevados de açúcar no sangue (hiperglicemia), exibindo duas categorias etiopatogénicas: *diabetes mellitus* tipo 1 ou auto-imune e *diabetes mellitus* tipo 2 ou não-dependente de insulina. A *diabetes mellitus* tipo 2 afeta mais de 9% da população mundial, sendo que as opções terapêuticas de primeira-linha incluem a administração de metformina (biguanida), numa fase inicial, à qual se equaciona a simultaneidade com sulfonilureias (por exemplo, glibenclamida) com o agravamento da condição.

A produção de co-cristais de glibenclamida nesta tese foi executada através do método de co-cristalização por moagem utilizando um moinho de bolas. O fármaco alvo foi testado em combinação com seis potenciais co-formadores distintos: adenina, nicotinamida, ácido málico, manitol, ácido p-aminobenzóico e trometamina. Os testes foram realizados utilizando 1mmol de fármaco e de potencial co-formador utilizando duas bolas de moagem de 12mm durante 3 horas a uma velocidade de 600 rpm. Os os produtos obtidos foram caracterizados quanto a propriedades de estado sólido por calorimetria diferencial de varrimento e por espectroscopia de infravermelho médio e infravermelho-próximo quanto ao seu perfil químico. Tendo em conta que, em princípio, um co-cristal apresenta características físicas e químicas diferentes dos precursores, todos os produtos obtidos após moagem foram caracterizados em comparação com a glibenclamida, respectivo potencial co-formador e mistura física de ambos. Verificou-se que no caso da nicotinamida e manitol não se obtiveram co-cristais. No sistema envolvendo adenina verificaram-se alterações nos espetros de infravermelho, embora esses resultados não fossem confirmados através de uma alteração visível do perfil de calorimetria térmica. A utilização de ácido p-aminobenzóico revelou também resultados promissores indicados por todas as técnicas analíticas usadas. Os sistemas que sobressaíram por apresentarem resultados bastante conclusivos relativamente à formação de co-cristais nestas condições envolveram os co-formadores ácido málico e trometamina. Os resultados obtidos pelo método de moagem encontram-se em linha com os obtidos por evaporação de solvente descritos na literatura. A utilização de condições de moagem diferentes, nomeadamente no que respeita à velocidade e tipologia das esferas de moagem deverá no futuro ser avaliada consistentemente para que sejam identificadas zonas ótimas de operação para produção de co-cristais, tendo em vista o rendimento e a sua pureza.

Acknowledgements

The accomplishment of this master's thesis counted on important supports, to which I will always be grateful.

First, I would like to express my sincere gratitude to my supervisor Professor João Almeida Lopes and co-supervisor Dr. Mafalda Sarraguça, for their guidance, total support, availability and the knowledge transmitted;

To Generis Farmacêutica S.A., for kindly providing the API;

To my parents and brother, for their unconditional support, encouragement, patience and total help in overcoming the obstacles that have arisen;

To my friends Mariana Silva and Joana Gomes, for the support shown, the companionship, strength and, above all, friendship;

To my best friend, Beatriz Forte, a special thank you for all the companionship over the last years, for the great friendship, for never doubting me and making me believe in me in the most difficult times, for teaching me to see life with other eyes but, above all, by the shoulder friend at all times.

Finally, I would like to express my gratitude to all those who, in one way or another, have made it possible to carry out this dissertation.

Contents

List of figures

List of tables

List of abbreviations

IND – Investigational New Drug

API – Active Pharmaceutical Ingredient

FDA – Food and Drug Administration

EMA – European Medicines Agency

GRAS – Generally Regarded As Safe

CSD – Cambridge Structural Database

BSM – Basic Structural Motifs

HSP – Hansen Solubility Parameters

RED – Relative Energy Difference

LAG – Liquid-assisted Grinding

HME – Hot Melt Extrusion

QbD – Quality by Design

ICH – International Conference on Harmonisation

PAT – Process Analytical Technology

PXRD – X-Ray Powder Diffraction

DSC – Differential Scanning Calorimetry

NIR – Near-Infrared

MIR – Mid-Infrared

SU – sulfonylureas

GBL – Glibenclamide

BCS – Biopharmaceutics Classification System

PABA – *p*-aminobenzoic acid

NICO – Nicotinamide

MAL – Malic Acid

ADE – Adenine

MAN – Mannitol

TRIS – Tromethamine

UV – Ultraviolet light

HIV – Human Immunodeficiency Virus

HBV – Hepatitis B Virus

CMV – Cytomegalovirus

NSAID - Non-steroidal Anti-inflammatory Drugs

PTFE – Polytetrafluoroethylene

ATR – Attenuated Total Reflectance

PM – Physical mixture

Chapter 1 – Introduction

1.1 – Drug development

The goal of pharmaceutical development is to design the best drug product possible and corresponding manufacturing process. The information obtained from pharmaceutical development studies provides scientific knowledge to support the establishment of the design space, specifications and manufacturing controls. (1,2) The development of a new medicinal product from a new compound is a complex procedure which involves different disciplines and can be broken down into five distinct stages: discovery and development, preclinical research, clinical research, drug review and post-market drug safety monitoring. Table 1 summarizes the main activities that occur at each stage. (3–6)

Table 1. Stages of drug development and respective activities.

Stages of drug development	Activities
Discovery and development	Several compounds may be potential candidates for development as a medical treatment. After identifying a promising compound for development, studies are conducted to gather information on: • how it is absorbed, distributed, metabolized and excreted; • best dosage and mechanism of action; • side effects and how it interacts with other drugs; • its effectiveness as compared with similar drugs.
Preclinical research	Studies are conducted to find out whether the drug has toxicity. These studies must provide detailed information on dosing and toxicity levels. At the end of this stage, it must be decided if the drug should be tested in people.
Clinical research	Drug developers must submit an investigational new drug (IND) application and then wait for the approval to begin the clinical trials. Clinical trials involve several phases: **Phase I** – lasts several months and aims to know if the drug is safe and its dosage. This phase encompasses studies related to: • pharmacokinetic, which studies the time course of drug absorption, distribution, metabolism, and excretion;

	• pharmacodynamic, which studies the relationship between drug concentration at the site of action and the resulting effect, including the time course and intensity of therapeutic and adverse effects; • pharmacovigilance, which studies the activities relating to the detection, assessment, understanding and prevention of adverse effects or any other drug-related problem; • tolerability, which represents the degree to which adverse effects can be tolerated by the patient.
	Phase II - lasts from several months to 2 years and aims to identify side effects and efficacy;
	Phase III – lasts from 1 to 4 years and aims to monitoring adverse reactions and its efficacy;
	Phase IV – the purpose of this phase is to study the safety and the efficacy of the tested drug.
Drug review	If after preclinical and clinical research, the drug in question presents evidence of being safe and effective, it can be filed an application to market the drug.
Post-market drug safety monitoring	At the time of the market approval, there is not a complete information about the safety of the drug. Therefore, the true picture of a product`s safety evolves over the years that make up a product`s lifetime in the marketplace. So, it is essential to monitoring the drug safety after the market approval.

1.2 – Solid Forms

One paramount procedure during the early stages of drug development is the screening and selection of existing solid state of the drug (or active pharmaceutical ingredient (API)) due to the fact that it may influence the API's physicochemical, mechanical properties and chemical stability. As solids, APIs can exist in crystalline or amorphous structures. However, the pharmaceutical industry is keener on the crystalline forms due to their characteristics which include superior stability, ease of purification, being their low solubility the major drawback. Amorphous forms have a higher mobility and energy state, which give them a higher solubility, but they have low stability and tend to recrystallize over time. The latter, make amorphous materials less appealing for the pharmaceutical industry. (7–9)

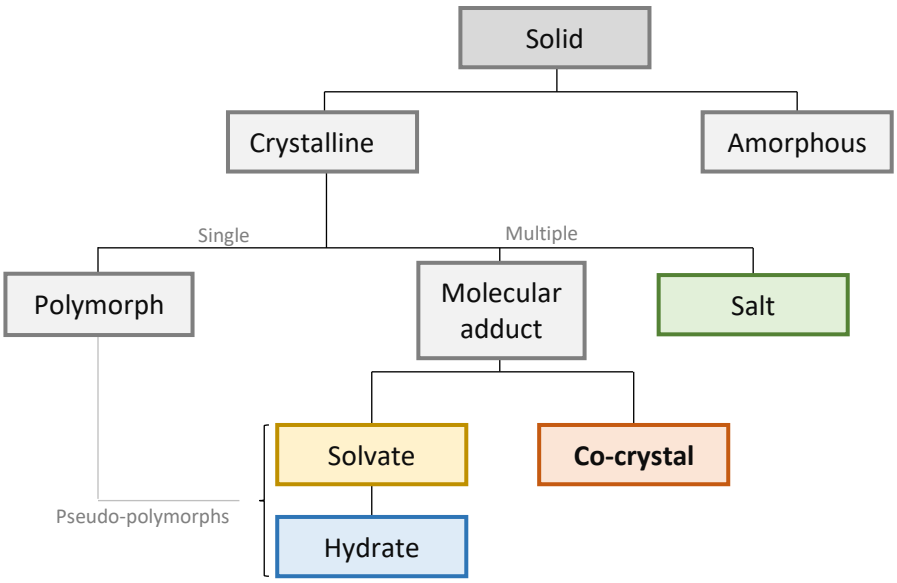

Figure 1. Schematic representation of solid forms.

As crystalline forms are more attractive to the pharmaceutical industry, a more detailed analysis will be given.

1.2.1 – Crystalline solids

Crystalline solids can exist in the form of polymorphs, solvates/hydrates, salts and co-crystals. (10)

Polymorphs exist when the drug substance crystallizes in different crystal packing arrangements, all of which having the same elemental composition. Physicochemical properties, such as solubility, melting point and crystal shape, vary with the polymorphic form, so it is extremely important to screen polymorphs for pharmaceutical applications. (10–13) Thus, the fact that polymorphs exhibit different characteristics is an advantage for their use. However, the major drawback is that the properties can change in such a way that the compound ceases to be pharmacologically active. (14)

Solvates often called pseudo-polymorphs due to the presence of the solvent molecules in the crystal lattice, are multiple component crystals, where the crystallization solvent is entrapped in the host lattice. These compounds have as a particularity the fact that one of the components is liquid at room temperature. When the liquid component is water, the solvate is called a hydrate. (2,3,5,6) The presence of solvent molecules influences the intermolecular interactions, thereby conferring different physical and chemical properties, such as thermodynamic properties and solubility, from those of the unsolvated form. Due to the solvent molecule, which can be lost during processing, solvates are typically viewed as a problem by the pharmaceutical industry. (14,15)

Most drug molecules on the market are salts and, usually, salts readily undergo crystallization leading to a resulting material which facilitates the subsequent processing. Thus, salt formation has become a widely used technique to increase both the dissolution rate and solubility of pharmaceutical drugs. A salt is a multicomponent system formed by an acid-base reaction between the API and an acidic or basic substance by proton transfer from acid (A) to base (B). (8,16–18) Although salts are widely used, the formation of salts is inadequate for non-ionizable drugs, which is an obvious disadvantage. (15,17)

Considering that all mentioned crystalline forms present disadvantages for the pharmaceutical industry, other alternatives might be considered. One of such alternatives may assume the form of co-crystals.

1.2.1.1 – Co-crystals

About 40 to 70% of drugs screened in industrial research have poor solubility and such problem led the pharmaceutical scientists to try to find a solution towards a drug with better solubility, dissolution rate and, hence, bioavailability. Co-crystallization allows to improve the API's physicochemical properties without changing its structure, thus, API activity remains intact. (12,19–22) The definition of co-crystals is still debated in the scientific literature, as the Food and Drug Administration (FDA) states that "co-crystals are a dissociable multicomponent solid crystalline supramolecular complex which contains two or more components within the same crystal lattice wherein the components are in neutral state and interact via non-ionic interactions" and European Medicines Agency (EMA) states that "co-crystals are in general defined as homogenous crystalline structures made up of two or more components in a definite stoichiometric ratio where the arrangement in the crystal lattice is not based on ion pairing". Despite this, the scientific community agrees that co-crystals enhance the bioavailability (are more soluble and stable) and do not affect its pharmacological action. In addition to these benefits, it can be introduced through the co-former, additional nutritional and health benefits. Co-crystals are held together by noncovalent interactions, usually hydrogen bonds due to their strength and directionality. Regarding the co-crystal formation, if $\Delta pKa>3$ then salt formation is expected, yet if $\Delta pKa<1$ there will be less than substantial proton transfer resulting in co-crystal formation. In instances where the difference in pKa values is between 1 and 3, the extent of proton transfer is usually not predictable and spectroscopic tools may be needed to probe the extent of ionization and therefore the location in the co-crystal/salt continuum.(12,16,23–25)

Regarding co-crystals development, studies have reported an enhancement in the dissolution rate. For example, GBL and oxalic acid (1:2) system determined an enhancement from 12% to 50% when compared to the pure API and GBL and

tromethamine (1:1) system determining an increase from 11% to 29% when compared with the pure drug. (26) Other examples that demonstrate the success of the co-crystal approach in enhancing properties of drugs are regarding the antifungal agent itraconazole, in which co-crystals of itraconazole-malic acid (Sporanox®) show a higher solubility and a faster dissolution rate, carbamazepine: saccharin co-crystals have shown an increasing of the carbamazepine bioavailability, the piracetam: tartaric acid co-crystals showed improved hygroscopic properties. Also, the dissolution rate of exemestane-megestrol and exemestane-maleic acid co-crystals were improved when using the co-crystallisation method. (16,22,23,27,28) Furthermore, in the last years several drugs were studied in order to obtain a co-crystal and the number of studied drugs for this purpose have been increasing, being estimated that the number of studied co-crystals will increase over the next years. (29) The last decade witnessed expedition of co-crystals from bench to successful drug products. Successfully marketed co-crystals products include Suglat® (ipragliflozin-proline), Entresto® (valsartan-sacubitril), Sporanox® (itraconazole-malic acid) and Steglujan® (ertugliflozin-sitagliptin), to prevent hyperglycaemia in type 2 *diabetes mellitus*. In addition, few combinations are in various stages of clinical trials, such as tramadol hydrochloride−celecoxib and TAK 020-gentisic acid. (27,30–32)

Co-former selection

Design of pharmaceutical co-crystals can be defined as the combination of theoretically and experimentally strategies employed to obtain the best co-crystal product. It is an approach that should be initiated by a drug complete characterization, followed by the selection of co-formers and the co-crystallization method. Considering that one of the aims of co-crystallization is to improve the solubility of the drug, it is necessary to realize the importance of co-former selection, since its solubility will be correlated with the solubility of the co-crystal. (33,34)

One of the main challenges in pharmaceutical co-crystal development is the selection of co-formers that are compatible with the designated drug and do not affect its pharmacological activity. Also, co-formers must be non-toxic and present no adverse side effects, reason why, co-formers should be approved as generally regarded as safe (GRAS). A crystal of an organic compound is the ultimate supermolecule and its assembly is achieved through hydrogen bonds between the individual molecules. In the structure of a crystal, during the regular repetition of crystal patterns, the pattern of interactions can be called a supramolecular synthon. They can be classified as: (24,35)

- Supramolecular homosynthons: made up of identical self-complementary functional groups;

- Supramolecular heterosynthons: made up of different but complementary functional groups.

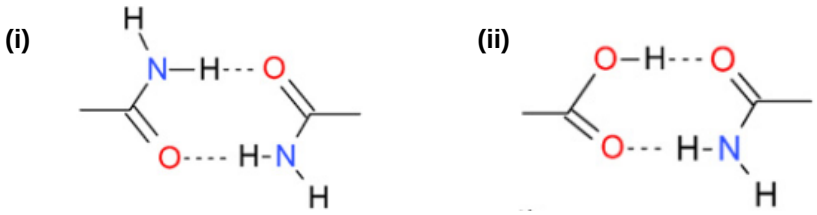

Figure 2. Examples of supramolecular synthons: (i) Homosynthon formed between amide dímer; (ii) Heterosynthon formed between carboxylic acid group and amide group.

"Trial and error" is still a widely used technique to choose co-formers, but in recent years, different approaches have been used using for example the Cambridge structural database (CSD), a repository for small molecule crystal structures. This platform allows the search for ordered, error-free organic crystal structures and incomplete or unreliable structures are filtered out. The remaining structures are exported to another software for further molecular statistical analysis. Thus, distribution models are constructed on parametric and nonparametric correlation coefficients between pairs of descriptors, such as simple atoms and bonds, resulting in the most probable final co-crystal structure. (20–22,34) This approach can be very efficient when it comes to relatively strong interactions, however, when it comes to comparing the strengths between different types of specific intermolecular interactions, like Van der Walls forces, it may be almost impossible due to the dependence of the energy of interactions on interatomic distances in different types of intermolecular interactions. (36) Moreover, for big molecules, the contribution of dispersion and electrostatic interactions to the total energy of interaction may be comparable to the energy of specific interactions. The only solution towards solving this issue is the application of comparative quantum-chemical calculations, determining the basic structural motifs (BSM) of a crystal. By applying this approach, it is possible to describe the structure of molecular crystals by a directional rhombus from molecule or molecular complex as a crystal-building unit for the three-dimensional structure of the crystal. This way, supramolecular synthons can be divided into four groups: (36,37)

- Local or basic – leading to the formation of molecular complexes;
- Primary – responsible for the formation of a BSM of the crystal;
- Secondary – providing the packing of BSMs;
- Auxiliary – depending on energies of the interactions between molecules.

Another approach includes the evaluation of the Hansen solubility parameters (HSP), which is used to predict the miscibility of a drug with the co-former. Such prediction is based on the premise that materials with similar solubility parameters are

miscible. Having this in mind, the total cohesive energy is divided into three individual components: dispersion, polar and H-bonding. HSP are used to compare the distance between two molecules (Ra): as smaller the distance is, the more likely the two molecules are to be compatible. Relative energy difference (RED) is given by combining the Ra with the interaction radius with the solvent. With this in mind: (36,37)

- If RED<1, the molecules are alike and will dissolve;
- If RED=1, the system will partially dissolve;
- If RED>1, the system will not dissolve.

The above-mentioned methods to assist co-crystals design and co-former selection can be used individually or combined.

In view of the studies already carried out on co-crystals, it is possible to address which co-formers are most used. Carboxylic acids have been studied as a co-former most extensively, which is due to the carboxylic acid moieties are one of the most commonly studied functional groups in crystal engineering. Examples of already studied combinations with carboxylic acid co-formers and APIs are caffeine-oxalic acid, fluoxetine hydrochloride-benzoic acid, itraconazole-malic acid and norfloxacin-maleic acid. Besides carboxylic acids, amides and alcohols are also mostly used as a co-former: ibuprofen-nicotinamide, baicalein-nicotinamide and dexlansoprazole-sorbitol, for example. (28,38–44)

1.3 – Co-crystallization techniques

A co-crystallization technique can be defined as any technique that allows combining two or more molecules, API and co-former in this case, through non-covalent interactions in a crystallization process. The selection of the suitable co-crystallization technique is of utmost importance to ensure appropriate co-crystal/particle properties, such as purity and particle size. To the pharmaceutical industry, it is also important that the co-crystallization technique can be easily scaled-up. (45,46) One possible classification towards co-crystallization techniques is related to the usability of solvent, being classified as solvent-based or solvent-free methods. Solvent-based methods are the most studied on a laboratory scale. (14) Therefore, they are the most common and well understood from a scientifically and technological perspective. Solvent-based methods are mainly used due to their simplicity and the possibility of process monitoring, but the fact that these methods are usually not scalable and the use of large amounts of hazardous solvents are huge disadvantages. On the other hand, solvent-free methods are less studied, but the co-crystals are produced in the absence of solvents, or by using

negligible amounts, and the excellent quality and purity, the fast processing times and the high throughputs make these methods a great deal with substantial industrial interest. (46,47)

1.3.1 – Mechanochemical methods

A mechanochemical reaction is a chemical reaction induced by the direct absorption of mechanical energy and the mechanochemical reactive sites are typically generated by methods such as grinding, stretching and shearing. Such methods have become increasingly attractive regarding the production of co-crystals, in particular by milling, since they can be applied to a wide range of compounds and are solvent-free. (14)

1.3.1.1 – Neat grinding method

Neat grinding, solid-state grinding or dry grinding, is based on mixing stoichiometric co-crystal components together in the solid state and grinding them manually by using a mortar and pestle, or mechanically by using a ball mill or vibratory mill. Since manual dry grinding has some problems with reproducibility, mechanical methods should be used to obtain a more efficient co-crystallization. (47) When using a ball mill for neat grinding, the components are loaded into a rotating chamber partially filled with small balls which can be of stainless steel, tungsten carbide or zirconium oxide, for example, and are subsequently mixed. (14) Depending on the driving-force, co-crystallization methods can be classified as thermodynamic or kinetic methods. In this case, neat grinding is considered a kinetic method, which involves non-equilibrium conditions, depending on the system energy and, correspondingly, to reaction duration. (14) Neat grinding has been a rising technique in the co-crystallization field and several studies have been successfully reported. For example piracetam-citric acid and piracetam-tartaric acid co-crystals (48), carbamazepine-nicotinamide co-crystal (49), carbamazepine–saccharin co-crystal (50), indomethacin-saccharin co-crystal (51) and ethenzamide-saccharin co-crystal (52).

Although mechanochemical methods are still less common, they offer advantages such as being environmentally friendly due to the absence of solvents and can be performed at room temperature. Despite the many advantages, a huge drawback with this solvent-free method, with no heating stage involved, is related with the energy required for the co-crystallization of compounds, often not enough. (47) Therefore, in some cases, the use of a small quantity of solvent can accelerate the process because the solvent acts as a catalyst increasing the kinetics of the process known as liquid-

assisted grinding (LAG). The systems piracetam-citric acid and piracetam-tartaric acid were used to compare LAG and neat grinding to produce co-crystals and it was concluded that both systems produced co-crystals through both methods, however, the LAG method produced co-crystals faster. (48) This fact can be explained by the increase in the possibility of molecular collisions and the increase in degrees of orientation and conformational freedom, leading to a kinetic improvement. It is not clear why LAG is more efficient compared with neat grinding, but this method provides other benefits over dry grinding, such as product crystallinity, ability to control polymorph formation and higher yield. (48,53)

1.4 – Pharmaceutical co-crystals manufacturing

Several co-crystallization techniques were described in the literature, however, not all of them can be considered for industrial purposes due to scale-up limitations. Scaling-up a method from laboratory scale to industrial production is a process that cannot compromise the product quality nor its characteristics. Regarding the techniques used in the pharmaceutical industry, spray drying is widely used for particle engineering and it is a technique easy to scale up to produce co-crystals. Despite being a technique relatively easy to scale up, further studies on how this technique can be used to produce co-crystals are still needed. A relatively new technique, spray congealing, is another technique that can be used for co-crystals production in industrial scale. However, because it is a fairly recent technique, more studies are needed to better understand this technique. Hot melt extrusion (HME) is a broadly studied technique in the co-crystals field and it is a promising technique for the industrial production of co-crystals. HME is a relatively simple technique and the reported studies have shown that it produces co-crystals with good quality. (14,54–56)

1.4.1 – Product development and process monitoring

Quality of the final product is extremely important for the pharmaceutical industry and, nowadays, the concept of quality control is overcome by embedding the product quality from the beginning of its development, through design strategies. Product development can be approached in various ways and the applicant can either choose an empirical approach or a systematic approach, or even a combination of both. Quality-by-design (QbD) appears as a systematic approach and it is defined as “a systematic approach to development that begins with predefined objectives and emphasizes product and process understanding and process control, based on sound science and quality risk management” by the International Conference on Harmonisation (ICH).

Moreover, QbD is found in optimization and understanding of how the design of a product and its manufacturing process can affect the final product quality. (2,14,57–59) Due to the necessity of building the quality into the product, a deep control and understanding of the manufacturing process are needed. Thus, process analytical technology (PAT) can provide the tools to deepen the knowledge of the manufacturing process. The ICH defines PAT as “a system for designing, analysing, and controlling manufacturing through timely measurements of critical quality and performance attributes of raw and in-process materials and processes with the goal of ensuring final product quality”, being PAT recommend by FDA and EMA. PAT is boosted to assist QbD implementation by reducing risks to regulatory and quality concerning while improving efficiency. (2,57–59)

QbD concepts and PAT tools have already been used to design and monitor co-crystallization techniques. However, due to their simplicity and the possibility of easily integrate PAT tools, most of the monitored techniques were solvent-based techniques. PAT tools increase process understanding while monitoring co-crystallization processes and can aid the scale-up process. So, to achieve co-crystals with desired quality, real-time monitoring can be an added value allowing process optimization at all stages to be accomplished. (2,14,60)

1.4.2 – Co-crystals continuous manufacturing

Currently, most industrial co-crystallization manufacturing processes adopted the batch processing mode. However, batch production encompasses disadvantages, such as multiple sequential steps and interruptions, which is not favourable for scale-up, consumption of raw materials and requirement of extensive validation. So, continuous manufacturing emerged as an alternative to batch mode, also in the co-crystallization field. Continuous manufacturing has many advantages when compared to the batch mode because it is simple to scale-up and allows a more automated way of manufacturing. (14,61,62) Carbamazepine - trans-cinnamic acid co-crystals, (61) and carbamazepine-nicotinamide co-crystals were produced in lab-scale in continuous mode by spray-drying (62). Vertex Pharmaceuticals has already adopted continuous manufacturing to produce Orkambi® (lumacaftor-ivacaftor), a drug product to target cystic fibrosis. (23,61) In the pharmaceutical industry, continuous manufacturing is still recent and its use for co-crystallization processes is very scarce. Despite that, the interest in shifting from batch manufacturing to continuous is markedly increasing. (14,64,65)

1.5 – Characterization methods

It is essential in co-crystallization studies to confirm phase transformation and to characterize co-crystal product(s). Thus, it is of paramount importance to apply the appropriate characterization methods to select the most promising co-crystal candidates. Regarding the characterization techniques, powder x-ray diffraction (PXRD), differential scanning calorimetry (DSC) and vibrational spectroscopy are the most used. (22,66,67) PXRD is a technique that detects changes in the crystal lattice, providing fundamental structural information about a co-crystal formation. This technique is mainly used since different crystalline phases show distinctly different PXRD patterns. Regarding the DSC technique, it is based on the heating of binary physical mixtures of the complex drug- co-former and the fact that it is not a time-consuming technique makes DSC a widely used approach for co-crystal detection. Both near- and mid-infrared spectroscopy methods are broadly used for co-crystallization detection regarding vibrational spectroscopy. Near-infrared spectroscopy (NIR) can give physical and chemical information, however mid-infrared spectroscopy (MIR) is a technique that gives more information because it provides information on the molecular structure. (68–70)

1.5.1 – Differential scanning calorimetry

Differential scanning calorimetry (DSC) is a thermoanalytical technique that has been reported as a simple and rapid approach towards co-crystal screening. DSC is based on the heating of the two potential co-crystal components, beyond the eutectic point.(14,68) The use of this technique assumes that the melting point of the co-crystal differs from that of forming components, which is confirmed with the fact that in more than 50% of the cases, co-crystals showed a lower melting point compared with both components. When analysing a DSC scan, co-crystallization is considered possible if an endothermic peak associated with the eutectic melting is followed by an exothermic peak, corresponding to the co-crystal formation (Fig. 3a). Co-crystallization is considered not possible when an endothermic peak representing the eutectic melting is present together with further peaks revealing melt or degradation points of the individual compounds (Fig. 3b). (68,71)

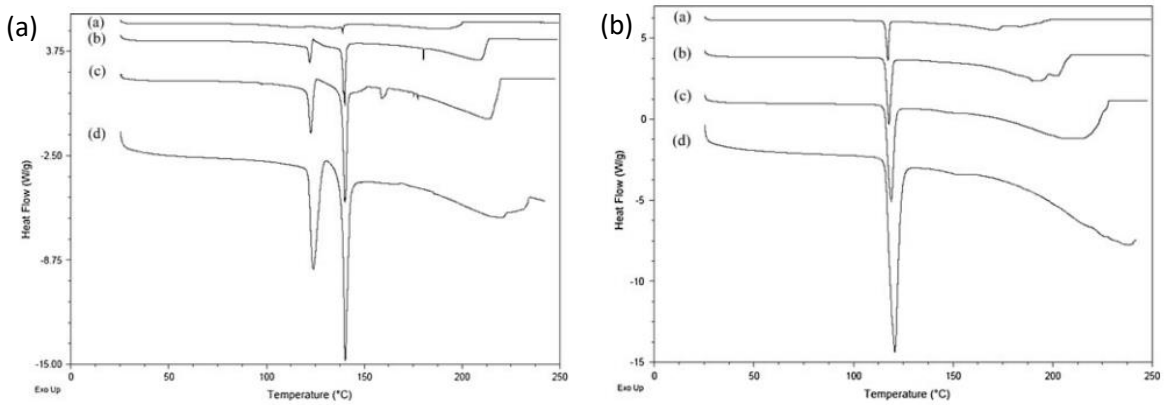

Figure 3. Examples of DSCs: (a) DSC in which co-crystallization is possible and (b) DSC in which co-crystallization is not possible.

It was reported how DSC can be important regarding co-former selection because from selecting a co-former with a melting point greater or lesser than the API, it is possible to raise or lower the melting point of the co-crystal. A reported article, in which a drug was studied with several co-formers, has shown that the melting point of the final drug depends on the chosen co-former. (72)

1.5.2 – Powder x-ray diffraction

Powder x-ray diffraction (PXRD) is a paramount technique for the study of crystalline solid-state materials since this technique detects changes in the crystal lattice. This technique allows to verify whether there are new links between API and co-former through the existence of new peaks in the PXRD pattern. In the case of new links, it is required to determine together with other techniques if the formation of a co-crystal actually occurred. (69,70) Although this technique is widely used to verify the formation of co-crystal, a disadvantage is the long measurement times. (69,70)

1.5.3 – Vibrational spectroscopy

Vibrational spectroscopic methods, such as near-infrared (NIR) and mid-infrared (MIR) spectroscopy are two important techniques for co-crystals characterization. The NIR spectral region is defined from 780 to 2500nm, which comprises combination and overtone bands, the strongest being of OH, CH, NH and SH groups, and it is usually measured in the reflectance mode on powder samples. Due to the fact that this technique has a low energy, no pre-treatment is needed for the sample because the signal will never be saturated. NIR is a powerful technique giving information of physical (e.g. particle size through scattering) and chemical properties and regarding co-crystal characterization, the spectrum of the sample is usually compared to the physical mixture spectrum. In the case of new vibrational bands, it may indicate the formation of new links

between the API and co-former, i.e., a co-crystal might have been formed. The implantation of NIRs as a PAT tool for the on-line monitoring of co-crystallization was already studied and reported (22) and the fact that NIR can be successfully used as a PAT tool is very appealing to the pharmaceutical industry. (70) In Figure 4, the correlation chart used for the NIR spectra results interpretation is displayed.(29)

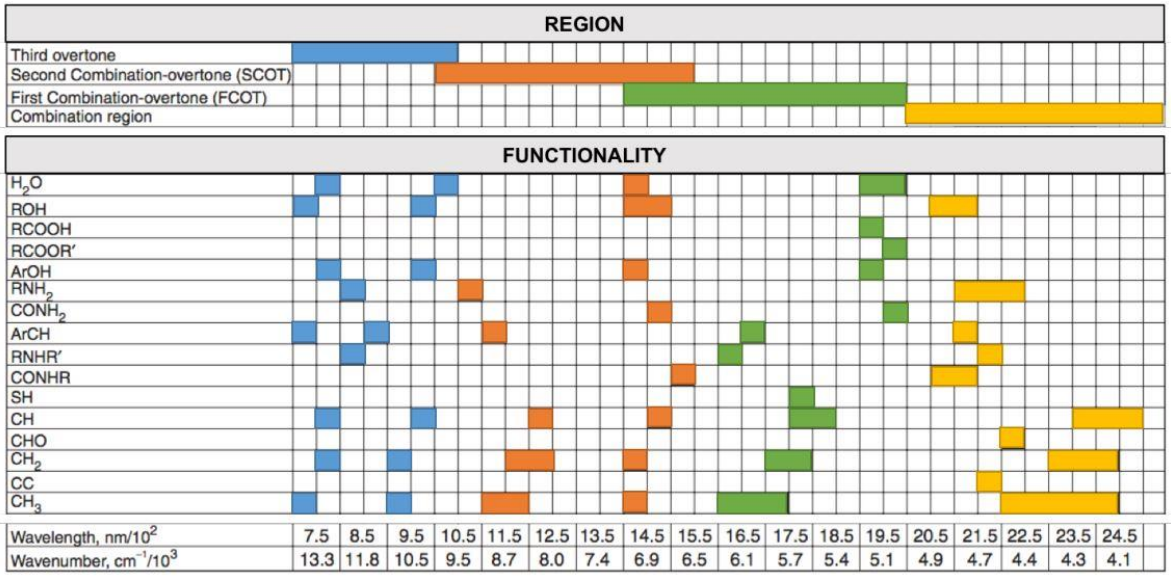

Figure 4. Major absorption bands found on NIR spectra.

MIR spectral region is defined from 2500 to 25000nm and the vibrational transitions occur at distinct wavelengths, which depends on the molecular structure of the compound. This technique has been widely applied in a pharmaceutical setting and in the last decade, it has been used to characterize co-crystals because if there is a new vibration if there is a new existing vibration it may indicate that the co-crystal was formed. One major advantage of this technique in the pharmaceutical field is that samples can be measured in different states, i.e., liquid, solid or gas. (14,74) In Figure 5 the correlation chart used for the MIR spectra results interpretation is displayed. (29)

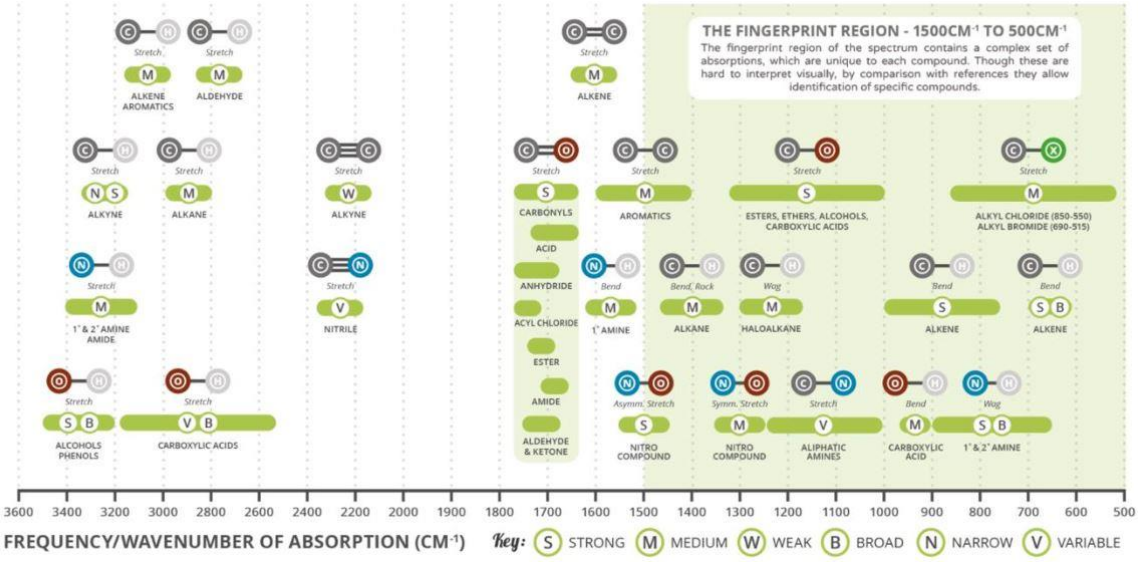

Figure 5. Major absorption bands found on MIR spectra.

Although both techniques highlight different co-crystal characteristics, for a detailed characterization it is necessary to use several techniques at the same time and, thus obtaining more information about the newly formed product.

1.6 – *Diabetes mellitus*

Diabetes mellitus is defined as a group of metabolic diseases characterized by increased blood glucose levels (hyperglycaemia), mainly caused by a deficient insulin action on target tissues. *Diabetes mellitus* typical symptoms involve polyuria, polydipsia, weight loss, polyphagia and blurred vision. (29,75–77) *Diabetes mellitus* can be categorized in two different etiopathogenetic categories: (29,75,76)

- *Diabetes mellitus* type 1: an autoimmune disease, which represents approximately 10% of the total diagnosed diabetic population;
- *Diabetes mellitus* type 2: non-insulin-dependent, which represents 90% of the total diagnosed diabetic population.

Diabetes mellitus type 2 is caused either by a mechanism of insulin, which is triggered by an insensitivity of glucose-utilizing tissues to insulin due to a progressive loss of β-cell function (which primary function is to store and release insulin) in the pancreas or by a relative impairment in the insulin secretion process. Its incidence has been increasing worldwide due to environmental factors, unhealthy eating habits, sedentary lifestyle and stress. As a result, *Diabetes mellitus* type 2 is considered one of the biggest epidemic diseases of the twenty-first century. (29,75,78–80) The treatment for *Diabetes mellitus* type 2 is divided in two ways: a lifestyle management and drug therapy. For drug therapy treatment, there are several main drugs prescribed: (79,81–83)

- Sulfonylureas (glipizide, glibenclamide, gliclazide, glimepiride) improve glucose homeostasis by stimulating insulin secretion on b-cells;
- Biguanides (metformin) decrease hepatic glucose production;
- Alpha-glucosidase inhibitors (acarbose, voglibose, miglitol) decrease carbohydrate absorption.

Besides these therapies, there are also incretin-based therapies composed of glucagon-like peptide-1 analogues or receptor agonists, dipeptidyl-peptidase-4 inhibitors, thiazolidinediones, and newest classes such as sodium-glucose cotransporter-2 inhibitors. (82,83)

1.6.1 – Sulfonylureas

Sulfonylureas (SU) hypoglycemic activity was discovered during the Second World War when an SU derivate p-amino benzene sulfonamide-isopropyl thiodiazole was tested as a typhoid fever treatment. The patients who received that treatment suffered from convulsion and coma, which are only reversed by glucose administration. (84–86) SU are classified into two different generation, according to their appearance:

- First generation such as acetohexamide, tolbutamide, chlorpropamide and tolazamide;
- Second generation such as glibenclamide, gliclazide, glimepiride and glipizide.

Regarding both generations, they are mostly differentiated by the potency of their correspondent agents, being the second generation of SU more potent than the first. Noninsulin-dependent *diabetes mellitus* treatment using SU is restricted to the second-generation agents because the first-generation agents marked toxicity combined with long half-lives and high protein bounding, but low albumin affinity, increase the risk of drug interactions. (87,88) In comparison with other antidiabetic drugs, SU display fast onset of action and generics availability reduces its cost. On the other hand, SU disadvantages include weight gain and increased risk of hypoglycaemic, mainly glibenclamide (GBL).

Mechanism of action

SU are insulin secretagogues, acting by stimulating insulin release from β-cells of the pancreas to the plasma, leading that the effectiveness of this drug depends on the presence of residual pancreatic-β-cells. SU mechanism of action involves the binding, and respective blockage, of the sulfonylurea type 1 receptor subunit (SUR1) of the ATP-sensitive potassium channels (K(ATP)) on the pancreatic-β-cells plasma membrane. The formed complex, SU-SUR1(K(ATP)) prevents the inward current flow of potassium ions

(K^+) within the β-cell and induces calcium ions (Ca^{2+}) influx through voltage-sensitive calcium channels, which trigger the exocytosis of insulin. (84,89)

After the aforementioned mechanism, SU increase insulin secretion, which takes place as insulin granules are translocated to the β-cells membrane. Later, in the second phase, the mechanism only happens if β-cell function is preserved, involving the progressive formation of new insulin granules. The risk of severe hypoglycaemia is a serious disadvantage, which occurs due to the independence of the mechanism to blood glucose levels. (84,89)

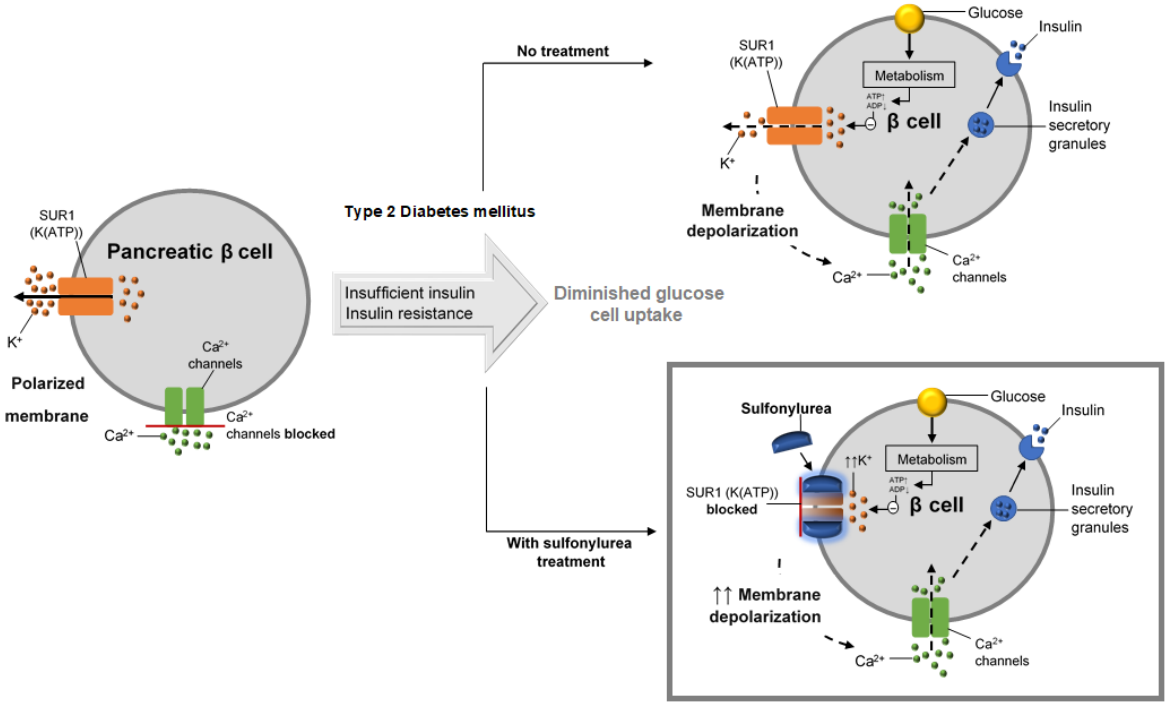

Figure 6. Scheme of sulfonylurea mechanism of action.

1.6.1.1 – Glibenclamide

Glibenclamide (GBL) or glyburide is a sulphonamide urea derivate with antihyperglycemic activity, which belongs to the sulfonylureas antidiabetic pharmaceutical class of compounds. As a solid, GBL appears as a white or an almost white crystalline powder, which is insoluble in water (4mg/L at 27ºC), leading to poor dissolution rate and subsequent decrease of its gastrointestinal absorption, slightly soluble in alcohol and freely soluble in dichloromethane. GBL chemical structure and formula are represented in Figure 7. (26,89–91)

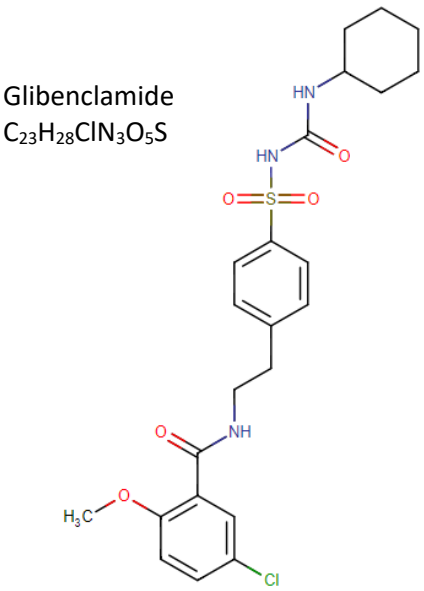

Figure 7. GBL chemical structure and molecular formula.

In Table 2, physicochemical properties of GBL are displayed. From these parameters, GBL is considered insoluble in water and from the pKa value it is possible to state that the absorption occurs in stomach and initial duodenum portion. (89,89,91)

Table 2. Physicochemical properties of GBL.

API	Water solubility (mg/L)	BCS class	pKa	logP	Melting point (°C)
Glibenclamide	4.0	II	4.32 (strongest acidic) -1.2 (strongest basic)	4.70	169

About GBL pharmacodynamics, it lowers blood glucose acutely by stimulating the release of insulin from the pancreas. On type 2 patients with chronic administration, the blood glucose lowering effect persists despite a gradual decline in the insulin secretory response to the drug. In addition to its blood glucose lowering actions, GBL produces a mild diuresis by enhancement of renal free water clearance. Pharmacokinetics parameters are displayed in Table 3. (89)

Pharmacokinetic parameter	
Bioavailability	1
Absorption	Significant absorption within 1 hour; Peak plasma levels are reached in 2 to 4 hours.
Half-life	1.4-1.8 hours (unchanged drug); 10 hours (metabolites included)
Volume of distribution	Steady state V_d=0.125 L/kg V_d during elimination phase=0.155 L/kg
Clearance	78 ml/hr/kg in healthy adults. It may be substantially decreased in those with severe renal impairment.

Table 3. Pharmacokinetic parameters of GBL.

GBL is a Biopharmaceutics Classification System (BCS) class II compound, i.e., low solubility and high permeability, making it a case of interest for studies related to the solubility and dissolution enhancement. So, for dissolution enhancement, particle size and morphology modifications are the most selected methods, including solid dispersion formulations, micronization and nanomization. Solid dispersion formulations between GBL and hypromellose, microcrystalline cellulose, polyethylene glycol and other polymers have been published extensively in the last decade regarding the improvement of dissolution rate. Furthermore, regarding particle size control, nanomization of GBL determined, approximately, 10 times higher drug release percentage. However, solid dispersion formulations and particle size reduction are limited to a set of APIs because they can result in decreased dissolution rate on ageing, caused by moisture absorption or phase separation, and in drug degradation. (92–97)

1.7 – Co-formers

In this work six different co-formers were tested for co-crystallization of GBL: *p*-aminobenzoic (PABA), nicotinamide (NICO), malic acid (MAL), adenine (ADE), *D*-mannitol (MAN) and tromethamine (TRIS). Such co-formers for GBL co-crystals were selected according to ongoing research works developed at the LAQV/REQUIMTE, Departamento de Ciências Químicas, Faculdade de Farmácia, Universidade do Porto, Portugal in collaboration with a second research group from Brazil (Centro de Ciências Sociais, Saúde e Tecnologia, Universidade Federal do Maranhão, Imperatriz, MA, Brazil). (29,98,99)

PABA or *p*-aminobenzoic acid (Figure 8) is an aminobenzoic acid isomer, which combined with pteridine and glutamic acid, forms folic acid and is a vitamin B complex

member. When PABA is exposed to light, absorbs ultraviolet (UV) light and emits excess energy via a photochemical reaction, causing damage to DNA and consequently skin cancer. Such DNA defects lead to the withdrawal from the market of sunscreen formulations containing PABA. (100,101)

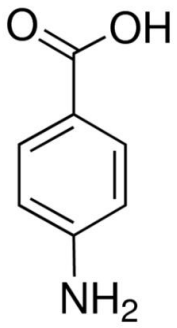

Figure 8. PABA molecular structure.

PABA may also increase oxygen uptake, enhancing monoamine oxidase activity to promote degradation of serotonin, revealing antifibrotic properties. As a solid, this substance appears as a white powder, slightly soluble in water and freely soluble in alcohol. (90,100,101)Regarding co-crystals studies, PABA has been successfully tested in systems with furosemide, hydrochlorothiazide, carbamazepine, acemetacin, niclosamide, ketoconazole and nitrofurantoin. (60,102–107)

Nicotinamide or NICO (Figure 9) is the active form of vitamin B3 (3-pyridine carboxamide) and a component of the coenzyme nicotinamide adenine dinucleotide (NAD), which as many pharmacological actions and therapeutic uses. (108–110)

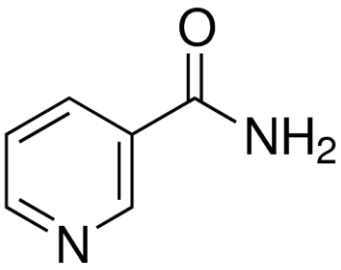

Figure 9. NICO molecular structure.

After oral administration, NICO is readily absorbed from the gastrointestinal tract and is widely distributed to the body tissues after metabolic conversion into N-methyl nicotinamide, 2- pyridone and 4-pyridone derivatives. NICO is primarily used for the prevention of deficiency in vitamin B3, which is characterized by skin lesion with hyperpigmentation and hyperkeratinisation, diarrhoea, abdominal pain, glossitis, stomatitis, loss of appetite, headache, lethargy and mental and neurological disturbances. As an API, NICO can also be used as a vasodilator, anti-hyperlipidaemia agent it can be useful in the treatment of mild-to-moderate inflammatory acne. (90,108–

110). NICO appears as a white crystalline powder or colourless crystals and it is freely soluble in water and in dehydrated alcohol. Regarding the co-crystals, NICO has successfully been tested in systems with furosemide, aceclofenac, theophylline, indomethacin, carbamazepine, naproxen, fenofibrate and gliclazide (90,98,111–117)

Malic acid or MAL (Figure 10) is an organic dicarboxylic acid, and when on its ionized form it`s malate, which is an intermediate of the citric acid (TCA) cycle along with fumarate. MAL has been used in trials studying the treatment of xerostomia, depression and hypertension. In the pharmaceutical formulation, malic acid s used as an acidifier, flavour and as an alternative to citric acid in effervescent powders. MAL is typically used with benzoic acid and salicylic acid for desloughing of ulcers, burns and wounds, and with arginine in preparations for the treatment of liver disorders. (90,118,119)

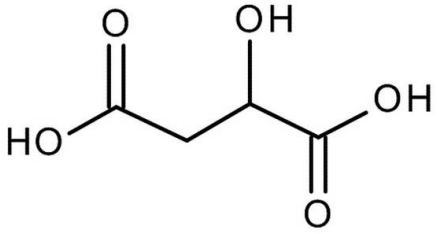

Figure 10. MAL molecular structure.

Regarding co-crystals studies, MAL has successfully been tested in systems with itraconazole, sulfamethoxazole and caffeine. (40,120,121)

Adenine or ADE (Figure 11) is one of the components of adenine nucleotides that form nucleic acids and it is also a constituent of many coenzymes. ADE has been used to manage white blood cell disorders and alcoholism and it is known to prevent loss of cell viability of red cells during long-time storage. (90,122,123)

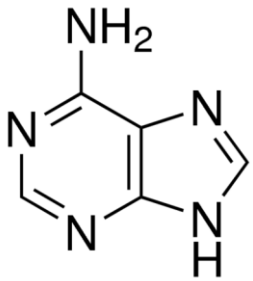

Figure 11. ADE molecular structure.

As an API, ADE derivates have significant antiviral and cytostatic activity. So, several ADE derivates have been marketed for the treatment of human immunodeficiency virus (HIV), hepatitis B virus (HBV), Cytomegalovirus (CMV) and other virus-infected diseases. (124,125)As a solid, ADE appears as a white powder, very slightly soluble in water and in alcohol. This substance dissolves in dilute mineral acids and in dilute solutions of alkali hydroxides. (90) Regarding co-crystals studies, ADE has

been successfully tested in systems with fumaric acid, furosemide, succinic acid, fumaric acid and maleic acid. (22,126,127)

D-Mannitol or MAN (Figure 12) is an alcohol and a sugar, which can be used to treat oliguria associated with kidney failure or other manifestations of inadequate renal function. MAN is commonly used to increase urine production, being part of the diuretics. (128–130)

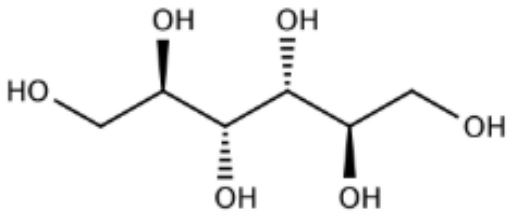

Figure 12. MAN molecular structure.

MAN can also be used to treat or prevent medical conditions that are caused by an increase in body fluids/water, being used to open the blood-brain barrier, which allows anticancer medicines to enter the brain and treat brain tumours. MAN is frequently given along with other diuretics, such as furosemide and chlorothiazide, and/or IV fluid replacement. (131) As a solid, MAN appears as a white or almost white crystalline powder and it is freely soluble in water and very slightly soluble in alcohol. (90)

Tromethamine or TRIS (Figure 13) is an organic amine proton acceptor and it has several uses in the pharmaceutical industry. TRIS, as an API, can be administered as an analgesic, anti-inflammatory and antipyretic, belonging to the pyrrolo-pyrrole group on non-steroidal anti-inflammatory drugs (NSAID). (90,132,133)

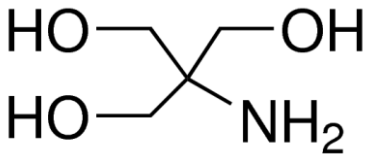

Figure 13. TRIS molecular structure.

As an NSAID member, TRIS can inhibit both cyclooxygenase-1 and -2 cascade mechanisms, blocking the production of prostaglandins. TRIS can also be used in the treatment of metabolic acidosis due to its alkalinizing effect and acts as a weak osmotic diuretic, which makes it suitable to administrate during cardiac arrest and cardiac bypass surgery. (90,132,133) As a solid, TRIS appears as a white or an almost white crystalline powder and it is freely soluble in water, sparingly soluble in alcohol and very slightly soluble in ethyl acetate. Regarding co-crystals, TRIS has been used in systems with glibenclamide and gliclazide. (90,134,135)

Chapter 2 – Materials and methods

2.1 – Materials

GBL was provided by Generis Farmacêutica S.A.. PABA (>99.5% purity) was acquired from Sigma-Aldrich (St. Louis, MO, USA). NICO (>99.5% purity) was acquired from Sigma–Aldrich (St. Louis, Missouri). MAL (>99.5% purity) was acquired from Merck (Germany). ADE (>99.0% purity) was acquired from Sigma-Aldrich (USA). MAN (>99.0% purity) was acquired from Riedel-de-Haën (Germany). TRIS (≥99% purity) was acquired from Sigma-Aldrich (St. Louis, MO, USA). Methanol was acquired from Sigma-Aldrich® (≥99,8% purity) and ethanol from Carlo Erba, DasitGroup®.

2.2 – Grinding method

The co-crystallization experiments were performed in a planetary ball mill PM 100 from Retsch® with a grinding jar of 50ml, maximum speed of 600rpm and the stainless-steel grinding balls were also acquired from Retsch® with a diameter of 12mm. (136,137) In each experiment, it was placed 1gr of powder (API and respective co-former) and, approximately, 800 mg of powder was recovered after grinding due to the adherence to the jar walls.

2.3 – Co-crystals production

In this work, several experiments where performed by co-crystallizing GBL with the six different co-formers (PABA, MAN, ADE, NICO, MAL and TRIS) using a ball mill. GBL co-crystals were synthetized through grinding using a ball mill with no-solvent involved but also with ethanol and methanol. GBL co-crystallization was tested with PABA, MAN, ADE, NICO, MAL and TRIS. Equimolar quantities of API and co-former (1:1) were used. The grinding jar was filled with the grinding balls and with both components and then milled for 3 hours with a speed of 600rpm, the maximum allowed by the equipment. When using ethanol and methanol to the GBL co-crystallization, two drops were added to the grinding jar. In Table 4 all co-crystals systems ratio and respective quantities are displayed.

Table 4. Co-crystals systems ratio and respective quantities.

Co-crystal test	Ratio	GBL	PABA	MAL	MAN	TRIS	NICO	ADE	Ethanol	Methanol
GlibPaba	1:1	500mg	137mg	-	-	-	-	-	-	-
GlibPaba	1:1	500mg	137mg	-	-	-	-	-	2 drops	-
GlibPaba	1:1	500mg	137mg	-	-	-	-	-	-	2 drops

GlibMal	1:1	500mg	-	134mg	-	-	-	-	-	-
GlibMal	1:1	500mg	-	134mg	-	-	-	-	2 drops	-
GlibMal	1:1	500mg	-	134mg	-	-	-	-	-	2 drops
GlibMan	1:1	500mg	-	-	182mg	-	-	-	-	-
GlibMan	1:1	500mg	-	-	182mg	-	-	-	2 drops	-
GlibMan	1:1	500mg	-	-	182mg	-	-	-	-	2 drops
GlibTris	1:1	500mg	-	-	-	121mg	-	-	-	-
GlibTris	1:1	500mg	-	-	-	121mg	-	-	2 drops	-
GlibTris	1:1	500mg	-	-	-	121mg	-	-	-	2 drops
GlibNico	1:1	500mg	-	-	-	-	122mg	-	-	-
GlibNico	1:1	500mg	-	-	-	-	122mg	-	2 drops	-
GlibNico	1:1	500mg	-	-	-	-	122mg	-	-	2 drops
GlibAde	1:1	500mg	-	-	-	-	-	135mg	-	-
GlibAde	1:1	500mg	-	-	-	-	-	135mg	2 drops	-
GlibAde	1:1	500mg	-	-	-	-	-	135mg	-	2 drops

2.4 – Characterization Methods

GBL, co-formers and products obtained by ball milling were characterized by NIR, MIR and DSC.

2.4.1 – Differential scanning calorimetry

The thermograms were obtained with a differential scanning calorimeter (TA instruments, Q200, USA) purged with nitrogen. For the analysis, approximately 3 mg were placed in aluminium non-hermetic crucibles and then heated at a rate of 10°C/min from 0ºC to 200ºC (except the GlibAde systems which were heated from 0ºC to 400ºC).

Table 5. Melting points of all pure compounds.

Pure compounds	Melting Point (ºC)
Glibenclamide	173
Adenine	360
Malic acid	134
Nicotinamide	129
***p*-aminobenzoic acid**	189
Tromethamine	172
Mannitol	167

2.4.2 – Near-infrared spectroscopy

To characterize the obtained systems a Fourier-transform near-infrared analyser (FTLA2000, ABB, Québec, Canada) was used and it was equipped with an InGaAs detector. The measurements of the samples were made in diffuse reflectance mode using a powder sampling accessory with a 2 cm diameter window. The background was obtained with a reflectance certified material (polytetrafluoroethylene, PTFE). Spectra were acquired with a resolution of 8 cm^{-1} and stored as the average of 64 scans in the range between 10.000 and 4.000 cm^{-1}. For each sample, three spectral replicates were taken.

2.4.3 – Mid-infrared spectroscopy

A Fourier-transform infrared analyser FT-IR Spectrometer Frontier™ (PerkinElmer Inc., MA, USA) equipped with an attenuated total reflectance (ATR) accessory was used (single relfection diamond crystal). Each spectrum was acquired with a resolution of 4 cm^{-1} as the average of 32 scans in the range between 4.000 cm^{-1} and 600 cm^{-1}. For each sample, two spectral replicates were taken.

Chapter 3 – Results and discussion

This chapter presents the analysis for the thermal characterization and spectroscopic characterization for each API and co-former system. Furthermore, a summary of the characterization results is presented. Firstly, the obtained products through grinding were characterized by DSC and by vibrational spectroscopic techniques. The possibility of co-crystal formation is discussed for each case based on the results of the characterization techniques. All grinded products were characterized by DSC. In this technique, the potential co-crystal was compared with the API, respective co-former and physical mixture. Table 6 summarizes the results for the thermal characterization of the pure compounds by DSC.

Table 6. Transition temperature and enthalpy variation for the pure compounds used in this study.

Pure components	**1st peak**		**2nd peak**	
	T_{peak} (°C) ±st.dev.	ΔH (J/g) ±st.dev.	T_{peak} (°C) ±st.dev.	ΔH (J/g) ±st.dev.
GBL	173.44 ±0.01	-76.42 ±5.07	-	-
ADE	361.46 ±0.00	-117.3 ±12.3	-	-
MAL	134.37 ±0.02	-212.7 ±23.3	-	-
MAN	167.05 ±0.05	-285.0 ±17.0	-	-
NICO	129.78 ±0.00	-190.3 ±11.9	-	-
PABA	188.73 ±0.02	-172.6 ±17.5	-	-
TRIS	142.61 ±0.10	-236.70 ±16.10	172.39 ±0.01	-23.92 ±1.71

Regarding the pure compounds, all of them were thermally characterized by one single endothermic peak, corresponding to the melting point, except for TRIS. Such co-former exhibit an enthalpy variation endothermic peak at 142.61±0.10°C (ΔH=-236.70±16.10 J/g), corresponding to a plastic deformation from a crystalline orthorhombic to a body-centred cubic structure, and a second endothermic peak at 172.39±0.01°C (ΔH=-23.92 ±1.71 J/g), which is the melting point. (138) GBL was thermally stable up to 173.44±0.01ºC (ΔH= -76.42±5.07 J/g), which corresponds to the referred temperature value in the literature (169-180ºC).(89,135) Table 7 displays the results for the thermal characterization of the physical mixtures (PM) and the milled products by DSC.

Table 7. Transition temperatures and enthalpy variation for the systems under study and respective PM.

	1st peak		2nd peak		3rd peak	
	T_{peak} (°C) ±st.dev.	ΔH (J/g) ±st.dev.	T (°C) ±st.dev.	ΔH (J/g) ±st.dev.	T (g°C) ±st.dev.	ΔH (J/g) ±st.dev.
System GlibAde						
GlibAde PM	172.46 ±0.01	-60.72 ±2.78	-	-	-	-
GlibAde (Sol.: None)	174.63 ±0.00	-71.14 ±7.75	-	-	-	-
GlibAde (Sol.: Ethanol)	171.15 ±0.00	-57.00 ±4.98	-	-	-	-
GlibAde (Sol.: Methanol)	173.46 ±0.00	47.26 ±1.31	-	-	-	-
System GlibMal						
GlibMal PM	134.91 ±0.01	-125.6 ±12.8	142.58 ±0.01	-	-	-
GlibMal (Sol.: None)	124.52 ±0.26	-	131.43 ±0.07	-25.95 ±5.57	154.65 ±0.01	-
GlibMal (Sol.: Ethanol)	107.61 ±0.26	-1.90 ±1.14	138.89 ±0.34	-15.38 ±11.3	157.98 ±0.01	-
GlibMal (Sol.: Methanol)	133.03 ±0.03	-14.92 ±6.65	143.65 ±0.30	-	159.00 ±0.01	-
System GlibMan						
GlibMan PM	166.34 ±0.01	-1.79 ±1.60	170.14 ±0.14	-11.13 ±16.41	-	-
GlibMan (Sol.: None)	167.15 ±0.01	-125.3 ±20.8	-	-	-	-
GlibMan (Sol.: Ethanol)	168.99 ±0.00	-96.58 ±23.62	-	-	-	-
GlibMan (Sol.: Methanol)	169.04 ±0.00	-134.0 ±13.4	-	-	-	-
System GlibNico						
GlibNico PM	125.43 ±0.03	-70.25 ±15.11	139.49 ±0.08	-2.860 ±1.56	-	-
GlibNico (Sol.: None)	122.08 ±0.00	-44.56 ±7.81	141.82 ±0.02	-5.306 ±3.33	-	-
GlibNico (Sol.: Ethanol)	121.45 ±0.01	-23.94 ±2.14	157.19 ±0.17	-23.97 ±9.73	-	-
GlibNico (Sol.: Methanol)	120.64 ±0.10	-19.74 ±10.48	149.12 ±0.13	-11.42 ±8.58	-	-
System GlibPaba						
GlibPaba PM	143.61 ±0.10	-9.08 ±2.37	-	-	-	-
GlibPaba (Sol.: None)	61.25 ±0.10	-2.67 ±1.64	91.74 ±0.02	-	128.08 ±0.00	-34.46 ±11.72
GlibPaba (Sol.: Ethanol)	138.56 ±0.00	-37.27 ±10.1	172.89 ±0.00	-0.317 ±0.09	-	-
GlibPaba (Sol.: Methanol)	139.22 ±0.43	-22.70 ±10.99	154.23 ±0.03	-0.591 ±0.07	-	-

Table 7(continuation). Transitions temperature and enthalpy variation for the systems under study and respective PM.

System GlibTris						
GlibTris PM	124.86 ±0.00	-0.834 ±0.01	137.28 ±0.02	-154.7 ±19.7	-	-
GlibTris (Sol.: None)	118.71 ±0.10	-20.66 ±1.88	135.43 ±0.01	-1.15 ±0.10	140.71 ±0.01	-6.59 ±0.16
GlibTris (Sol.: Ethanol)	135.06 ±0.02	-1.326 ±1.04	142.42 ±0.00	-16.34 ±7.52	-	-
GlibTris (Sol.: Methanol)	133.14 ±0.01	-2.562 ±1.94	143.92 ±0.00	-39.33 ±15.2	-	-

Regarding the spectroscopic characterization, the NIR and MIR spectroscopic analysis aims to verify whether there was molecular bond formation between GBL and the six co-formers. In this way, by comparison with the PM it is observed if there are new or shifted bonds, corresponding to new vibration between GBL and co-formers.

3.1 – GlibAde system

When analysing the thermograms for the GlibAde (1:1) without solvent, GlibAde (1:1) Ethanol and GlibAde (1:1) Methanol systems (Fig. 14) and the values present in Table 7, we can verify that all milled systems express a similar behaviour with the PM. From the DSC results it can be inferred that no co-crystal was produced in this case.

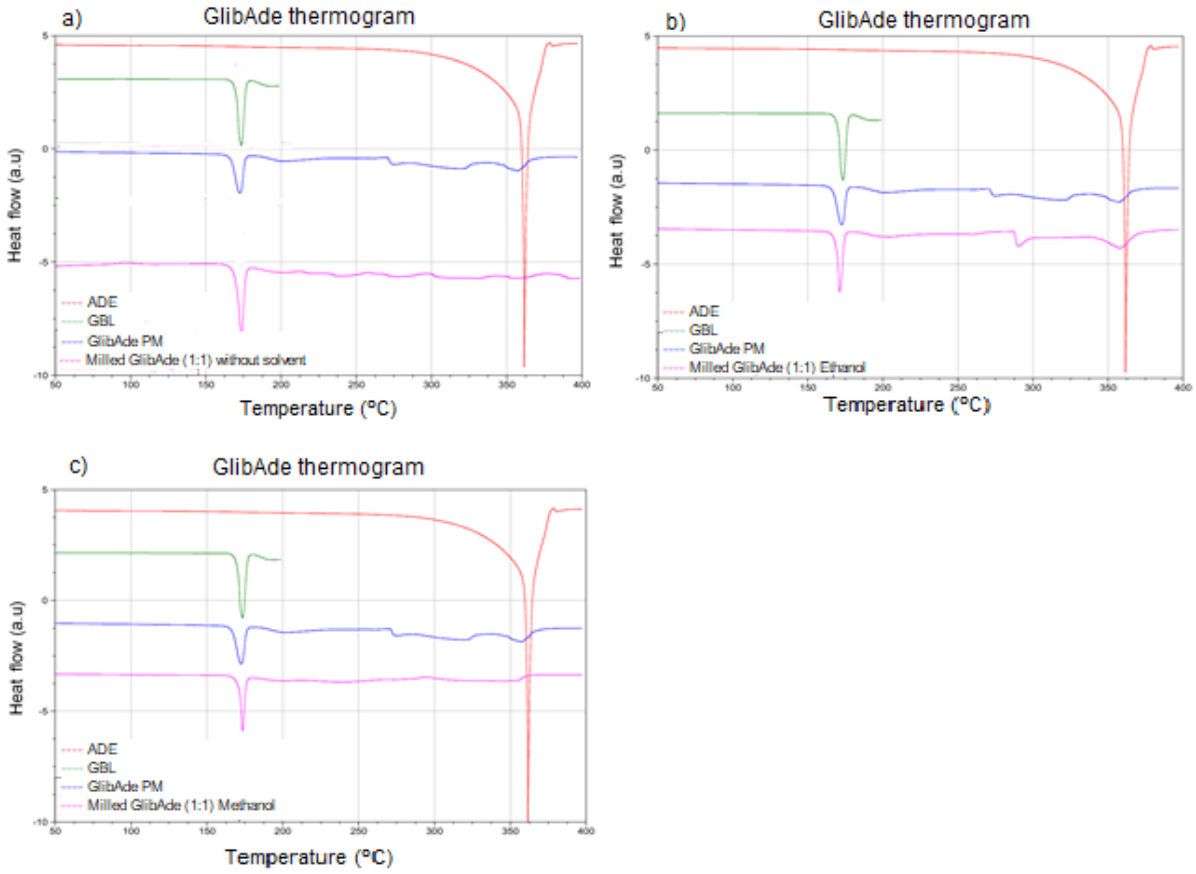

Figure 14. Thermograms of the GlibAde system: (a) GlibAde (1:1) without solvent, (b) GlibAde (1:1) Ethanol, (c) GlibAde (1:1) Methanol.

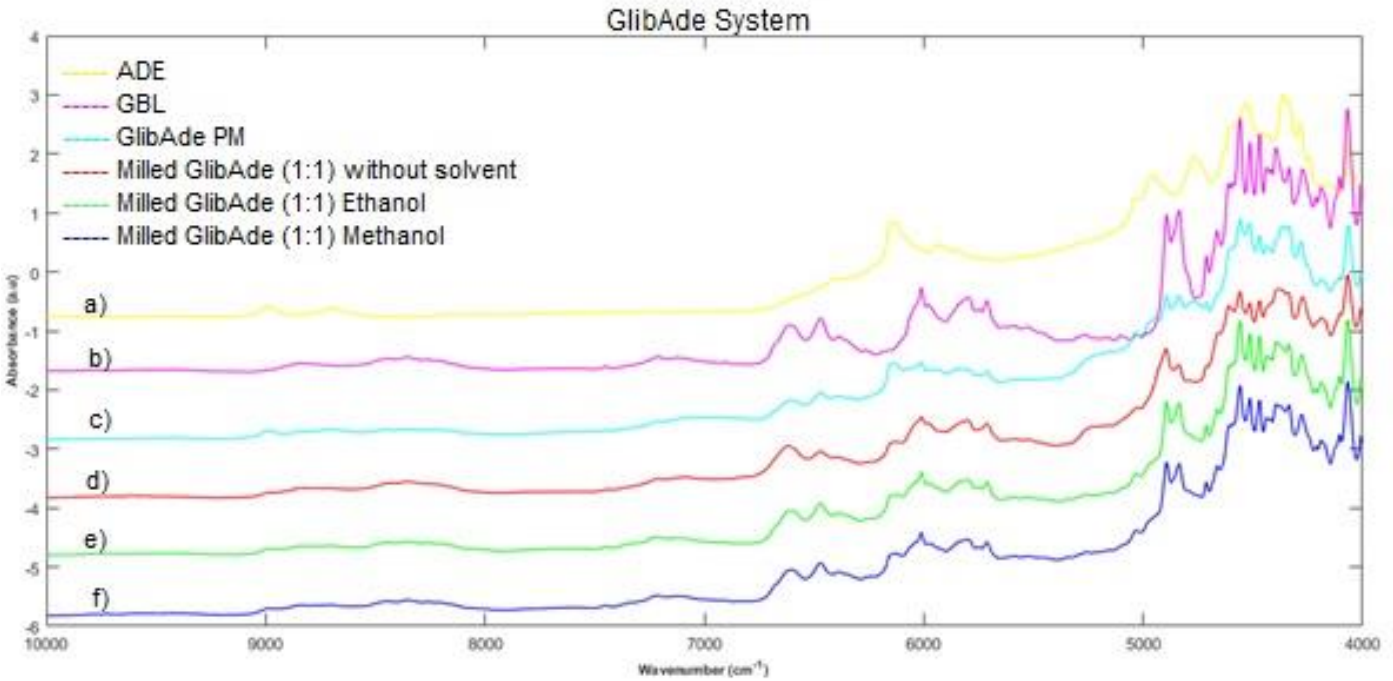

Figure 15. Spectroscopic characterization: (a) NIR spectra for the pure compound ADE; (b) NIR spectra for the pure compound GBL; (c) NIR spectra for the GlibAde PM; (d) NIR spectra for the GlibAde(1:1) without solvent; (e) NIR spectra for the GlibAde (1:1) Ethanol and (f) NIR spectra for the GlibAde (1:1) Methanol.

The NIR spectrum of the GlibAde (1:1) system without solvent shows a difference in the spectral region (Fig.15):

- Between 5000-4500 cm^{-1}, which corresponds to the combination region of the vibration of the amine (RNH_2) and amide (CONH-R);

The NIR spectrum of the GlibAde (1:1) Ethanol and GlibAde (1:1) Methanol systems do not show significant differences.

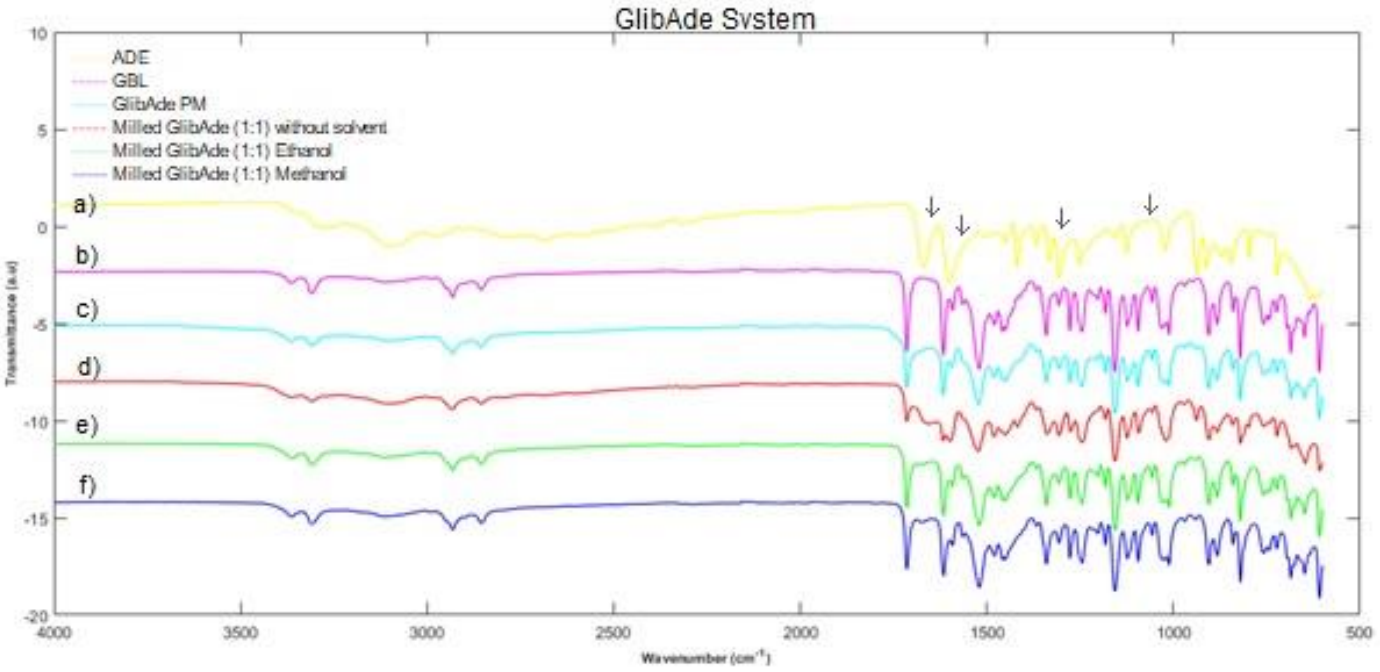

Figure 16. Spectroscopic characterization: (a) MIR spectra for the pure compound ADE; (b) MIR spectra for the pure compound GBL; (c) MIR spectra for the GlibAde PM; (d) MIR spectra for the GlibAde (1:1) without solvent; (e) MIR spectra for the GlibAde (1:1) Ethanol and (f) MIR spectra for the GlibAde (1:1) Methanol.

The MIR spectrum of the GlibAde (1:1) system without solvent shows differences in the spectral region (Fig.16):

- at ≈ 1020 cm^{-1} (fingerprint region), which may be due to the stretching of the C-N amine vibration;
- at ≈ 1420 cm^{-1} (fingerprint region), corresponding to the bending of the C-H in the methyl group;
- at ≈ 1600 cm^{-1}, which may result of the stretching of C=C;
- at ≈ 1660 cm^{-1}, result of the stretching of C=C.

The MIR spectrum of the GlibAde (1:1) Ethanol and GlibAde (1:1) Methanol systems (Fig. 16) do not show significant differences.

3.2 – GlibMal system

The GlibMal PM thermogram (Fig. 17) presents an endothermic peak corresponding to the eutectic melting following by an exothermic peak that may correspond to the co-crystal formation followed by the co-crystal melting. This behaviour is consistent with the possibility of co-crystal formation between these two compounds. (14) The thermogram of the GlibMal (1:1) system without solvent shows a complex behaviour with several endothermic peaks followed by what seems to be an exothermic

event. This behaviour can be due to the presence of the co-crystal impure, i.e., in a mixture with the pure components, or the presence of different polymorphs of the cocrystal.

The thermogram of the GlibMal (1:1) Ethanol system (Fig. 17b) shows an endothermic peak, which may be due to solvent presence, followed by another endothermic peak and an exothermic peak. This behaviour is consistent with the possibility of co-crystal formation. The thermogram of the GlibMal (1:1) Methanol (Fig. 17c) system exhibits a desolvation peak at ≈ 65°C, corresponding to the presence of methanol in the mixture. The desolvation peak is followed by several endothermic peaks and what seems to be an exothermic event. This behaviour is similar to the GlibMal (1:1) without solvent system, leading to the conclusion that this behaviour can be due to the presence of an impure co-crystal and is consistent with the possibility of co-crystal formation.

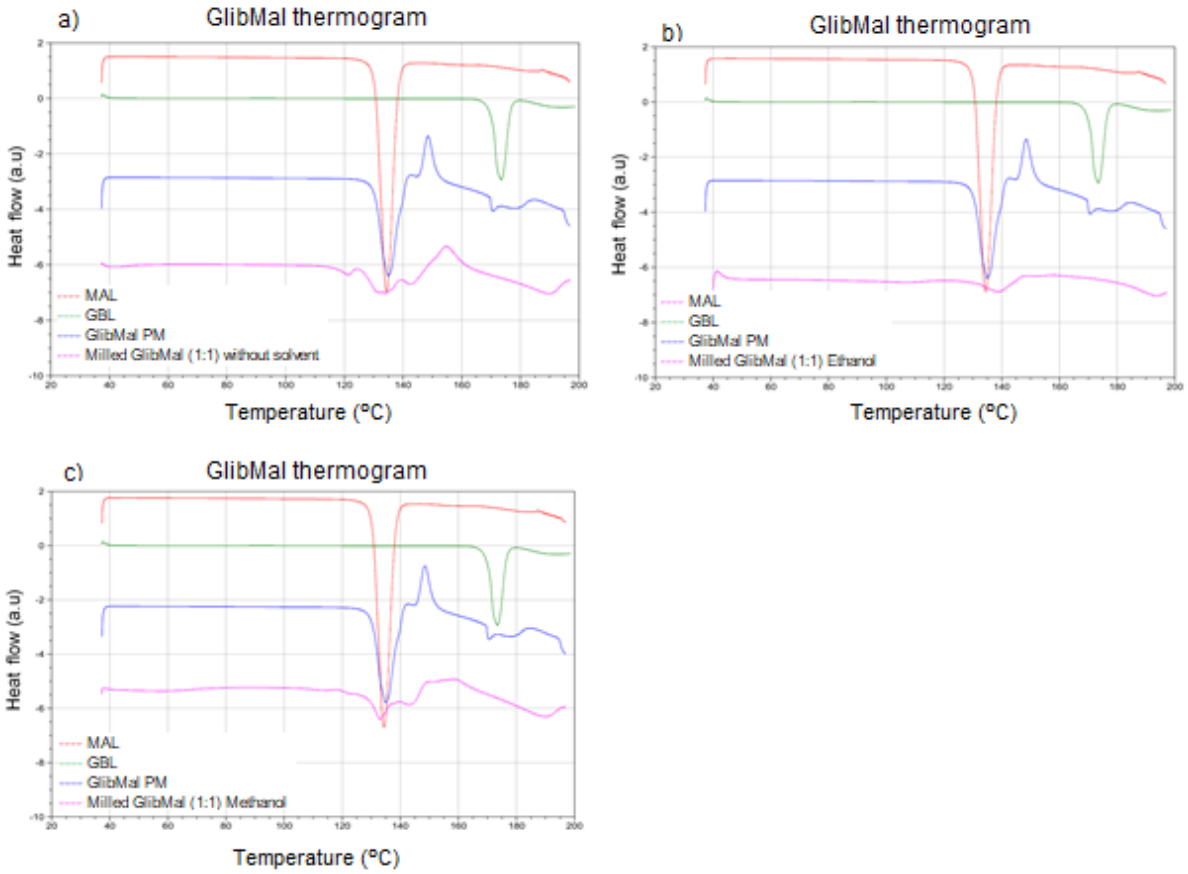

Figure 17. Thermograms of the GlibMal system: (a) GlibMal (1:1) without solvent, (b) GlibMal (1:1) Ethanol, (c) GlibMal (1:1) Methanol.

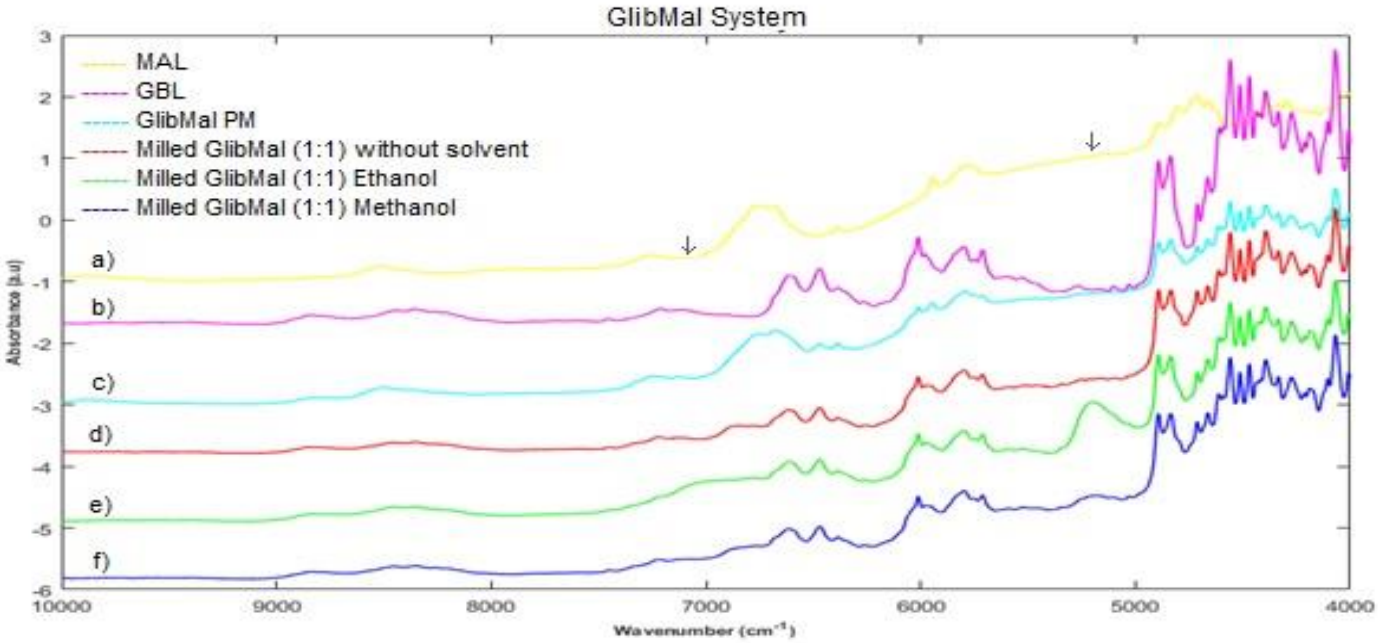

Figure 18. Spectroscopic characterization: (a) NIR spectra for the pure compound MAL; (b) NIR spectra for the pure compound GBL; (c) NIR spectra for the GlibMal PM; (d) NIR spectra for the GlibMal(1:1) without solvent; (e) NIR spectra for the GlibMal (1:1) Ethanol and (f) NIR spectra for the GlibMal (1:1) Methanol.

Concerning the NIR spectrum of the GlibMal system without solvent, differences are shown (Fig. 18):

- between 6000-5900 cm^{-1}, corresponding to the first overtone of the C-H bound in the methyl group;
- between 6900-6650 cm^{-1}, in the second overtone region corresponding to the $CONH_2$, CONH-R, NH_2 and OH groups vibrations.

The NIR spectra of the GlibMal (1:1) Ethanol and Methanol systems (Fig. 18) exhibits the same differences as the GlibMal (1:1) system without solvent, except the differences regarding to solvent presence, which is most notable in the system with ethanol:

- at ≈ 5200 and 7000 cm^{-1}, a characteristic band of OH vibration is visible in the first overtone region, being due to solvent presence;

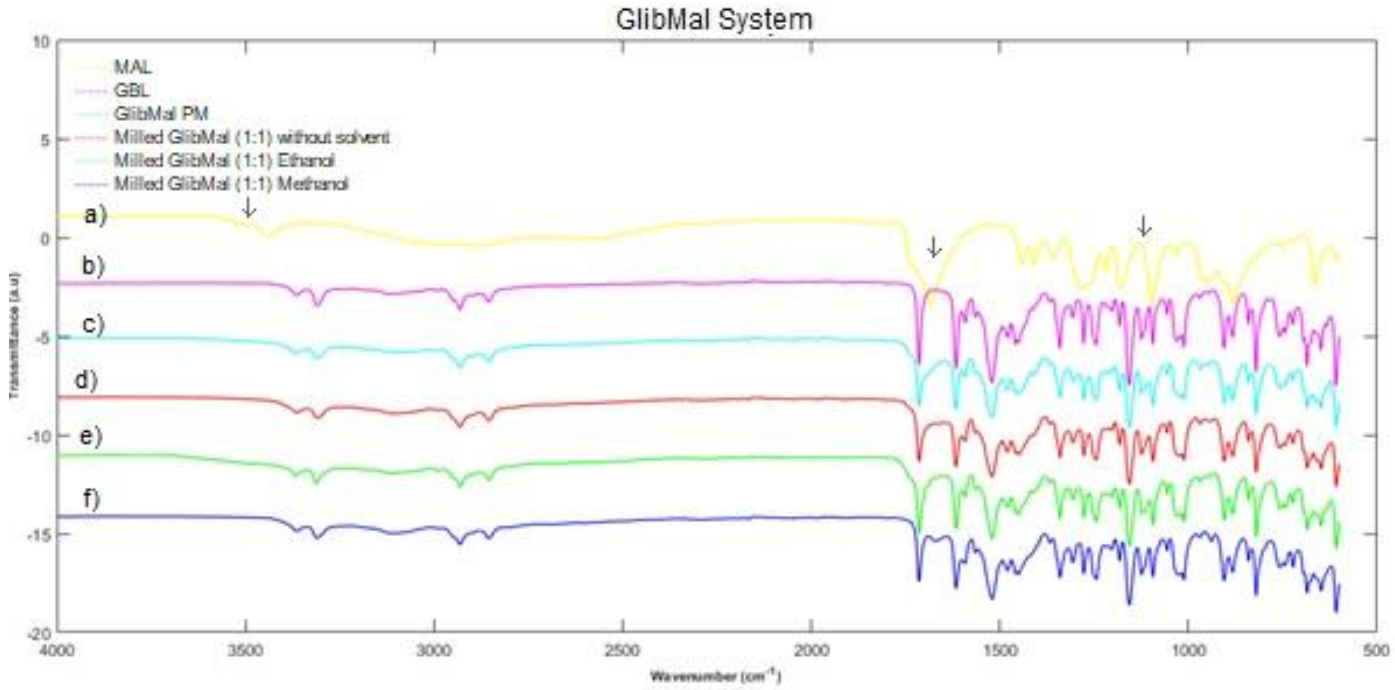

Figure 19. Spectroscopic characterization: (a) MIR spectra for the pure compound MAL; (b) MIR spectra for the pure compound GBL; (c) MIR spectra for the PM GBL:MAL (1:1); (d) MIR spectra for the GBL:MAL (1:1) w/solvent; (e) MIR spectra for the GBL:MAL (1:1) Ethanol and (f) MIR spectra for the GBL:MAL (1:1) Methanol.

The MIR spectrum of the GlibMal (1:1) system without solvent shows a difference (Fig. 19):

- at ≈ 1690 cm^{-1}, a characteristic vibration band corresponding to the C=O stretching.

Regarding the systems with solvent, the MIR spectrum of the GlibMal (1:1) Ethanol (Fig. 19) shows differences:

- at ≈ 1150 cm^{-1} (fingerprint region), corresponding to the C=O stretching.
- at ≈ 3500 cm^{-1}, corresponding to the OH stretching band, which is due to the solvent presence;

In the MIR spectrum of GlibMal (1:1) Methanol system, the observed differences for the GlibMal (1:1) Ethanol are also valid for the system with methanol.

3.3 – GlibMan system

The GlibMan PM thermogram exhibits two endothermic peaks (Fig. 20), which may be due to the pure compounds, because they are close to the respective melting points. All systems with MAN exhibit a similar behavior with the PM. Therefore, it can be concluded that no co-crystal was formed.

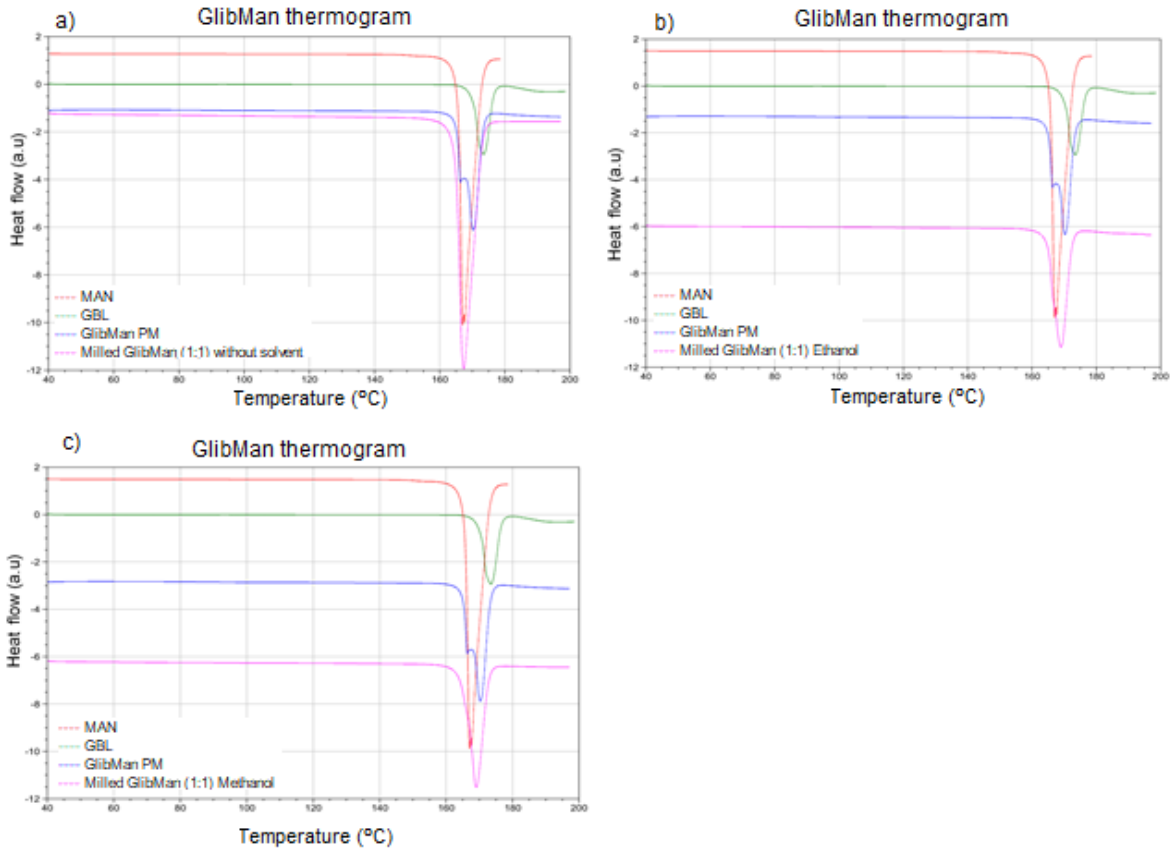

Figure 20. Thermograms of the GlibMan system: (a) GlibMan (1:1) without solvent, (b) GlibMan (1:1) Ethanol, (d) GlibMan (1:1) Methanol.

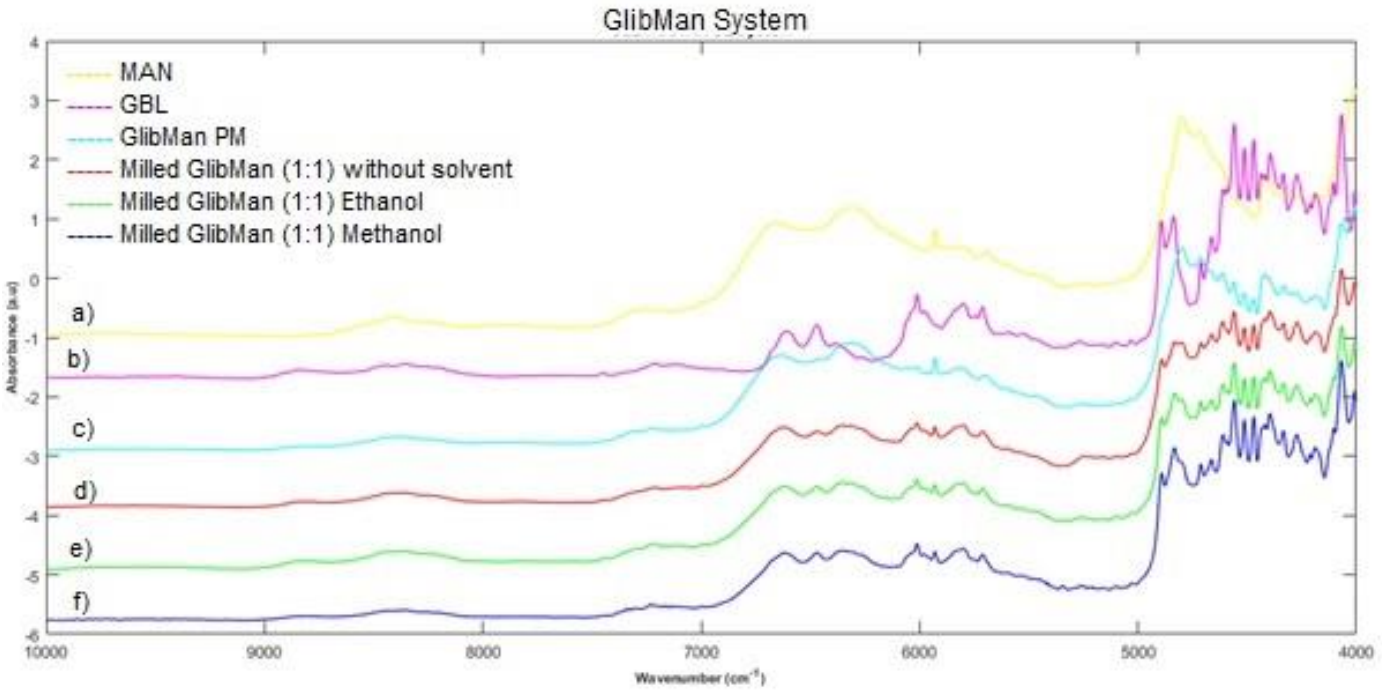

Figure 21. Spectroscopic characterization: (a) NIR spectra for the pure compound MAN; (b) NIR spectra for the pure compound GBL; (c) NIR spectra for the GlibMan PM; (d) NIR spectra for the

GlibMan(1:1) without solvent; (e) NIR spectra for the GlibMan (1:1) Ethanol and (f) NIR spectra for the GlibMan (1:1) Methanol.

The NIR spectra of the GlibMan (1:1) system without solvent and GlibMan (1:1) Ethanol and Methanol systems (Fig. 21) did not exhibit differences between the samples and the PM.

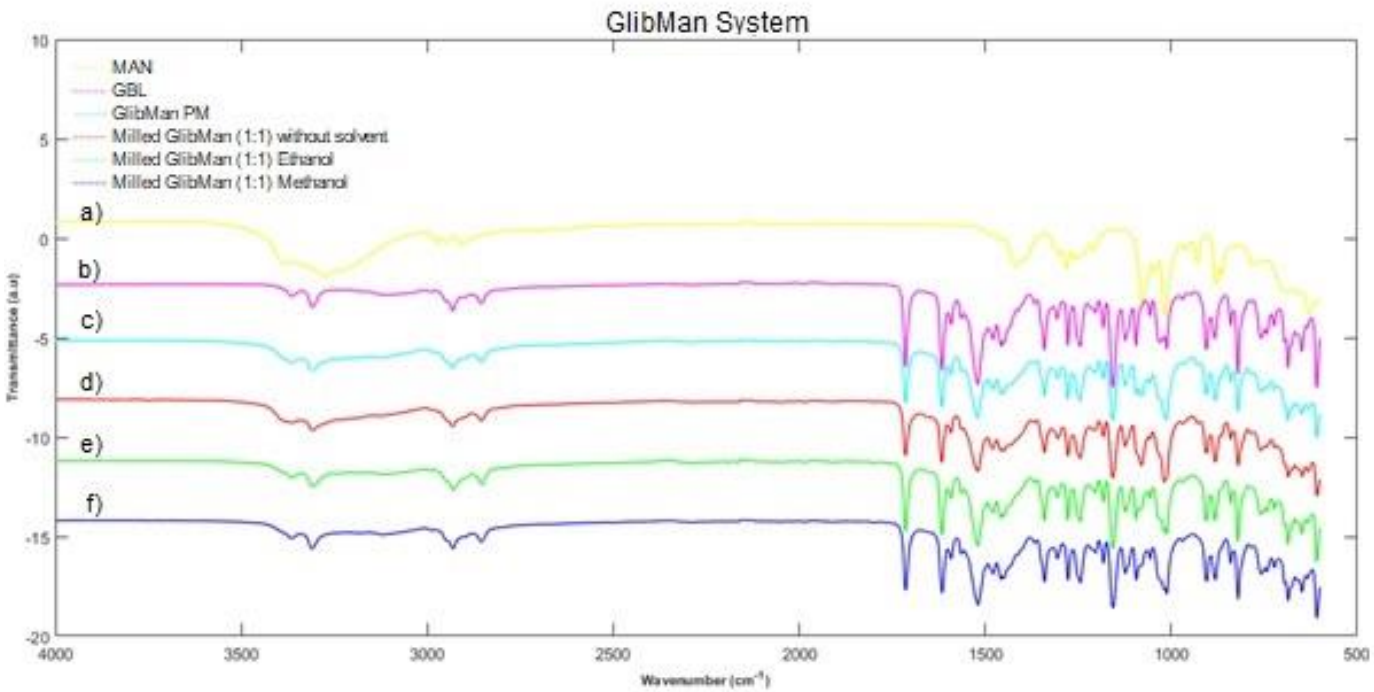

Figure 22. Spectroscopic characterization: (a) MIR spectra for the pure compound MAN; (b) MIR spectra for the pure compound GBL; (c) MIR spectra for the GlibMan PM; (d) MIR spectra for the GlibMan (1:1) without solvent; (e) MIR spectra for the GlibMan (1:1) Ethanol and (f) MIR spectra for the GlibMan (1:1) Methanol.

Regarding the MIR spectra of the GlibMan (1:1) system without solvent, GlibMan (1:1) Ethanol and GlibMan (1:1) Methanol systems (Fig. 22), no differences were found between the milled and the physical mixtures of each sample.

3.4 – GlibNico system

The thermograms of the GlibNico (1:1) system without solvent and GlibNico (1:1) Ethanol and Methanol exhibit one endothermic peak followed by another endothermic peak (Fig. 23). This behaviour is consistent with the melting of the pure compounds, therefore, there was no co-crystal formation.

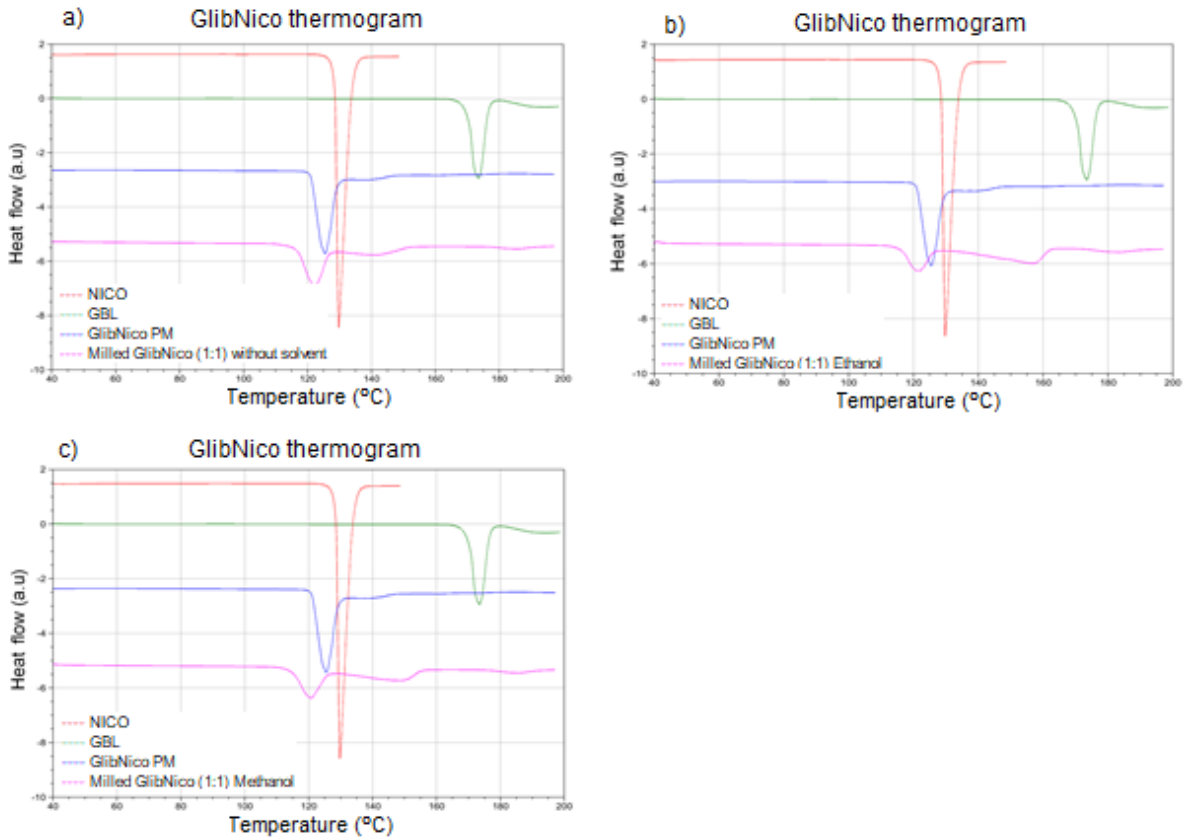

Figure 23. Thermograms of the GlibNico system: (a) GlibNico (1:1) without solvent, (b) GlibNico (1:1) Ethanol, (d) GlibNico (1:1) Methanol.

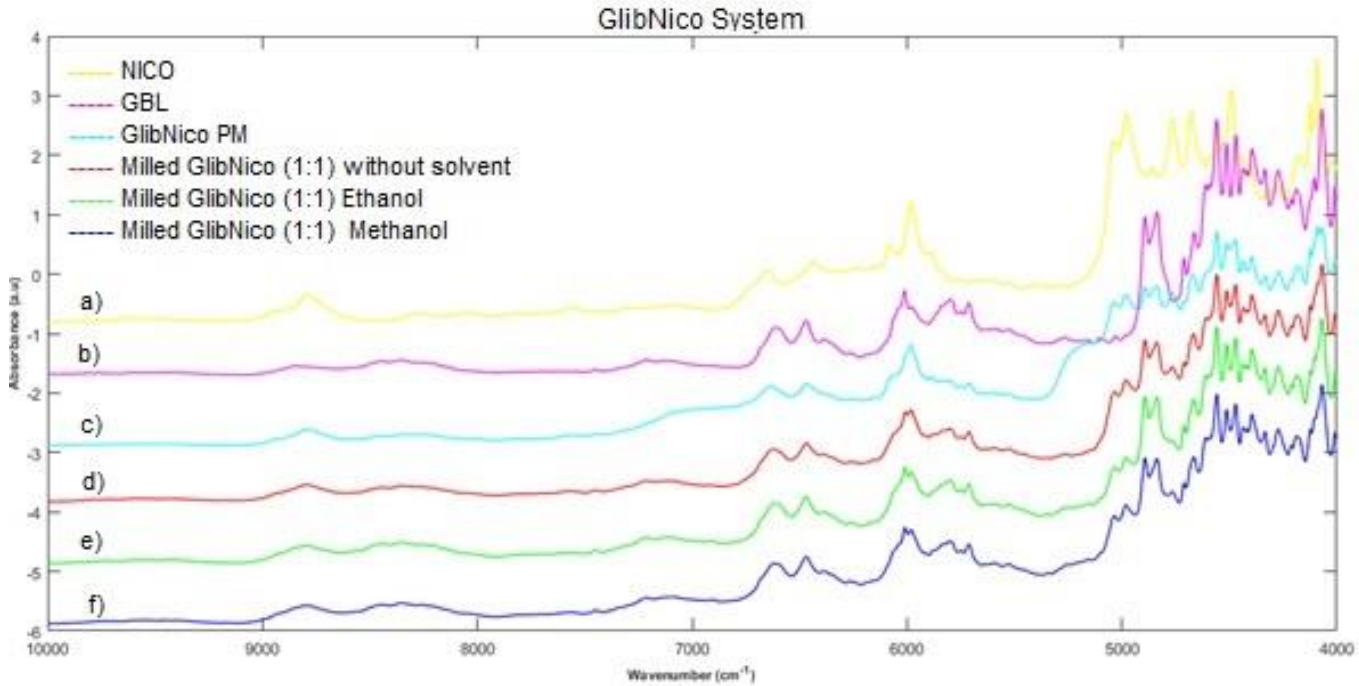

Figure 24. Spectroscopic characterization: (a) NIR spectra for the pure compound NICO; (b) NIR spectra for the pure compound GBL; (c) NIR spectra for the GlibNico PM; (d) NIR spectra for the GlibNico (1:1) without solvent; (e) NIR spectra for the GlibNico (1:1) Ethanol and (f) NIR spectra for the GlibNico (1:1) Methanol.

The NIR spectra for GlibNico (1:1) system without solvent and GlibNico (1:1) Ethanol and Methanol systems (Fig. 24), only exhibit in the combination region, at ≈ 4850 cm^{-1}, a vibration band of the OH group, however, it is due to traces of water in the physical mixture sample.

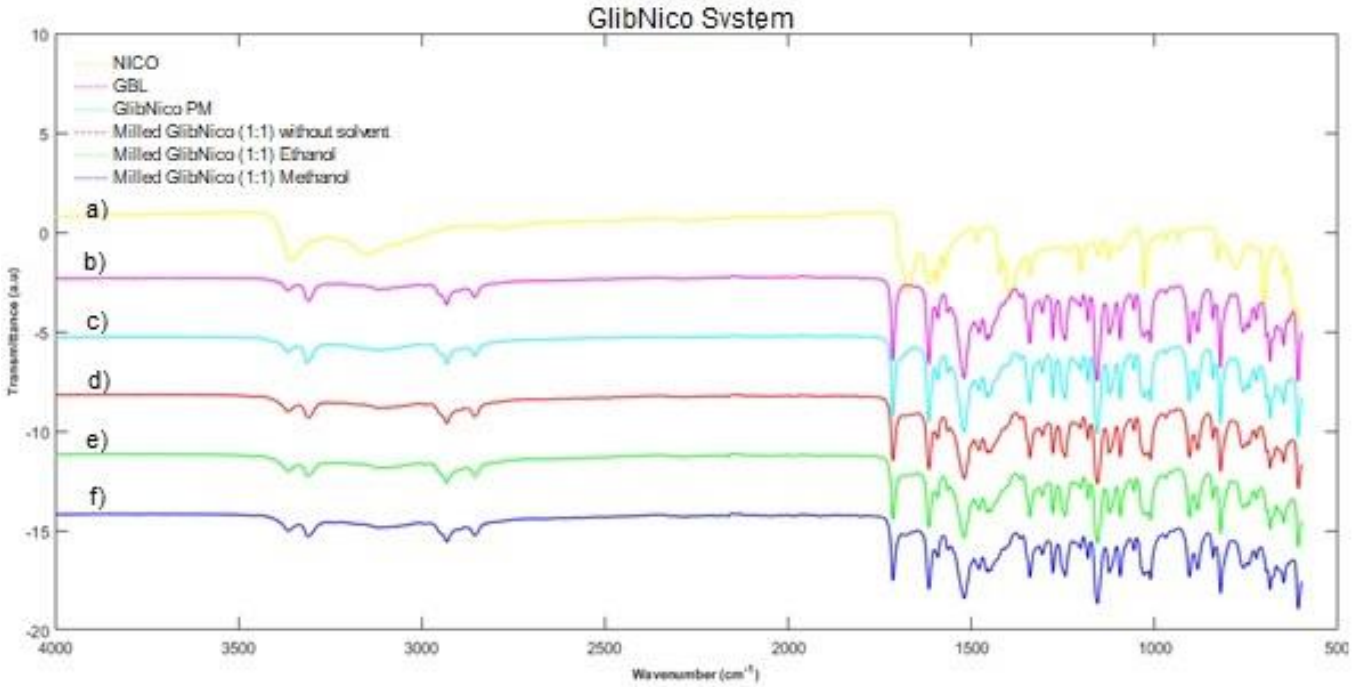

Figure 25. Spectroscopic characterization: (a) MIR spectra for the pure compound NICO; (b) MIR spectra for the pure compound GBL; (c) MIR spectra for the GlibNico PM; (d) MIR spectra for the GlibNico (1:1) without solvent; (e) MIR spectra for the GlibNico (1:1) Ethanol and (f) MIR spectra for the GlibNico (1:1) Methanol.

In the MIR spectrum of the GlibNico (1:1) system without solvent and GlibNico (1:1) Ethanol and Methanol systems (Fig. 25), no differences between the milled mix and the physical mixture were found.

3.5 – GlibPaba system

The thermograms of the GlibPaba (1:1) Ethanol and Methanol display two endothermic peaks, one followed by the other (Fig. 26). This behaviour is consist to the melt of the pure compounds, therefore, no co-crystal was formed. (14) The thermogram of the GlibPaba (1:1) system without solvent (Fig. 26) exhibits an endothermic peak followed by an exothermic peak and after another endothermic peak. The first endothermic peak may the melt of a co-crystal polymorph, followed by what seems to be the formation of a second polymorph and followed by the melt of the second polymorph.

This behaviour is consistent with the possibility of co-crystal formation between these two compounds.

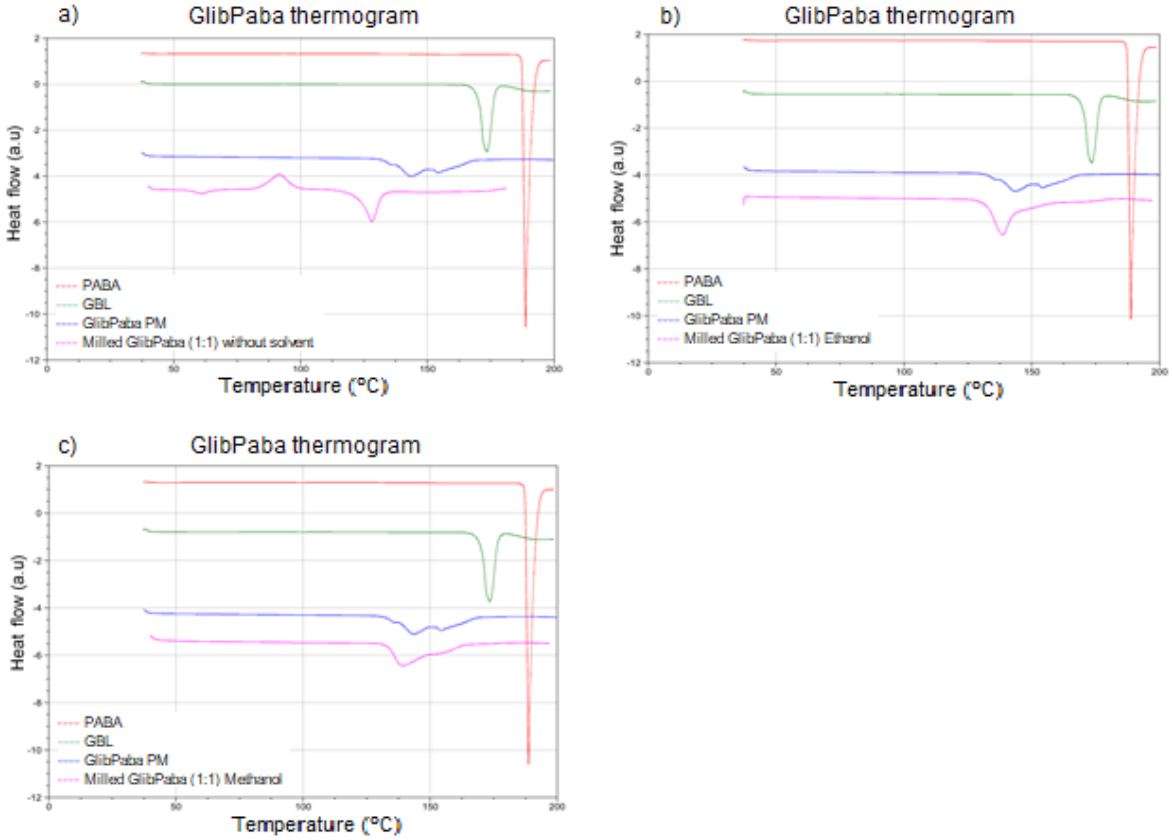

Figure 26. Thermograms of the GlibPaba system: (a) GlibPaba (1:1) without solvent, (b) GlibPaba (1:1) Ethanol, (c) GlibPaba (1:1) Methanol.

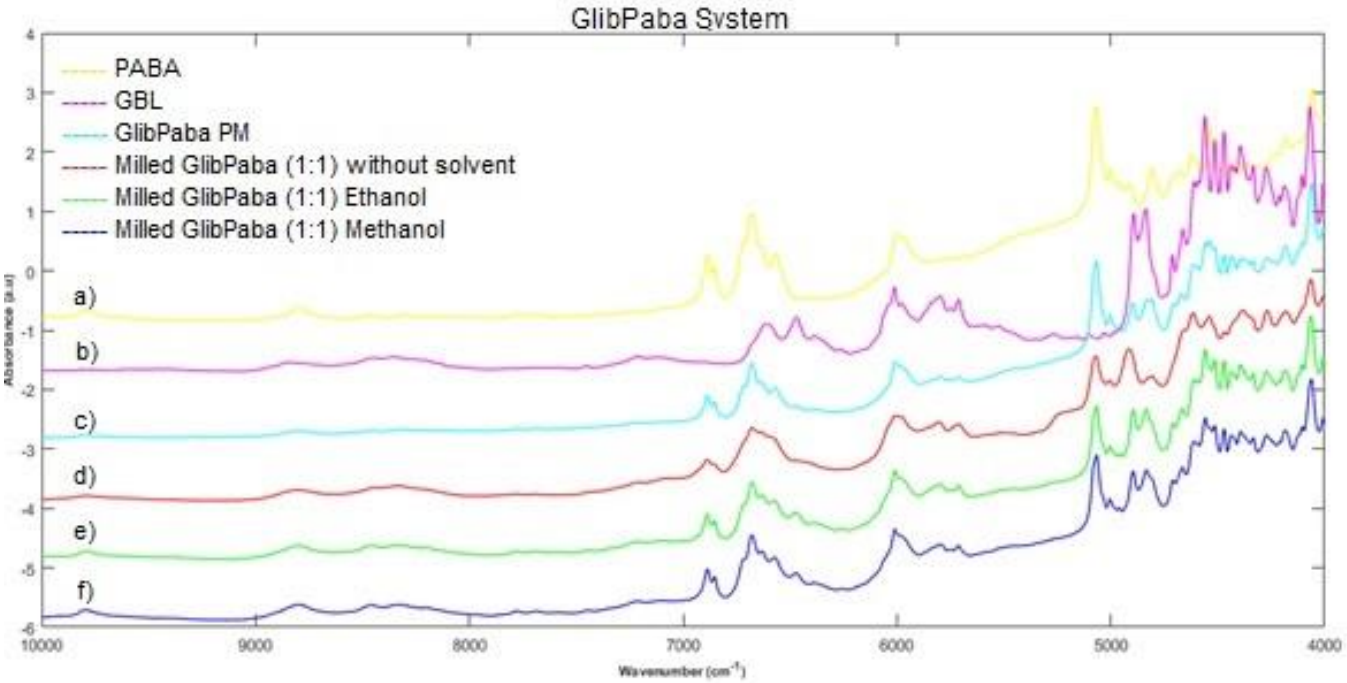

Figure 27. Spectroscopic characterization: (a) NIR spectra for the pure compound PABA; (b) NIR spectra for the pure compound GBL; (c) NIR spectra for the GlibPaba PM(1:1); (d) NIR spectra for the GlibPaba (1:1) without solvent; (e) NIR spectra for the GlibPaba (1:1) Ethanol and (f) NIR spectra for the GlibPaba (1:1) Methanol.

In the NIR spectrum of the GlibPaba (1:1) system without solvent (Fig. 27), several differences are visible:

- between 5000-4450 cm^{-1}, in the combination region band corresponding to the C-H vibration of the methyl group and amine group;
- at ≈ 4950 cm^{-1}, corresponding to the amine group vibration in the combination group;
- at ≈ 5100 cm^{-1}, which is due to the amide vibration in the first overtone region;
- at ≈ 5200 cm^{-1}, corresponding to the carboxylic acid group vibration in the first overtone region;
- at ≈ 6700 cm^{-1}, which corresponds to the second overtone region, in which is exhibit vibrations of the amine, amide and OH groups;
- between 7000-6500 cm^{-1}, corresponding to the second overtone of the CH bound and the alcohol (ROH) vibration band;
- between 9000-8500 cm^{-1}, which is due to the second overtone of the CH bound and the amine (RNH_2) vibration band.

In the NIR spectrum of the GlibPaba (1:1) Ethanol and GlibPaba (1:1) Methanol systems (Fig. 27), no significant differences were observed.

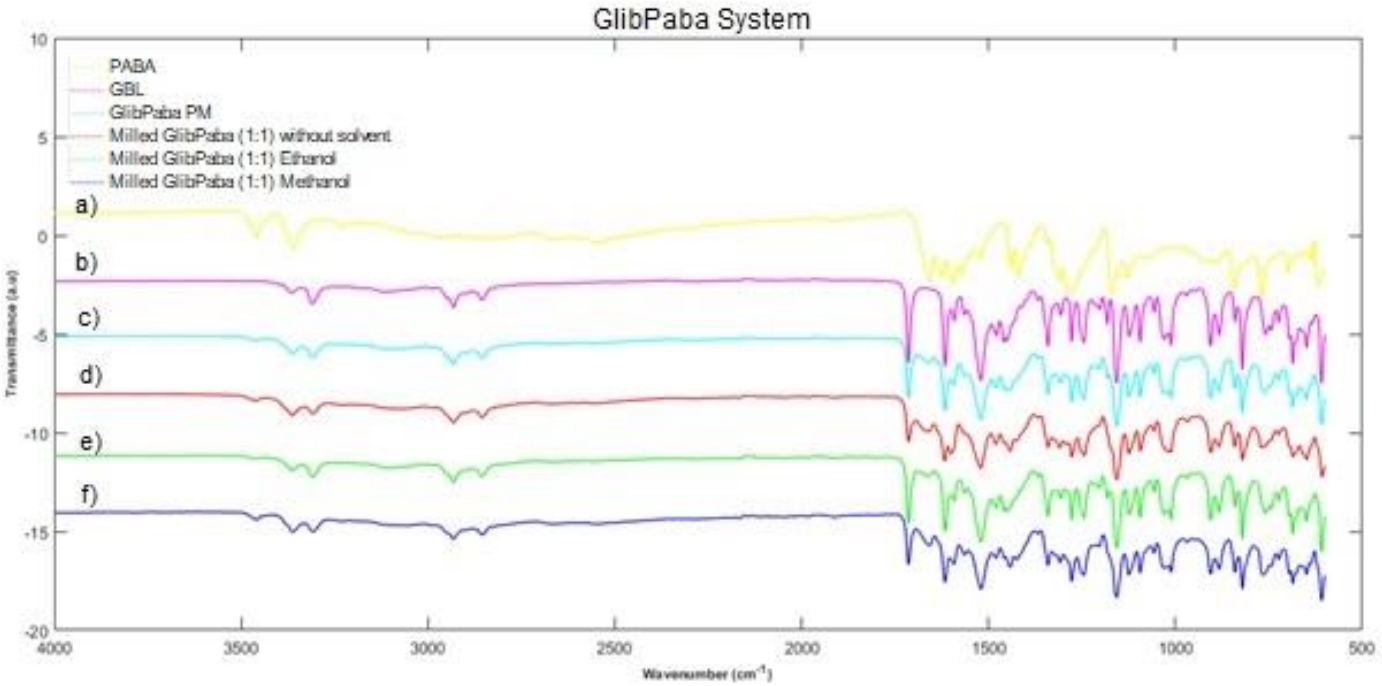

Figure 28. Spectroscopic characterization: (a) MIR spectra for the pure compound PABA; (b) MIR spectra for the pure compound GBL; (c) MIR spectra for the GlibPaba PM (1:1); (d) MIR spectra for the GlibPaba (1:1) without solvent; (e) MIR spectra for the GlibPaba (1:1) Ethanol and (f) MIR spectra for the GlibPaba (1:1) Methanol.

Regarding the MIR spectrum of GlibPaba (1:1) system without solvent (Fig. 28), it shows differences between the milled mix and the physical mixture:

- at ≈ 1170 cm^{-1}, which corresponds to the carboxylic acid C=O stretching vibration;
- at ≈ 1290 cm^{-1}, corresponding to the C=O of the carboxylic acid stretching vibration band;
- at ≈ 1600 cm^{-1}, which is due to N-H vibration of the amine group and C=C from the aromatics stretching vibration bands.

In the MIR spectrum of the GlibPaba (1:1) Ethanol and GlibPaba (1:1) Methanol systems (Fig. 28), no significant differences were observed.

3.6 – GlibTris system

Taking into account a previous study in which this particular system was studied through solvent evaporation, the respective thermogram showed a single and well-defined endothermic peak at ≈144°C, corresponding to the co-crystal melting point (Fig. 29). (29) However, in this work the GlibTris systems do not display a single endothermic peak. The thermogram of the GlibTris (1:1) system without solvent shows a complex behaviour with three endothermic peaks. The third endothermic peak, displayed at 140.71°C, happens in a similar temperature to the one reported in the previous study.

This behaviour can be due to the presence of the co-crystal impure, i.e., in a mixture with the pure components, or the presence of different polymorphs of the cocrystal. The thermograms of the GlibTris (1:1) Ethanol and Methanol (Fig. 29) exhibit two endothermic peaks, the same behaviour as the PM. The second endothermic peak in both GlibTris (1:1) solvent systems and PM is exhibit in a temperature near to the reported temperature in the previous study. This can be due to the presence of the co-crystal impure; however, the co-crystal formation seems to be possible.

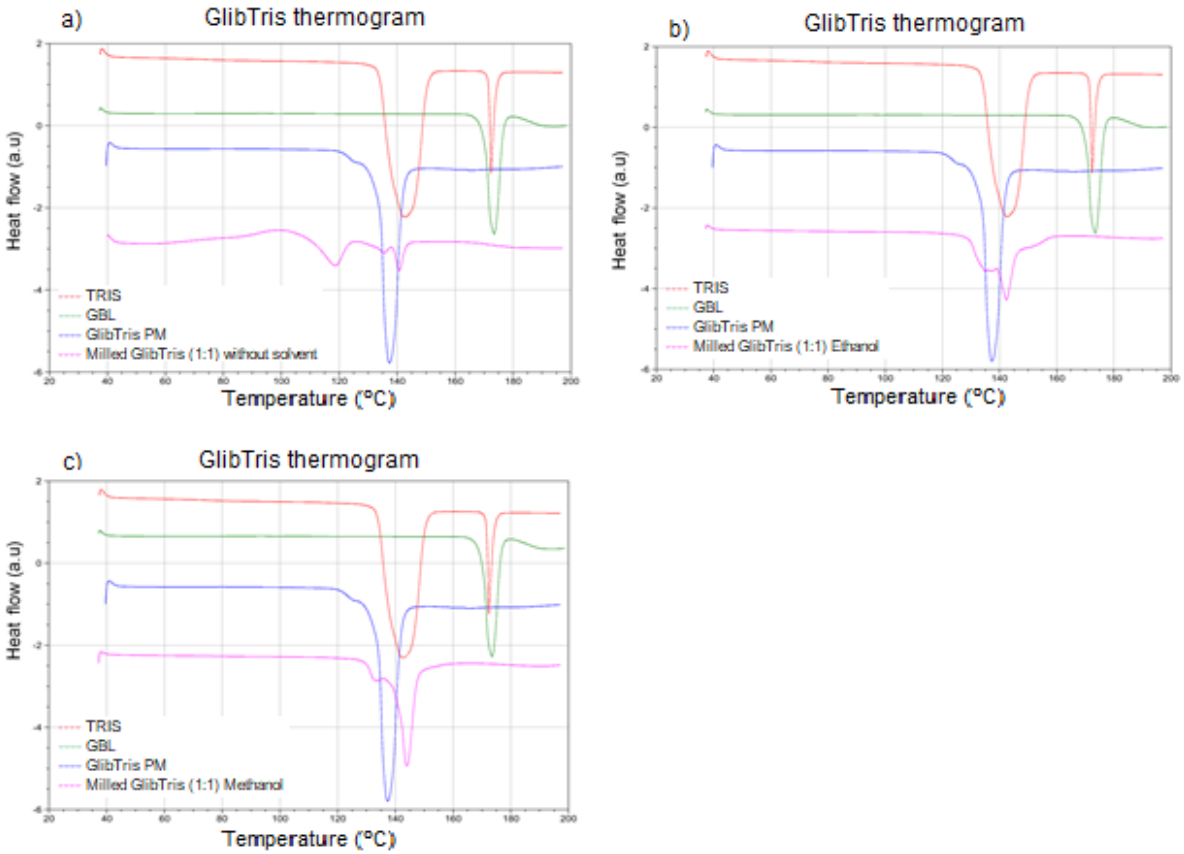

Figure 29. Thermograms of the GlibTris system: (a) GlibTris (1:1) without solvent, (b) GlibTris (1:1) Ethanol, (d) GlibTris (1:1) Methanol.

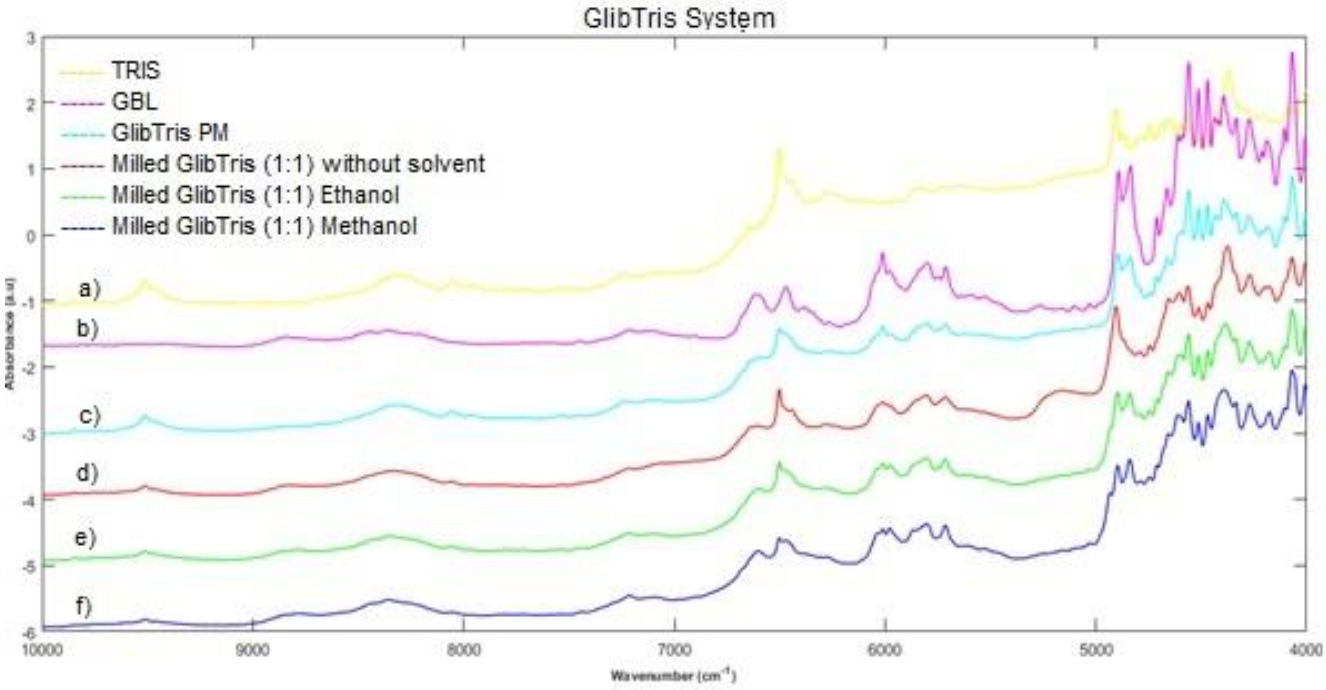

Figure 30. Spectroscopic characterization: (a) NIR spectra for the pure compound TRIS; (b) NIR spectra for the pure compound GBL; (c) NIR spectra for the GlibTris PM; (d) NIR spectra for the GlibTris (1:1) without solvent; (e) NIR spectra for the GlibTris (1:1) Ethanol and (f) NIR spectra for the GlibTris (1:1) Methanol.

In the NIR spectrum of the GlibTris (1:1) system without solvent (Fig. 30), some differences were found:

- at ≈ 4400 and ≈ 4450 cm^{-1}, which corresponds to the CHO group vibration band in the combination region;
- at ≈ 4500 and ≈ 4550 cm^{-1}, corresponding to the CHO group vibration and the amine vibration in the combination region;
- at ≈ 4900 cm^{-1}, in the first overtone region is it exhibit differences regarding the amide vibration;
- at ≈ 5200 cm^{-1}, which corresponds to H_2O in the first overtone region and leading to the conclusion that this sample contained water;
- at ≈ 6900 cm^{-1}, it is exhibit, in the second overtone, region an amide group vibration.

According to the paper published with this system, the differences found in this work correspond to the differences referred in that article. Although the wavenumbers may differ, the vibration bands are the same, which may imply the co-crystal formation. (29)

The NIR spectra of the GlibTris (1:1) Ethanol and Methanol systems (Fig. 30) do not exhibit significant differences between the PM and the milled systems. However, two differences are shown in both Ethanol and Methanol spectra:

- at ≈ 4450 cm^{-1}, which corresponds to the CHO group vibration band in the combination region;
- at ≈ 4600 cm^{-1}, corresponding to the CHO group vibration and the amine vibration in the combination region.

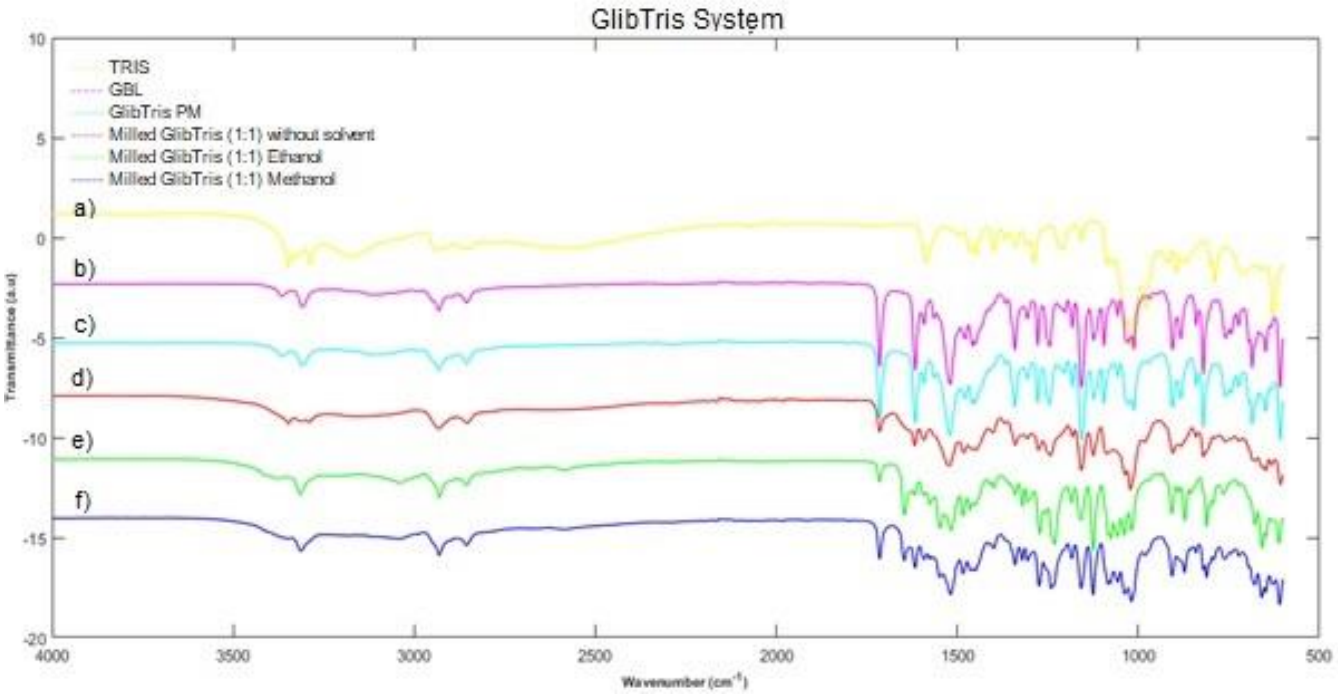

Figure 31. Spectroscopic characterization: (a) MIR spectra for the pure compound TRIS; (b) MIR spectra for the pure compound GBL; (c) MIR spectra for the GlibTris PM; (d) MIR spectra for the GlibTris (1:1) without solvent; (e) MIR spectra for the GlibTris (1:1) Ethanol and (f) MIR spectra for the GlibTris (1:1) Methanol.

The MIR spectrum of the GlibTris (1:1) system without solvent (Fig. 31), the fingerprint region displays several differences:

- at ≈ 750 cm^{-1} and ≈ 1700 cm^{-1}, it is displayed two vibrations bands corresponding to the primary amine (NH) wagging and bending vibrations, respectively;
- at ≈ 800 cm^{-1} and ≈ 1250 cm^{-1}, corresponding to two vibration stretches characteristic of amine vibrations;
- at ≈ 1050 cm^{-1}, which corresponds to the C-N stretching vibration band from the amine group;
- at ≈ 3250 cm^{-1} and ≈ 3400 cm^{-1}, two amine stretching vibrations are exhibit in the spectra region.

According to the reported article referring this system, the differences found in this work correspond to the differences referred in the same article. Although the wavenumbers may differ and the fact that above the wavenumber of 3000 cm^{-1} no differences were observed, the vibration bands observed are the same, which may imply the co-crystal formation. (29)

The MIR spectrum of the GlibTris (1:1) Ethanol system (Fig. 31), shows several differences in the fingerprint region:

- at ≈ 850 cm^{-1} and ≈ 1600 cm^{-1}, it is displayed two vibrations bands corresponding to the primary amine (NH) wagging and bending vibrations, respectively;
- at ≈ 1050 cm^{-1} and ≈ 1100 cm^{-1}, which corresponds to the C-N stretching vibration band from the amine group;
- between 1400-1350 cm^{-1} spectra region, corresponding to alkane bending vibration characteristic band.

The MIR spectrum of the GlibTris (1:1) Methanol system (Fig. 31), it expresses several differences in the fingerprint region:

- at ≈ 850 cm^{-1} and ≈ 1600 cm^{-1}, it is displayed two vibrations bands corresponding to the primary amine (NH) wagging and bending vibrations, respectively;
- at ≈ 1100 cm^{-1}, which corresponds to the C-N stretching vibration band from the amine group;
- between 1400-1350 cm^{-1} spectra region, corresponding to alkane bending vibration characteristic band.

3.3 – Summary of the characterization results

All the mentioned characterization methods were valuable tools to determine if a co-crystal was formed (or not) and each one gave different insights over the co-crystallization process and product. For the analysis of whether a co-crystal was formed or not, the milled product characteristics were compared to the pure API (GBL), the pure co-former and the physical mixture of both. Table 8 summarizes the conclusions withdrawn from the characterization results, i.e., whether there were differences observed between the milled mixture and the respective physical mixture.

Table 8. Summary of the conclusion from the characterization methods. (YES= differences found; NO= differences not found)

	DSC	MIR	NIR
GlibAde system			
GlibAde (1:1) without solvent	No	Yes	Yes
GlibAde (1:1) Ethanol	No	No	No
GlibAde (1:1) Methanol	No	No	No
GlibMal system			
GlibMal (1:1) without solvent	**Yes**	**Yes**	**Yes**
GlibMal (1:1) Ethanol	**Yes**	**Yes**	**Yes**
GlibMal (1:1) Methanol	**Yes**	**Yes**	**Yes**
GlibMan system			
GlibMan (1:1) without solvent	No	No	No
GlibMan (1:1) Ethanol	No	No	No
GlibMan (1:1) Methanol	No	No	No
GlibNico system			
GlibNico (1:1) without solvent	No	No	No
GlibNico (1:1) Ethanol	No	No	No
GlibNico (1:1) Methanol	No	No	No
GlibPaba system			
GlibPaba (1:1) without solvent	**Yes**	**Yes**	**Yes**
GlibPaba (1:1) Ethanol	No	No	No
GlibPaba (1:1) Methanol	No	No	No
GlibTris system			
GlibTris (1:1) without solvent	**Yes**	**Yes**	**Yes**
GlibTris (1:1) Ethanol	**Yes**	**Yes**	**Yes**
GlibTris (1:1) Methanol	**Yes**	**Yes**	**Yes**

To further solidify the analysis performed previously and presented in Table 8, a mathematical calculation was performed (in Matlab) to evaluate differences obtained in infrared spectra. The goal was to identify differences between the spectrum of a mixture (GLB and co-former) and the milling product, highlighting the possibility of the production of a new form. The idea was based on the fact that, for both MIR and NIR, a spectrum of a mixture can be reconstructed from the spectra of the pure components. Basically, the spectrum of a mixture can be estimated from a linear combination of the pure components spectra. However, because the co-crystal evidence differences from a spectrum of a pure mixture, the reconstruction from the pure components spectra should be more difficult (and therefore present a higher reconstruction error). Therefore, an algorithm was constructed for the optimal reconstruction of spectra of mixtures and potential cocrystals from pure components spectra. The difference between the reconstruction and the experimental spectrum reveals the ability or not of the reconstruction. The results presented below compare the result of the best possible

reconstruction (always a linear combination of the pure components spectra) with the experimental spectra for FTIR and FTNIR.

In Table 8, regarding the GlibAde system without solvent, it is showed that no differences were found in the DSC thermogram; however, differences were found when analysing the NIR and MIR spectra. This is in accordance with the results showed in Figure 32, i.e., both NIR and MIR experimental spectra cannot be reconstructed from the original spectra of GBL and ADE. This leads to the conclusion that a different compound was formed, although it was not detected in the DSC. It is however unclear the reason for this difference. The new compound may not even be a co-crystal.

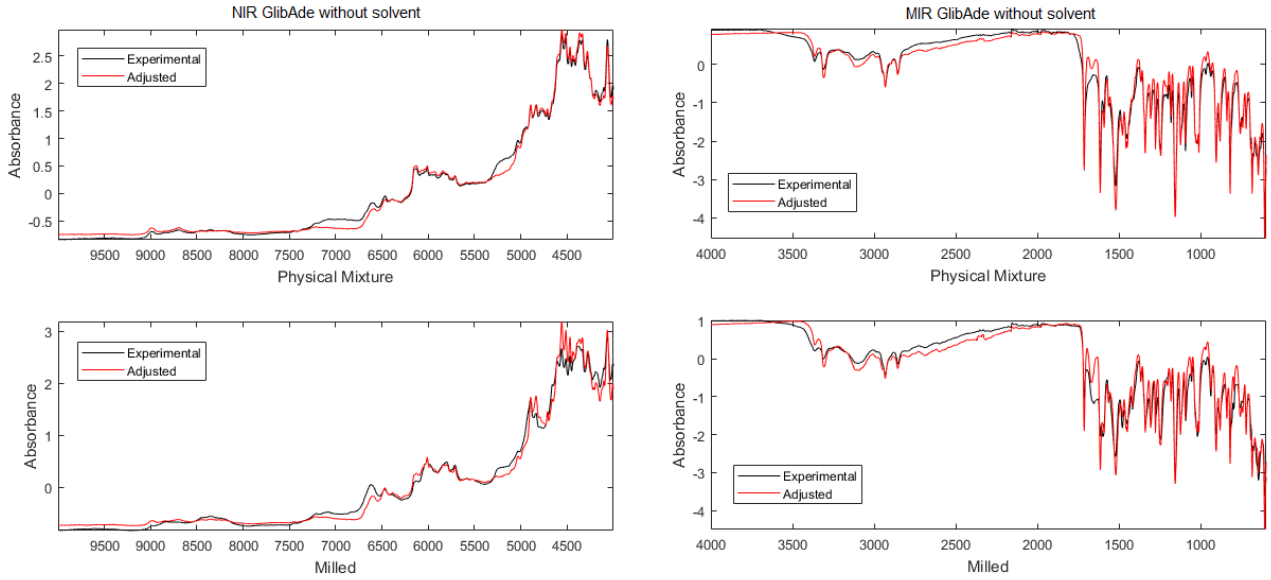

Figure 32. Results obtained for the GlibAde system without solvent using the mathematical model.

The GlibAde Ethanol and Methanol systems did not show differences in the DSC thermogram and in the NIR and MIR spectra. When analysing the results from the mathematical reconstruction (Fig. 33 and 34) it is observed that the experimental NIR and MIR spectra can be built from its precursors (GBL and ADE) by using the mathematical model. Therefore, it is possible to conclude that these systems were not successful and that the result of the grinding method was just a combination of both original crystals.

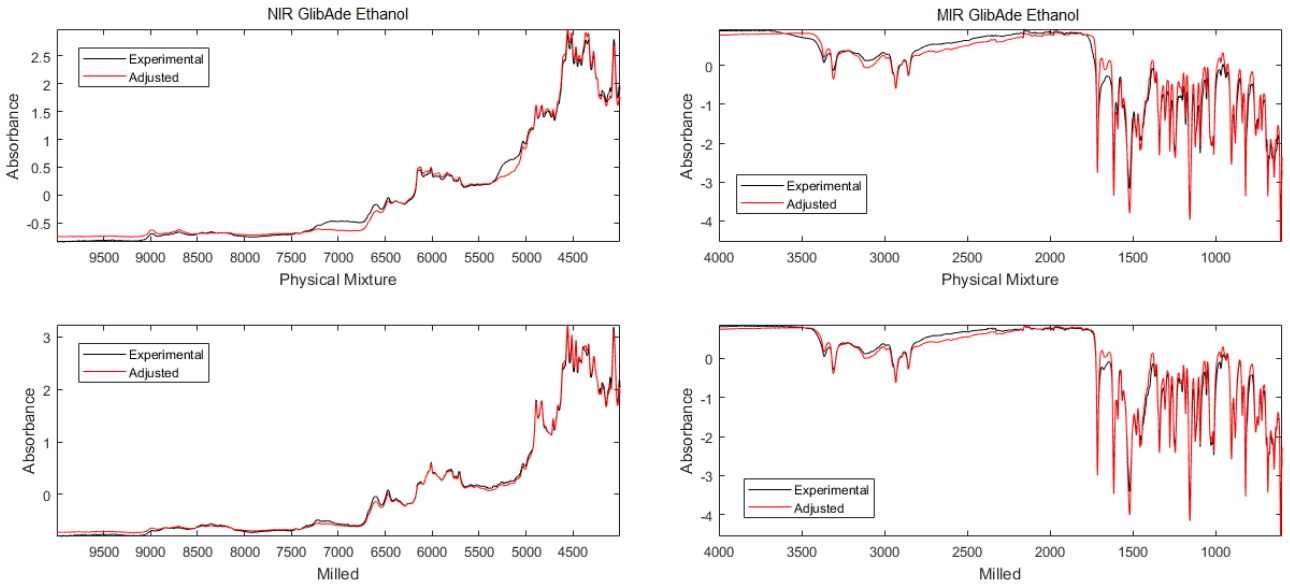

Figure 33. Results obtained for the GlibAde Ethanol system using the mathematical model.

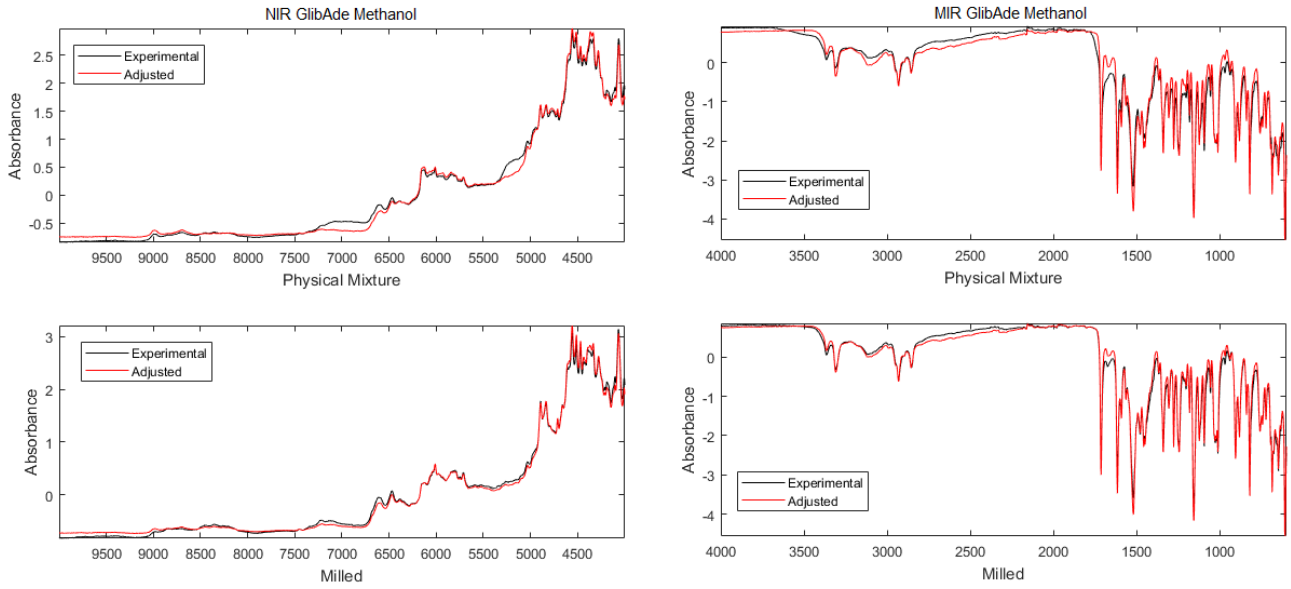

Figure 34. Results obtained for the GlibAde Methanol system using the mathematical model.

The co-crystallization process with GBL and co-former MAL is a promising system because differences were observed in the thermal characterization method and in the vibrational spectroscopy characterization methods (Table 8). Moreover, when analysing the spectra obtained through the mathematical reconstruction (Fig. 35, 36 and 37) it is possible to verify that the experimental NIR and MIR spectra cannot be estimated accurately from the original GBL and MAL spectra. However, it should be noted that both NIR and MIR physical mixture spectra cannot be reconstructed through the original spectra of GBL and MAL, which may indicate an interaction between these two compounds even before they are milled.

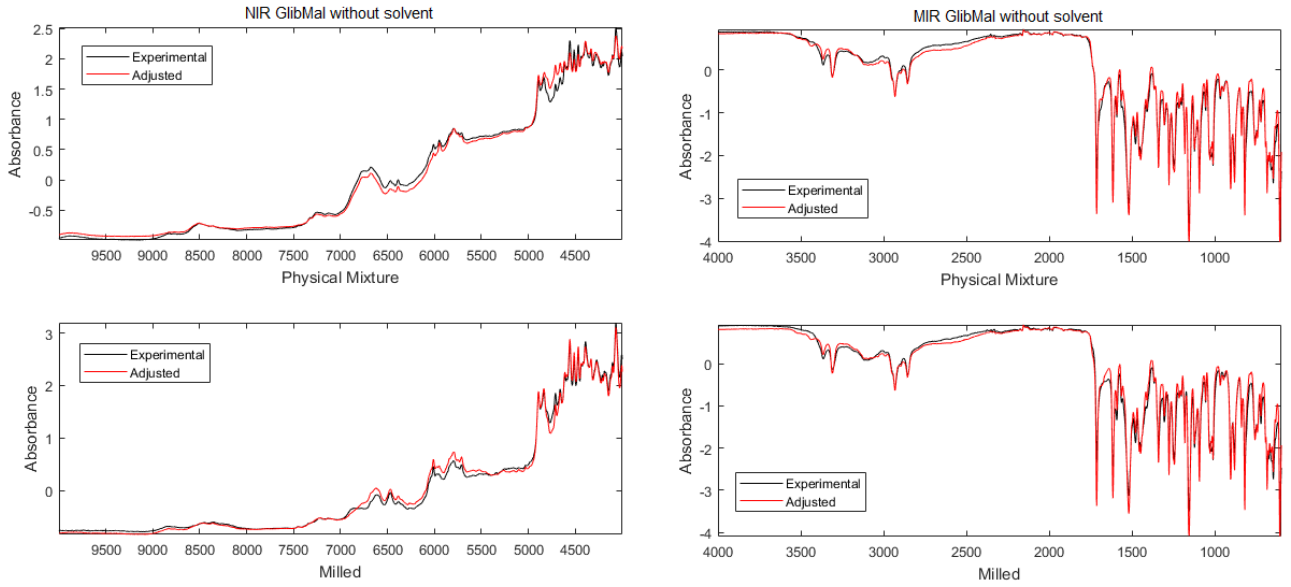

Figure 35. Results obtained for the GlibMal system without solvent using the mathematical model.

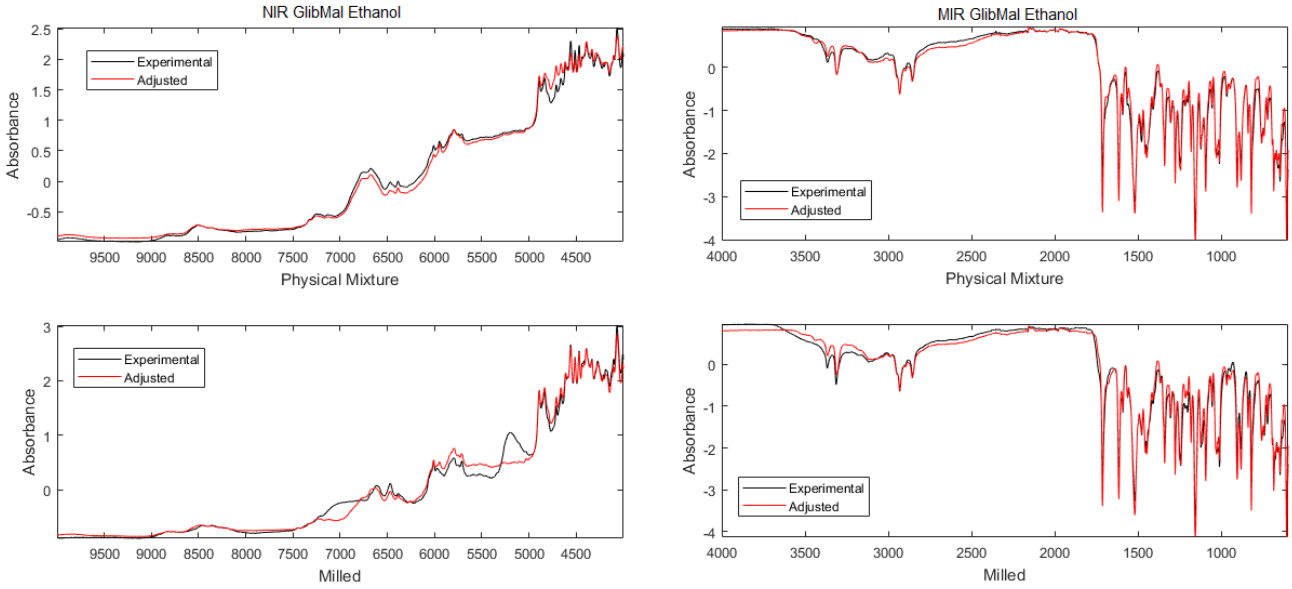

Figure 36. Results obtained for the GlibMal Ethanol system using the mathematical model.

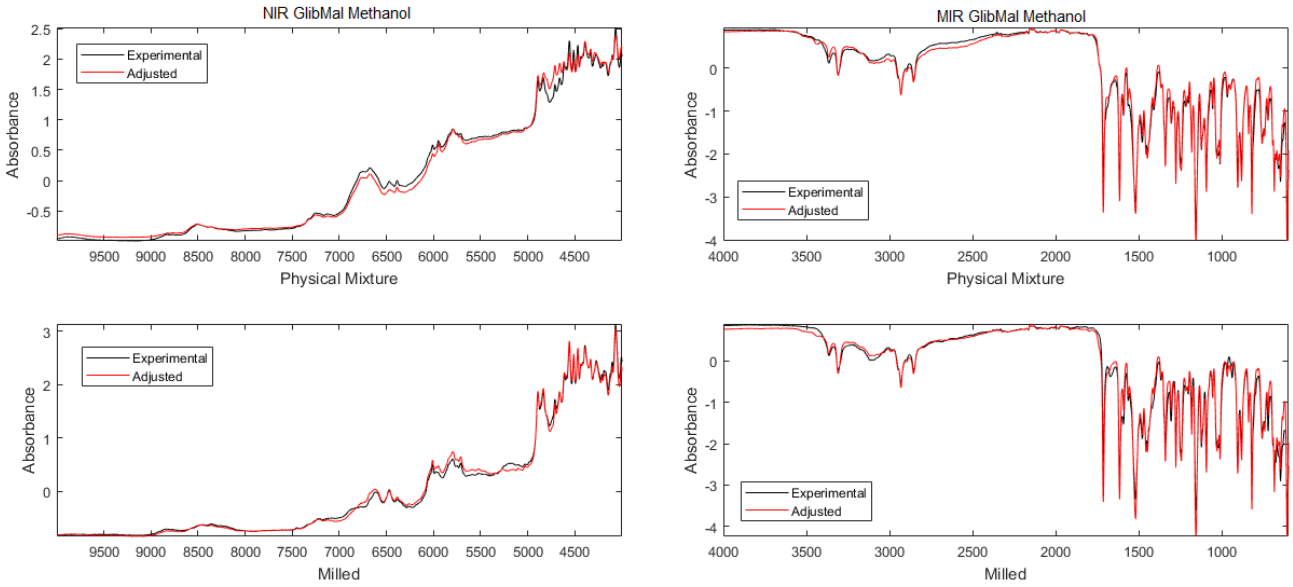

Figure 37. Results obtained for the GlibMal Methanol system using the mathematical model.

By analysing the summary results (Table 8) for the GlibMan systems, it is possible to conclude that this system was not successful because it did not exhibit any differences regarding the DSC thermograms and the NIR and MIR spectra, both for the system without solvent and for ethanol and methanol systems. Furthermore, when analysing the spectra obtained through the mathematical model (Fig. 38, 39 and 40) it is possible to verify that the experimental NIR and MIR spectra can be reconstructed from the original GBL and MAN spectra. Therefore, these systems without solvent and with ethanol and methanol are not successful as a co-crystallization process.

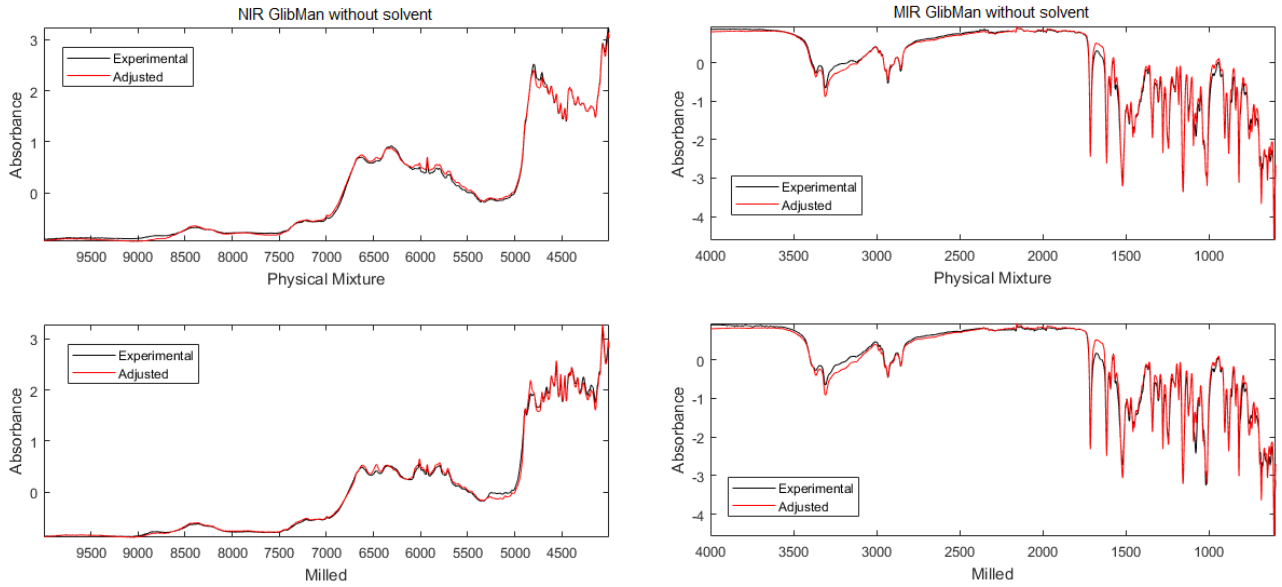

Figure 38. Results obtained for the GlibMan system without solvent using the mathematical model.

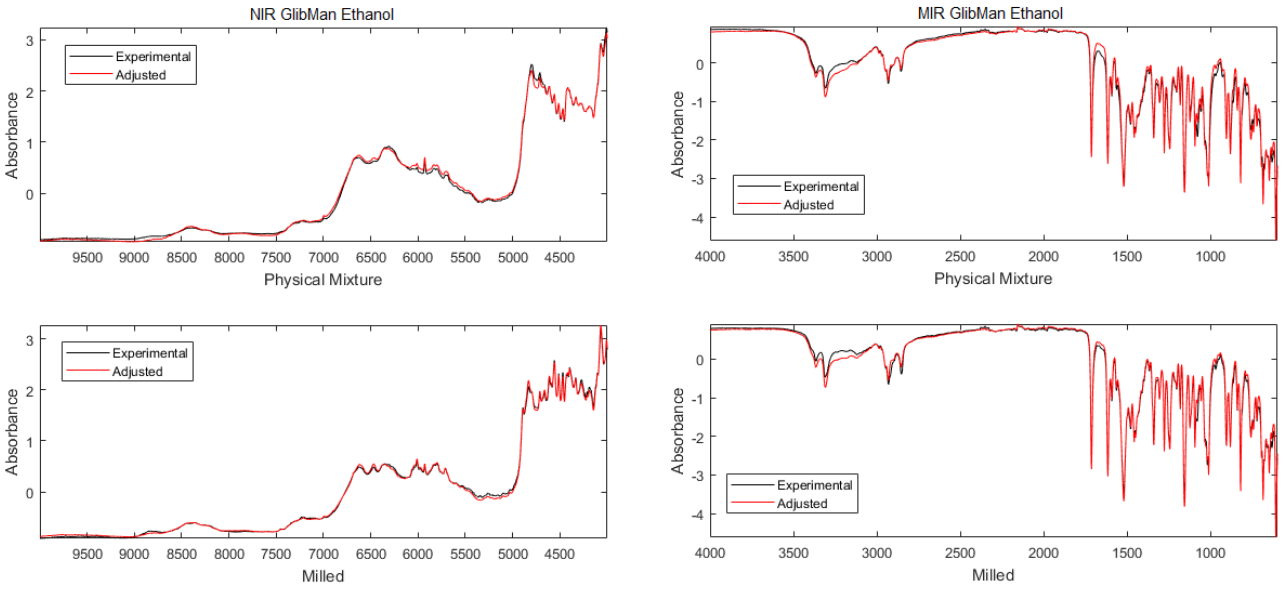

Figure 39. Results obtained for the GlibMan Ethanol system using the mathematical model.

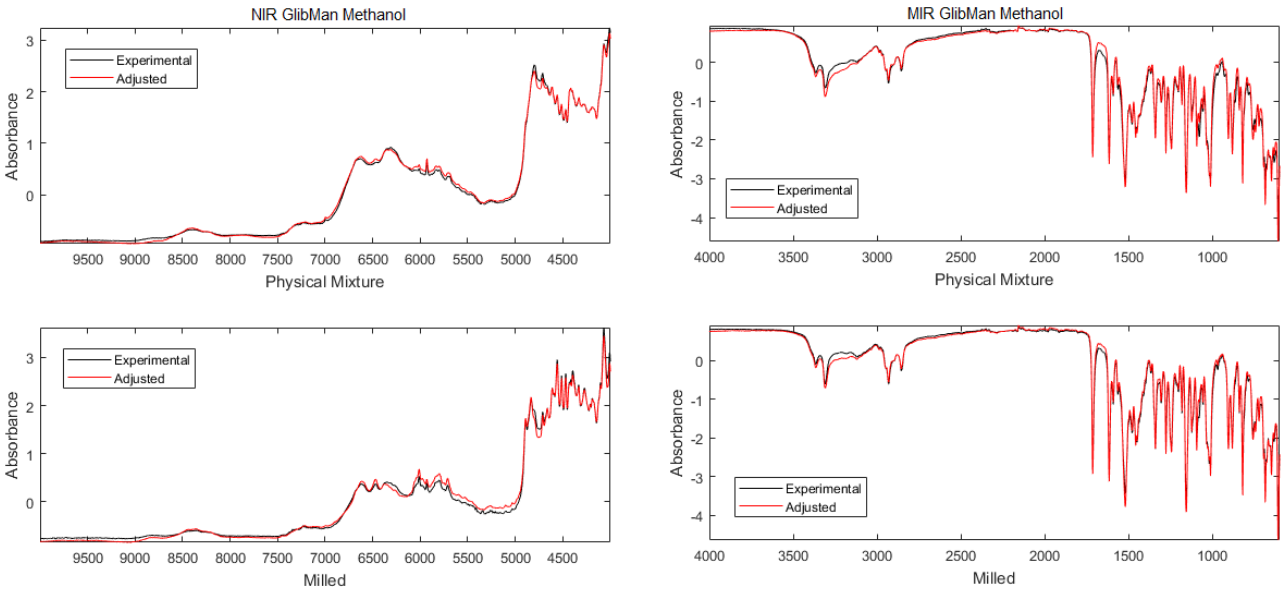

Figure 40. Results obtained for the GlibMan Methanol system using the mathematical model.

In Table 8, for the GlibNico systems, it is possible to conclude that this system was not successful because it did not exhibit any differences regarding the DSC thermograms and the NIR and MIR spectra. Moreover, when analysing the spectra obtained through the mathematical reconstruction (Fig. 41, 42 and 43) it is possible to verify that the experimental NIR and MIR spectra can be estimated from the original GBL and NICO spectra. Therefore, these systems without solvent and with ethanol and methanol are not successful regarding the co-crystallization process. It is noteworthy that in the NIR spectra for all systems, differences between experimental and adjusted spectra are found. However, these differences are due to traces of water in the physical mixture.

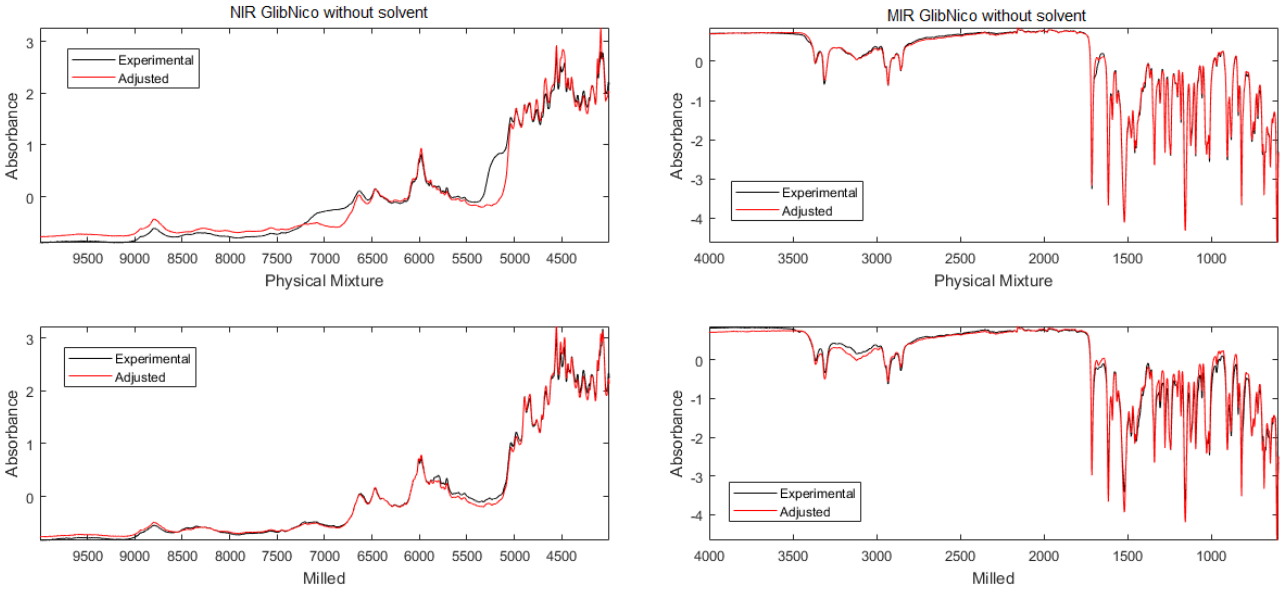

Figure 41. Results obtained for the GlibNico system without solvent using the mathematical model.

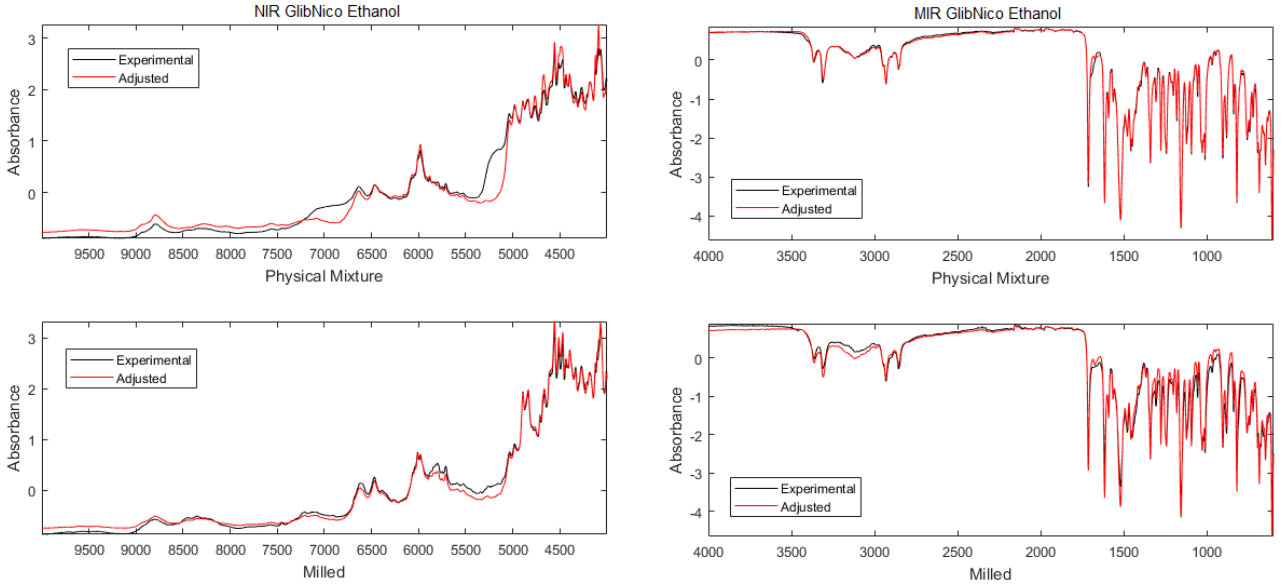

Figure 42. Results obtained for the GlibNico Ethanol system using the mathematical model.

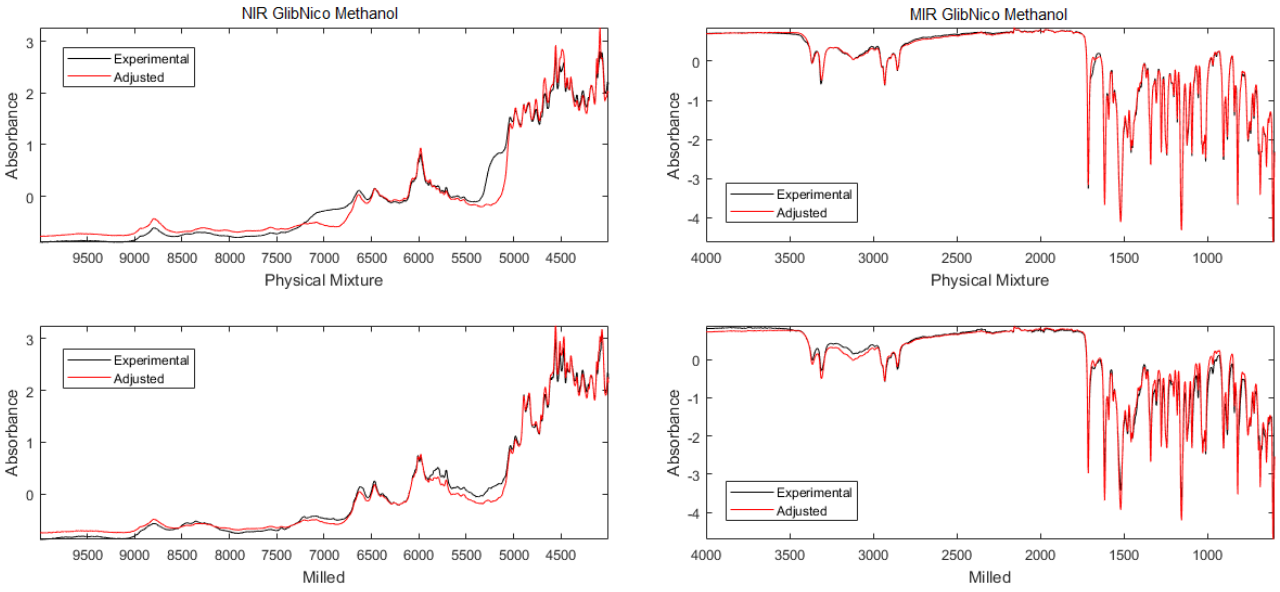

Figure 43. Results obtained for the GlibNico Methanol system using the mathematical model.

The co-crystallization process with GBL and PABA without solvent is a promising system because differences were observed in the thermal characterization method and in the vibrational spectroscopy characterization methods (Table 8). Moreover, when analysing the spectra obtained through the mathematical model (Fig. 44) it is possible to verify that the experimental NIR and MIR spectra cannot be reconstructed from its precursors.

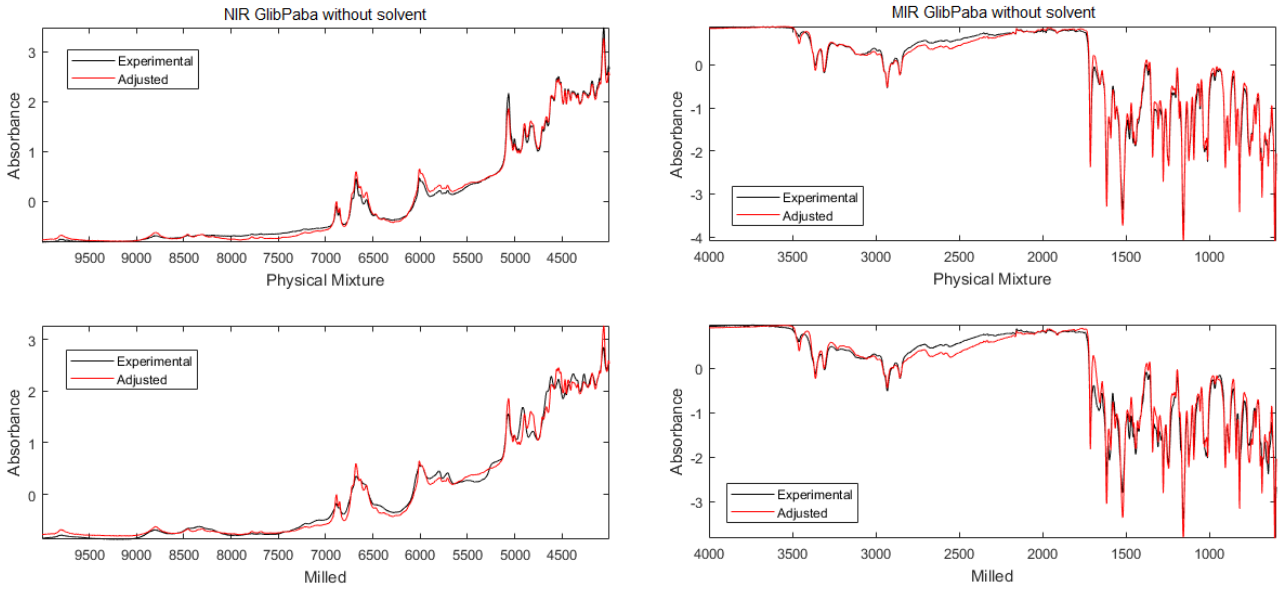

Figure 44. Results obtained for the GlibPaba system without solvent using the mathematical model.

The GlibPaba Ethanol and Methanol systems did not show differences in the DSC thermogram and in the NIR and MIR spectra. When analysing the results from the mathematical model (Fig. 45 and 46) it is observed that the experimental NIR and MIR

can be built from its precursors (GBL and PABA) by using the mathematical model. Therefore, it is possible to conclude that these systems were not successful.

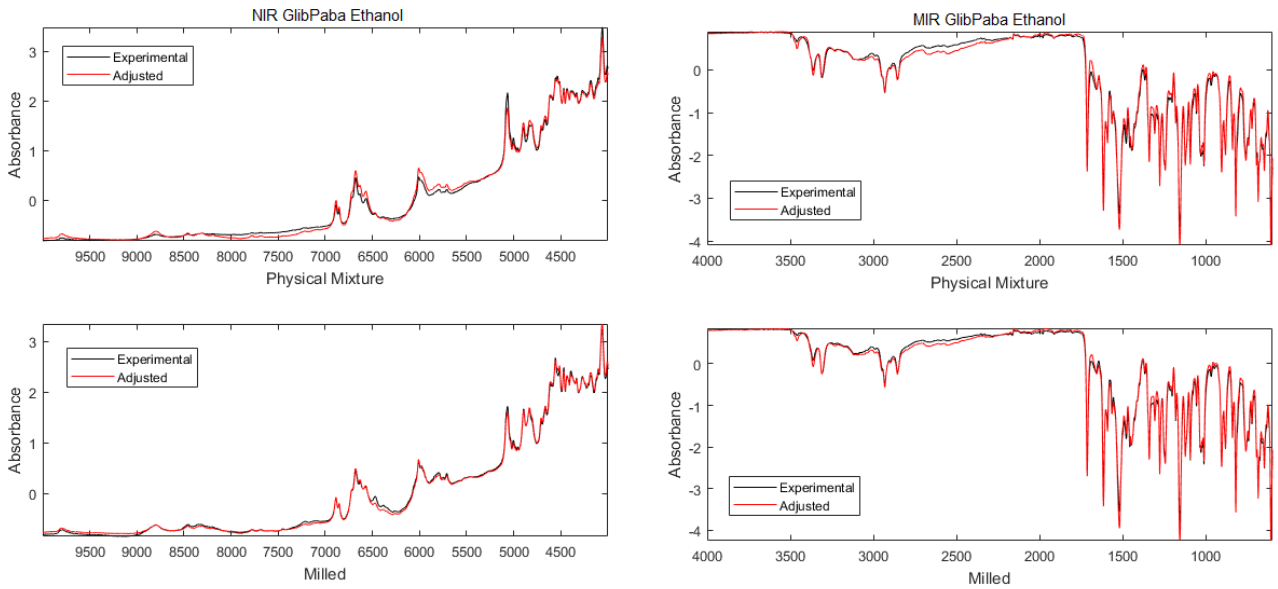

Figure 45. Results obtained for the GlibPaba Ethanol system using the mathematical model.

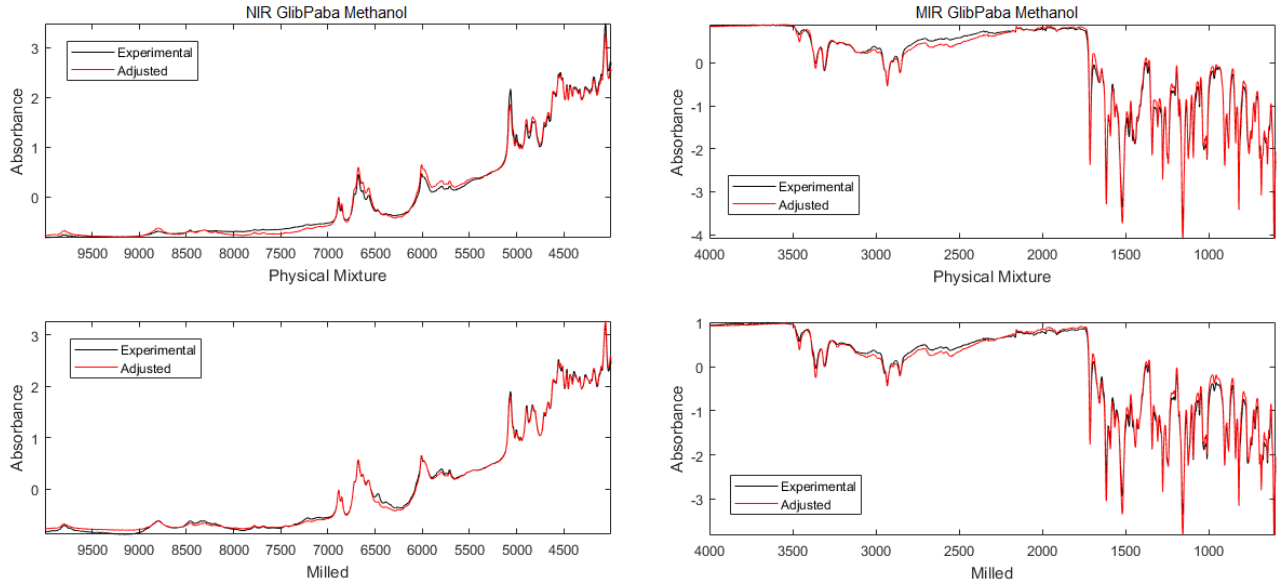

Figure 46. Results obtained for the GlibPaba Methanol system using the mathematical model.

The co-crystallization process with GBL and TRIS is a promising system since differences were observed in the thermal characterization method and in the vibrational spectroscopy characterization methods (Table 8). In addition, the mathematical model for the reconstruction of the NIR and MIR spectra of the physical mixtures (Fig. 47, 48 and 49) can reconstruct it from the precursors. However, upon rebuilt of the NIR and MIR

spectra of the milled products, the mathematical model fails, reporting to the fact that a co-crystal was formed. In this way, we conclude that this system was a success.

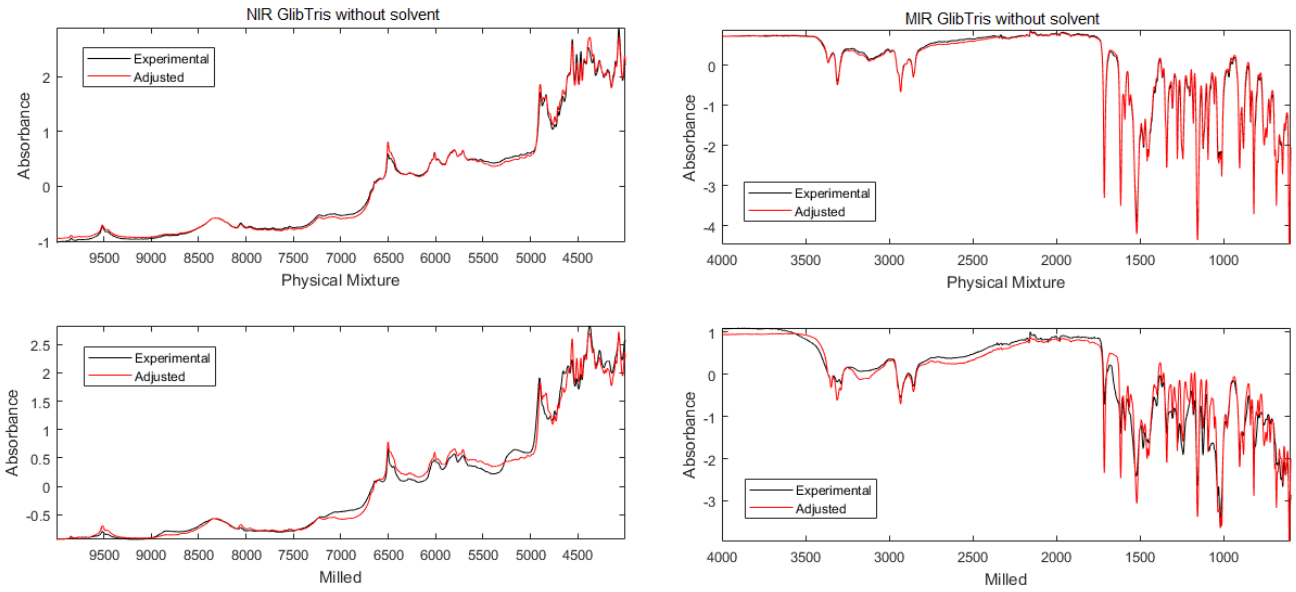

Figure 47. Results obtained for the GlibTris system without solvent using the mathematical model.

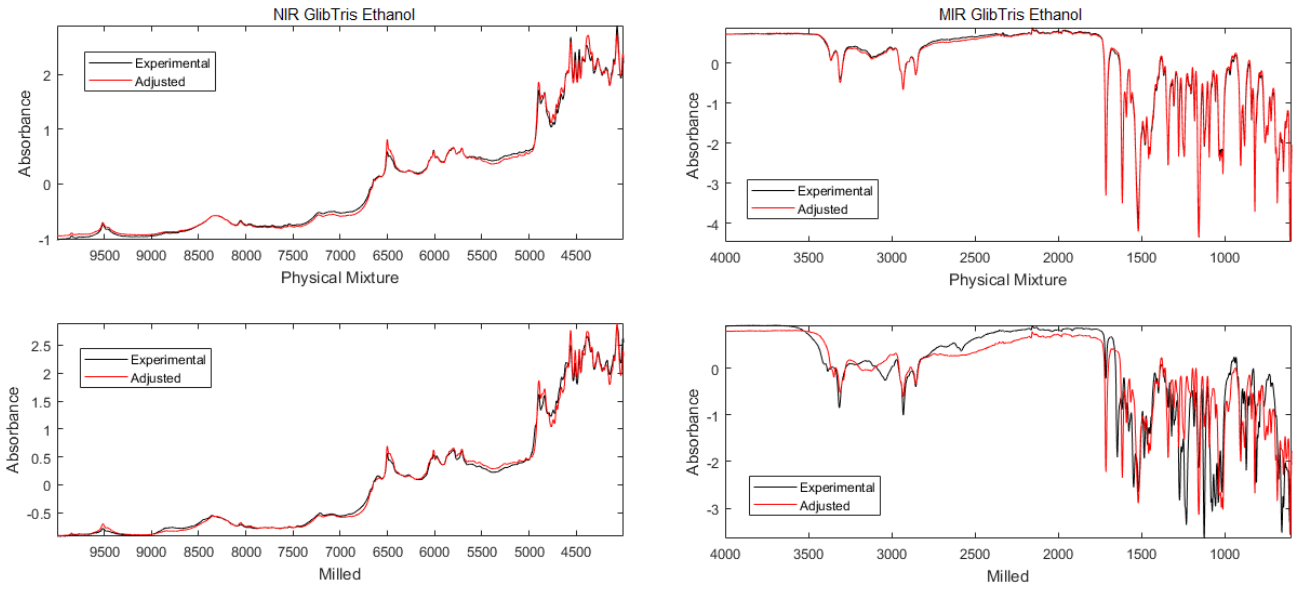

Figure 48. Results obtained for the GlibTris Ethanol system using the mathematical model.

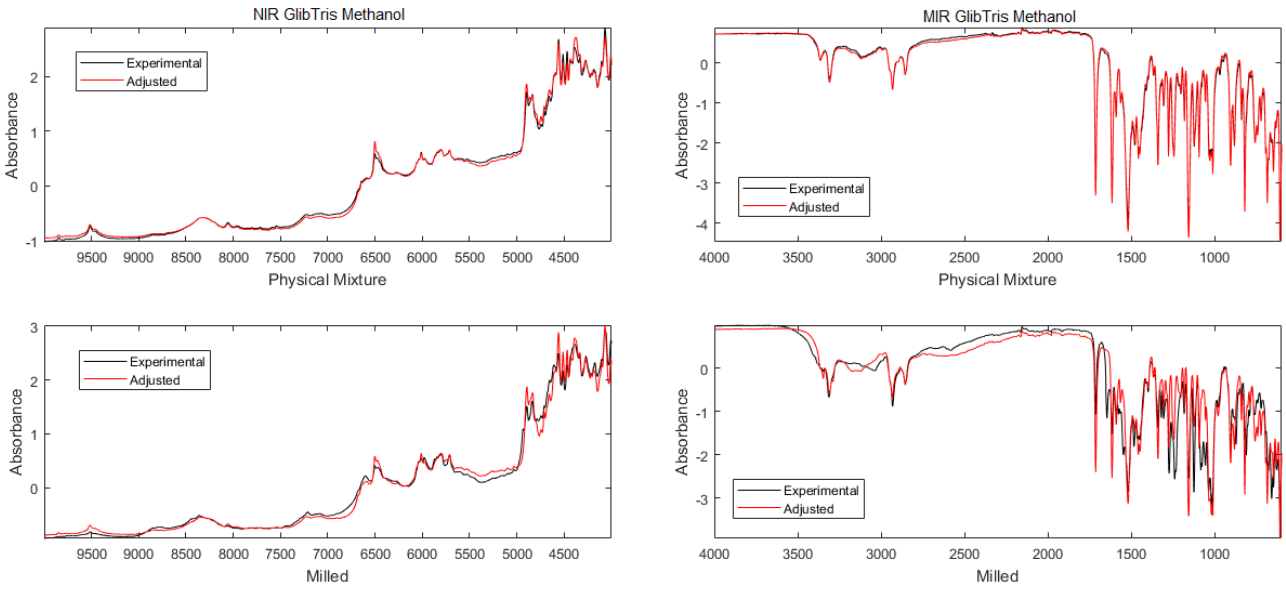

Figure 49. Results obtained for the GlibTris Methanol system using the mathematical model.

Chapter 4 – Conclusions and future perspectives

4.1 – Conclusions

The work involved the GBL co-crystallization process with six different co-formers (ADE, MAL, MAN, NICO, PABA and TRIS).

It was concluded that both systems involving mannitol and nicotinamide did not form any cocrystals after grinding in the ball mill. On the other hand, relatively to the system with adenine, it presented unsatisfactory results when using solvent (ethanol and methanol). However, for the system without solvent, the characterization by NIR and MIR revealed certain differences, implying the formation of a new compound. The system with glibenclamide and *p*-aminobenzoic acid presented similar conclusions to the system with glibenclamide and adenine, both systems with solvent had unsatisfactory results, i.e., no co-crystal was formed. For the system without solvent, there was co-crystal formation. Finally, the systems with malic acid and tromethamine co-formers presented results consisting to co-crystals formation in all cases. The system with glibenclamide and malic acid formed co-crystals for the three cases analysed, i.e., without solvent, with ethanol and with methanol, as well as the system involving tromethamine. In this way, it can be concluded that these two systems were the most satisfactory ones.

4.2 – Future perspectives

In what concerns the systems in which co-crystals were potentially obtained, the purity of must be assessed. For all systems in which co-crystals were not obtained or results were inconclusive, more experiments should be performed. These experiments should involve changing the ball mill rotation speed, number and size of milling spheres, milling time, and stoichiometry. Additionally, evaluating the impact of these process conditions towards the formation of co-crystals (purity and yield) is of upmost importance for the establishment of design-spaces crucial for process understanding, optimization, scaling up procedures and consistent manufacturing (reduced process variability). Additionally, products should be further analysed by powder X-Ray diffraction in order to validate the formation of co-crystals. Finally, solubility studies should be carried out in order to evaluate the changes in properties like the solubility (also the dissolution rate) and stability, the first ultimately the purpose of the production of pharmaceutical co-crystals.

References

1. Blagden N, de Matas M, Gavan PT, York P. Crystal engineering of active pharmaceutical ingredients to improve solubility and dissolution rates. Adv Drug Deliv Rev [Internet]. 2007;59(7):617–30. Available from: https://www.sciencedirect.com/science/article/pii/S0169409X07000828
2. International Conference on Harmonisation of Technical Requirements for Registration of Pharmaceuticals for Human Use. Pharmaceutical Development Q8(R2). ICH Harmon Tripart Guidel [Internet]. 2009;8(August):1–28. Available from: https://www.ich.org/fileadmin/Public_Web_Site/ICH_Products/Guidelines/Quality/Q8_R1/Step4/Q8_R2_Guideline.pdf
3. Gibson M. Pharmaceutical Preformulation and Formulation: A Practical Guide from Candidate Drug Selection to Commercial Dosage Form [Internet]. Vol. 199, Drugs and Pharmaceutical Sciences. 2009. 1-559 p. Available from: http://pubs.acs.org/doi/abs/10.1021/op050157h
4. Lertora JJL, Vanevski KM. Introduction to pharmacokinetics and pharmacodynamics [Internet]. Small Molecule Therapy for Genetic Disease. 2010. 35-54 p. Available from: https://www.ashp.org/-/media/store files/p2418-sample-chapter-1.pdf
5. World Health Organization. WHO Drug Information. 2018;32(1):1–88. Available from: http://apps.who.int/medicinedocs/en/d/Js23187en/
6. FDA - U.S. Department of Health and Human Services. The Drug Development Process. 2018; Available from: https://www.fda.gov/ForPatients/Approvals/Drugs/default.htm
7. Nanjwade VK, Manvi F V, M SA, Basavaraj K, Maste MM. New Trends in the Co-crystallization of Active Pharmaceutical Ingredients New Trends in the Co-crystallization of Active Pharmaceutical Ingredients. J Appl Pharm Sci [Internet]. 2011;8(2015):1–5. Available from: https://www.researchgate.net/publication/279205222_New_Trends_in_the_Co-crystallization_of_Active_Pharmaceutical_Ingredients
8. Sarma B, Chen J, Hsi HY, Myerson AS. Solid forms of pharmaceuticals: Polymorphs, salts and cocrystals. Korean J Chem Eng [Internet]. 2010;28(2):315–22. Available from: https://link.springer.com/article/10.1007/s11814-010-0520-0
9. Publication A. Physicochemical Evaluation and Developability Assessment of Co-amorphouses of Low Soluble Drugs and Comparison to the Co-crystals. Chem Pharm Bull [Internet]. 2016;2–26. Available from: https://www.jstage.jst.go.jp/article/cpb/64/12/64_c16-00604/_article
10. Vippagunta SR, Brittain HG, Grant DJW. Crystalline solids. Adv Drug Deliv Rev

[Internet]. 2001;48(1):3–26. Available from: https://www.sciencedirect.com/science/article/pii/S0169409X01000977?via%3Dihub

11. Haleblian, John; McCrone W. Pharmaceutical Applications of Polymorphism. J Pharm Sci [Internet]. 1971;60(9). Available from: https://www.sciencedirect.com/science/article/pii/S0022354915369562
12. Qureshi SA. Encyclopedia of Pharmaceutical Technology: Tablet Testing. 2007. 600-615 p.
13. Byrn S, Pfeiffer R, Ganey M, Hoiberg C, Poochikian G. Pharmaceutical Solids: A Strategic Approach to Regulatory Considerations [Internet]. Vol. 12, Pharmaceutical research. 1995. p. 945–54. Available from: https://link.springer.com/article/10.1023/A:1016241927429
14. Rodrigues M, Baptista B, Lopes JA, Sarraguça MC. Pharmaceutical cocrystallization techniques. Advances and challenges. Int J Pharm [Internet]. 2018;547(1–2). Available from: https://doi.org/10.1016/j.ijpharm.2018.06.024
15. Jones W, Motherwell WDS, Trask A V. Pharmaceutical Cocrystals : An Emerging Approach to Physical Property. MRS Bull [Internet]. 2006;31(11):875–9. Available from: https://www.cambridge.org/core/journals/mrs-bulletin/article/pharmaceutical-cocrystals-an-emerging-approach-to-physical-property-enhancement/7C1AFBD2B7CE0ABEAF7E57B56CDD2037
16. Agency EM. Reflection paper on the use of cocrystals and other solid state forms of active substances in medicinal products. Eur Med Agency [Internet]. 2014;1–10. Available from: http://www.ema.europa.eu/docs/en_GB/document_library/Scientific_guideline/2015/07/WC500189927.pdf
17. Serajuddin ATM. Salt formation to improve drug solubility. Adv Drug Deliv Rev [Internet]. 2007;59(7):603–16. Available from: https://www.ncbi.nlm.nih.gov/pubmed/17619064
18. Kumar L, Amin A, Bansal AK. Salt selection in drug development. Pharm Technol [Internet]. 2008;32(3):1–10. Available from: http://www.pharmtech.com/salt-selection-drug-development
19. Aakeröy C. Is there any point in making co-crystals? Struct Sci Cryst Eng Mater [Internet]. 2015;71(4):387–91. Available from: http://scripts.iucr.org/cgi-bin/paper?S2052520615010872
20. Steed JW. The role of co-crystals in pharmaceutical design. Trends Pharmacol Sci [Internet]. 2013;34(3):185–93. Available from: https://www.sciencedirect.com/science/article/pii/S0165614712002131

21. Blagden N, Coles SJ, Berry DJ. Pharmaceutical co-crystals – are we there yet? R Soc Chem [Internet]. 2014;16(26):5753–61. Available from: http://xlink.rsc.org/?DOI=C4CE00127C
22. Sarraguça MC, Ribeiro PRS, Santos AO, Silva MCD, Lopes JA. A PAT approach for the on-line monitoring of pharmaceutical co-crystals formation with near infrared spectroscopy. Int J Pharm [Internet]. 2014;471(1–2). Available from: http://dx.doi.org/10.1016/j.ijpharm.2014.06.003
23. FDA. Regulatory Classification of Pharmaceutical Co-Crystals: Guidance for Industry. 2013; Available from: http://www.fda.gov/downloads/Drugs/Guidances/UCM281764.pdf
24. Kotak U, Prajapati V, Solanki H, Jani G, Jha P. Co-crystallization Technique - Its rationale and recent progress. World J Pharm Pharm Sci [Internet]. 2015;4(4):1484–508. Available from: www.wjpps.com/download/article/1427970181.pdf
25. Desiraju GR. Pharmaceutical Salts and Co-crystals [Internet]. Royal Society of Chemistry. 2012. 9-88 p. Available from: http://ebook.rsc.org/?DOI=10.1039/9781849733502
26. Budiman A, Nurlatifah E, Amin S. Enhancement of Solubility and Dissolution Rate of Glibenclamide by Cocrystal Approach with Solvent Drop Grinding Method. Int J Curr Pharm Rev Res [Internet]. 2016;7(5):248–50. Available from: http://impactfactor.org/PDF/IJCPR/7/IJCPR,Vol7,Issue5,Article4.pdf
27. Chavan RB, Thipparaboina R, Yadav B, Shastri NR. Continuous manufacturing of co-crystals : challenges and prospects. Drug Deliv Transl Res [Internet]. 2018;8(40):1–14. Available from: https://www.ncbi.nlm.nih.gov/pubmed/29352367
28. Miroshnyk I, Mirza S, Sandler N. Pharmaceutical co-crystals–an opportunity for drug product enhancement. Expert Opin Drug Deliv [Internet]. 2009;6(4):333–41. Available from: http://www.tandfonline.com/doi/full/10.1517/17425240902828304
29. B. Baptista, J. Lopes and MS. From synthesis to formulation of gliclazide and glibenclamide cocrystal pharmaceutical solid dosage forms. 2017.
30. Almansa C, Mercè R, Tesson N, Farran J, Tomàs J, Plata-Salamán CR. Co-crystal of Tramadol Hydrochloride-Celecoxib (ctc): A Novel API-API Co-crystal for the Treatment of Pain. Cryst Growth Des [Internet]. 2017;17(4):1884–1892. Available from: https://pubs.acs.org/doi/pdf/10.1021/acs.cgd.6b01848
31. Id I. Healthy Volunteer Study to Evaluate Formulations of TAK-020. Heal Res Auth [Internet]. 2018;1(1):1–2. Available from: https://pubs.acs.org/doi/pdf/10.1021/acs.cgd.6b01848
32. FDA - U.S. Department of Health and Human Services. Fda approves sglt2 inhibitor steglatro ™ (ertugliflozin) and fixed- dose combination steglujan ™ (ertugliflozin

and sitagliptin) for adults with type 2 diabetes [Internet]. 2017. Available from: https://www.pfizer.com/news/press-release/press-release-detail/fda_approves_sglt2_inhibitor_steglatro_ertugliflozin_and_fixed_dose_combination_steglujan_ertugliflozin_and_sitagliptin_for_adults_with_type_2_diabetes

33. Ross SA, Lamprou DA, Douroumis D. Engineering and manufacturing of pharmaceutical co-crystals: a review of solvent-free manufacturing technologies. R Soc Chem [Internet]. 2016;52(57):8772–86. Available from: http://arxiv.org/abs/1612.08814
34. Sulbha R. Fukte; Milind P. Wagh; Shilpi Rawat. Coformer selection: An important tool in cocrystal formation. Int J Pharm Pharm Sci [Internet]. 2014;6(7):9–14. Available from: https://www.researchgate.net/publication/286768098_Coformer_selection_An_important_tool_in_cocrystal_formation
35. Desiraju GR. Supramolecular Synthons in Crystal Engineering—A New Organic Synthesis. Angew Chemie Int [Internet]. 1995;34(21):324–32. Available from: https://onlinelibrary.wiley.com/doi/abs/10.1002/anie.199523111
36. Shishkin O V., Zubatyuk RI, Shishkina S V., Dyakonenko V V., Medviediev V V. Role of supramolecular synthons in the formation of the supramolecular architecture of molecular crystals revisited from an energetic viewpoint. R Soc Chem [Internet]. 2014;16(14):6773–86. Available from: http://xlink.rsc.org/?DOI=c3cp55390f
37. Hansen CM. Hansen Solubility Parameters [Internet]. 1999. p. 1. Available from: https://www.taylorfrancis.com/books/9781420049312
38. Parmar VK, Shah SA. Hydrochloride salt co-crystals: Preparation, characterization and physicochemical studies. Pharm Dev Technol [Internet]. 2013;18(2):443–53. Available from: https://www.ncbi.nlm.nih.gov/pubmed/22686294
39. Otsuka Y, Ito A, Takeuchi M, Tanaka H. Dry Mechanochemical Synthesis of Caffeine/Oxalic Acid Cocrystals and Their Evaluation by Powder X-Ray Diffraction and Chemometrics. J Pharm Sci [Internet]. 2017;106(12):3458–64. Available from: https://www.jpharmsci.org/article/S0022-3549(17)30560-9/pdf
40. Ober CA, Montgomery SE, Gupta RB. Formation of itraconazole/L-malic acid cocrystals by gas antisolvent cocrystallization. Powder Technol [Internet]. 2013;236(14):122–31. Available from: http://dx.doi.org/10.1016/j.powtec.2012.04.058
41. Basavoju S, Bostrom D, Velaga P. Pharmaceutical cocrystals and salts of Norfloxacin. Cryst Growth Des [Internet]. 2006;6(12):2699–2708. Available from: https://pubs.acs.org/doi/pdf/10.1021/cg060327x
42. Soares FLF, Carneiro RL. Green synthesis of ibuprofen-nicotinamide cocrystals and

in-line evaluation by Raman spectroscopy. Cryst Growth Des [Internet]. 2013;13(4):1510–1517. Available from: https://pubs.acs.org/doi/abs/10.1021/cg3017112

43. Huang Y, Zhang B, Gao Y, Zhang J, Shi L. Baicalein-nicotinamide cocrystal with enhanced solubility, dissolution, and oral bioavailability. J Pharm Sci [Internet]. 2014;103(8):2330–7. Available from: https://www.sciencedirect.com/science/article/pii/S0022354915304652
44. Tong Sun, Marlton; Shawn Watson CH. Sorbitol/dexlansoprazole co-crystals and method for making same [Internet]. 2012. p. 1–29. Available from: https://patents.google.com/patent/US8318943B1/en
45. Childs SL, Rodríguez-Hornedo N, Reddy LS, Jayasankar A, Maheshwari C, McCausland L, et al. Screening strategies based on solubility and solution composition generate pharmaceutically acceptable cocrystals of carbamazepine. CrystEngComm [Internet]. 2008;10(7):856–64. Available from: http://pubs.rsc.org/en/Content/ArticleLanding/2008/CE/b715396a#!divAbstract
46. Moradiya H, Islam MT, Woollam GR, Slipper IJ, Halsey S, Snowden MJ, et al. Continuous cocrystallization for dissolution rate optimization of a poorly water-soluble drug. Cryst Growth Des [Internet]. 2014;14(1):189–198. Available from: https://pubs.acs.org/doi/abs/10.1021/cg401375a
47. Douroumis D, Ross SA, Nokhodchi A. Advanced methodologies for cocrystal synthesis. Adv Drug Deliv Rev [Internet]. 2017;117:178–95. Available from: https://doi.org/10.1016/j.addr.2017.07.008
48. Rehder S, Klukkert M, Löbmann KAM, Strachan CJ, Sakmann A, Gordon K, et al. Investigation of the formation process of two piracetam cocrystals during grinding. Pharm J [Internet]. 2011;3(4):706–22. Available from: https://www.ncbi.nlm.nih.gov/pubmed/24309304
49. Chieng N, Hubert M, Saville D, Rades T, Aaltonen J. Formation Kinetics and Stability of Carbamazepine - Nicotinamide Cocrystals Prepared by Mechanical Activation. Cryst Growth Des [Internet]. 2009;9(5):2377–2386. Available from: https://pubs.acs.org/doi/abs/10.1021/cg801253f
50. Jayasankar A, Somwangthanaroj A, Shao ZJ, Rodríguez-Hornedo N. Cocrystal formation during cogrinding and storage is mediated by amorphous phase. Pharm Res [Internet]. 2006;23(10):2381–92. Available from: https://link.springer.com/article/10.1007%2Fs11095-006-9110-6
51. Basavoju S, Boström D, Velaga SP. Indomethacin-saccharin cocrystal: Design, synthesis and preliminary pharmaceutical characterization. Pharm Res [Internet]. 2008;25(3):530–41. Available from:

https://www.ncbi.nlm.nih.gov/pubmed/17703346

52. Tong Y, Zhang P, Dang L, Wei H. Monitoring of cocrystallization of ethenzamide-saccharin: Insight into kinetic process by in situ Raman spectroscopy. Chem Eng Res Des [Internet]. 2016;109:249–57. Available from: http://dx.doi.org/10.1016/j.cherd.2016.01.032
53. Shan N, Toda F, Jones W. Mechanochemistry and co-crystal formation: Effect of solvent on reaction kinetics. Chem Commun [Internet]. 2002;2(20):2372–3. Available from: http://pubs.rsc.org/en/Content/ArticleLanding/2002/CC/b207369m#!divAbstract
54. Thiry J, Krier F, Evrard B. A review of pharmaceutical extrusion: Critical process parameters and scaling-up. Int J Pharm [Internet]. 2015;479(1):227–40. Available from: http://dx.doi.org/10.1016/j.ijpharm.2014.12.036
55. Duarte Í, Andrade R, Pinto JF, Temtem M. Green production of cocrystals using a new solvent-free approach by spray congealing. Int J Pharm [Internet]. 2016;506(1–2):68–78. Available from: https://www.sciencedirect.com/science/article/pii/S037851731630285X?via%3Dihub
56. Alhalaweh A, Velaga SP. Formation of cocrystals from stoichiometric solutions of incongruently saturating systems by spray drying. Cryst Growth Des [Internet]. 2010;10(8):3302–3305. Available from: https://pubs.acs.org/doi/abs/10.1021/cg100451q
57. Bian L, Zhao H, Hao H, Yin Q, Wu S, Gong J, et al. Novel glutaric acid cocrystal formation via cogrinding and solution crystallization. Chem Eng Technol [Internet]. 2013;36(8):1–5. Available from: https://onlinelibrary.wiley.com/doi/abs/10.1002/ceat.201200720
58. Du S, Wang Y, Wu S, Yu B, Shi P, Bian L, et al. Two novel cocrystals of lamotrigine with isomeric bipyridines and in situ monitoring of the cocrystallization. Eur J Pharm Sci [Internet]. 2017;110(1):19–25. Available from: https://www.sciencedirect.com/science/article/pii/S0928098717303330?via%3Dihub
59. Gagniere E, Puel F, Mangin D, Valour JP, Rivoire A, Galvan JM, et al. In Situ Monitoring of Cocrystallization Processes - Complementary Use of Sensing Technologies. Chem Eng Technol [Internet]. 2012;35(6):1–5. Available from: https://www.scopus.com/citation/output.uri?origin=recordpage&view=&src=s&eid=2-s2.0-84861690813&outputType=exportPdf
60. Sarraguça MC, Paisana M, Pinto J, Lopes JA. Real-time monitoring of cocrystallization processes by solvent evaporation: A near infrared study. Eur J

Pharm Sci [Internet]. 2016;90(1):76–84. Available from: https://www.sciencedirect.com/science/article/pii/S0928098715300981

61. Moradiya HG, Islam MT, Halsey S, Maniruzzaman M, Chowdhry BZ, Snowden MJ, et al. Continuous cocrystallisation of carbamazepine and trans-cinnamic acid via melt extrusion processing. CrystEngComm [Internet]. 2014;16(17):3573–83. Available from: http://pubs.rsc.org/en/Content/ArticleLanding/2014/CE/C3CE42457J#!divAbstract
62. Patil SP, Modi SR, Bansal AK. Generation of 1:1 Carbamazepine:Nicotinamide cocrystals by spray drying. Eur J Pharm Sci [Internet]. 2014;62(1):251–7. Available from: http://dx.doi.org/10.1016/j.ejps.2014.06.001
63. Lee SL, O'Connor TF, Yang X, Cruz CN, Chatterjee S, Madurawe RD, et al. Modernizing Pharmaceutical Manufacturing: from Batch to Continuous Production. J Pharm Innov [Internet]. 2015;10(3):191–9. Available from: https://link.springer.com/article/10.1007/s12247-015-9215-8
64. Teżyk M, Milanowski B, Ernst A, Lulek J. Recent progress in continuous and semi-continuous processing of solid oral dosage forms: A review. Drug Dev Ind Pharm [Internet]. 2015;42(8):1195–214. Available from: https://www.tandfonline.com/doi/full/10.3109/03639045.2015.1122607
65. Plumb K. Continuous processing in the pharmaceutical industry: Changing the mind set. Chem Eng Res Des [Internet]. 2005;83(6):730–8. Available from: https://www.sciencedirect.com/science/article/pii/S0263876205727556?via%3Dihub
66. Bolla G, Chernyshev V, Nangia A. Acemetacin cocrystal structures by powder X-ray diffraction. IUCrJ [Internet]. 2017;4(3):206–14. Available from: https://www.ncbi.nlm.nih.gov/pubmed/28512568
67. Schultheiss N, Newman A. Pharmaceutical Cocrystals and Their Physicochemical Properties. Cryst Growth Des [Internet]. 2009;9(6):2950–2967. Available from: https://pubs.acs.org/doi/abs/10.1021/cg900129f
68. Saganowska P, Wesolowski M. DSC as a screening tool for rapid co-crystal detection in binary mixtures of benzodiazepines with co-formers. J Therm Anal Calorim [Internet]. 2017;133(1):785–795. Available from: https://doi.org/10.1007/s10973-017-6858-3
69. Padrela L, De Azevedo EG, Velaga SP. Powder X-ray diffraction method for the quantification of cocrystals in the crystallization mixture. Drug Dev Ind Pharm [Internet]. 2012;38(8):923–9. Available from: https://www.researchgate.net/publication/51809386_Powder_X-ray_diffraction_method_for_the_quantification_of_cocrystals_in_the_crystallization

_mixture

70. Elbagerma MA, Edwards HGM, Munshi T, Hargreaves MD, Matousek P, Scowen IJ. Characterization of new cocrystals by raman spectroscopy, powder X-ray diffraction, differential scanning calorimetry, and transmission raman spectroscopy. Cryst Growth Des [Internet]. 2010;10(5):2360–2371. Available from: https://pubs.acs.org/doi/abs/10.1021/cg100156a
71. Yamashita H, Hirakura Y, Yuda M, Teramura T, Terada K. Detection of cocrystal formation based on binary phase diagrams using thermal analysis. Pharm Res. 2013;30(1):70–80.
72. Ross SA, Lamprou DA, Douroumis D. Engineering and manufacturing of pharmaceutical co-crystals: a review of solvent-free manufacturing technologies. R Soc Chem [Internet]. 2016;52(57):8772–86. Available from: http://pubs.rsc.org/en/content/articlelanding/2016/cc/c6cc01289b#!divAbstract
73. Chavan RB, Bhargavi N, Lodagekar A, Shastri NR. Near infra red spectroscopy: a tool for solid state characterization. Drug Discov Today [Internet]. 2017;22(12):1835–43. Available from: http://dx.doi.org/10.1016/j.drudis.2017.09.002
74. Van Eerdenbrugh B, Taylor LS. Application of mid-IR spectroscopy for the characterization of pharmaceutical systems. Int J Pharm [Internet]. 2011;417(1–2):3–16. Available from: http://dx.doi.org/10.1016/j.ijpharm.2010.12.011
75. Porestsky L. Principles of diabetes mellitus (2nd ed.). 2009. 19-87 p.
76. Harvard Health Publications. Diagnosis and classification of diabetes mellitus. 2010;33(1):62–9. Available from: https://www.ncbi.nlm.nih.gov/pmc/articles/PMC2797383/
77. Tabish SA. Is Diabetes Becoming the Biggest Epidemic of the Twenty-first Century? Int J Health Sci (Qassim) [Internet]. 2007;1(2):5–8. Available from: https://www.ncbi.nlm.nih.gov/pmc/articles/PMC3068646/
78. Publications HH. Type 2 Diabetes Mellitus Guide: Causes, Symptoms and Treatment Options. 2012;37(7):28–37. Available from: http://content.wkhealth.com/linkback/openurl?sid=WKPTLP:landingpage&an=00006205-201207000-00010
79. Hawley JA. ZJR. Physical Activity and Type 2 Diabetes. 2008. 15-38 p.
80. Kumar A, Bharti SK, Kumar A. Diabetes mellitus type 2: One monster eating all. Apollo Med [Internet]. 2014;11(3):161–6. Available from: http://dx.doi.org/10.1016/j.apme.2014.01.009
81. Skyler JS. Diabetes mellitus: Pathogenesis and treatment strategies. J Med Chem [Internet]. 2004;47(17):4113–7. Available from:

https://www.ncbi.nlm.nih.gov/pubmed/15293979

82. D. T. The market for type 2 diabetes therapeutics - Key findings from a recent analysis of global drug development efforts. Drug Dev Deliv [Internet]. 2013;13(9):28–32. Available from: http://www.embase.com/search/results?subaction=viewrecord&from=export&id=L370305580%5Cnhttp://www.drug-dev.com/Uploads/Public/Nov Dev 2013 Web.pdf
83. Kenny, T Tidy C. Treatments for Type 2 Diabetes. Diabetes UK [Internet]. 2018;1(1):1–10. Available from: http://patient.info/health/treatments-for-type-2-diabetes
84. Sola D, Rossi L, Schianca GPC, Maffioli P, Bigliocca M, Mella R, et al. Sulfonylureas and their use in clinical practice. Arch Med Sci [Internet]. 2015;11(4):840–8. Available from: https://www.ncbi.nlm.nih.gov/pmc/articles/PMC4548036/
85. Groop LC. Sulfonylureas in NIDDM. Diabetes Care [Internet]. 1992;15(6):737–54. Available from: https://www.ncbi.nlm.nih.gov/pubmed/1600834
86. Ferner RE. Oral hypoglycemic agents. Med Clin North Am [Internet]. 1988;72(6):1323–35. Available from: http://dx.doi.org/10.1016/S0025-7125(16)30709-X
87. Rosa MM, Dias T. Commonly used endocrine drugs. Handb Clin Neurol [Internet]. 2014;120:809–24. Available from: https://www.ncbi.nlm.nih.gov/pubmed/24365354
88. Shimabukuro M, Higa N, Takasu N. Comparison of the antioxidant and vascular effects of gliclazide and glibenclamide in Type 2 diabetic patients. A randomized crossover study. J Diabetes Complications [Internet]. 2006;20(3):179–83. Available from: https://www.ncbi.nlm.nih.gov/pubmed/16632238
89. Number A, Molecule S. Glyburide [Internet]. 2018. p. 1–37. Available from: https://www.drugbank.ca/drugs/DB01016
90. Mucklow JC. Martindale: The Complete Drug Reference. Vol. 49, British journal of clinical pharmacology. 2000. 1-613 p.
91. Compounds S. Glyburide [Internet]. 2018. p. 1–42. Available from: https://pubchem.ncbi.nlm.nih.gov/compound/glyburide
92. Salem HF, Elbary AAA, Maher ME. In vitro and in vivo Evaluation of Glibenclamide using Surface Solid Dispersion (SSD) Approach. Br J Pharmacol Toxicol [Internet]. 2011;2(1):601–7. Available from: https://www.researchgate.net/publication/285053008_In_vitro_and_in_vivo_Evaluation_of_Glibenclamide_using_Surface_Solid_Dispersion_SSD_Approach
93. Dhillon B, Goyal NK, Sharma PK. Formulation and Evaluation of Glibenclamide Solid Dispersion Using Different Methods. Glob J Pharmacol [Internet]. 2014;8(4):1–4. Available from: https://idosi.org/gjp/8(4)14/13.pdf

94. Shah SR, Parikh RH, Chavda JR, Sheth NR. Glibenclamide nanocrystals for bioavailability enhancement: Formulation design, process optimization, and pharmacodynamic evaluation. J Pharm Innov [Internet]. 2014;9(3):227–237. Available from: https://link.springer.com/article/10.1007/s12247-014-9189-y
95. Department of Pharmaceutical Sciences. Dissolution enhancement of glibenclamide by preparing drug nanoparticles - Part B by nanoprecipitation. Dep Pharm Sci [Internet]. 2014;9(5):337–350. Available from: http://shodhganga.inflibnet.ac.in/bitstream/10603/33035/14/14_chapter 7.pdf
96. G. Van Den Mooter. Solid dispersions as a formulation strategy for poorly soluble compounds. Finish Soc Phys Pharm. 2009;1(1):1–37.
97. Sud S, Kamath A. Methods of Size Reduction and Factors Affecting Size Reduction in Pharmaceutics. Int Res J Pharm [Internet]. 2013;4(8):1–8. Available from: http://www.irjponline.com/admin/php/uploads/1934_pdf.pdf
98. Sarraguça MC, Ribeiro PRS, Santos AOD, Lopes JA. Batch Statistical Process Monitoring Approach to a Cocrystallization Process. J Pharm Sci [Internet]. 2015;104(12):4099–108. Available from: https://www.sciencedirect.com/science/article/pii/S0022354915000489
99. Silva AFT, Sarraguça MC, Ribeiro PR, Santos AO, De Beer T, Lopes JA. Statistical process control of cocrystallization processes: A comparison between OPLS and PLS. Int J Pharm [Internet]. 2017;520(1–2):29–38. Available from: http://dx.doi.org/10.1016/j.ijpharm.2017.01.052
100. Chemical AT. Aminobenzoic Acid [Internet]. 2011. p. 1–71. Available from: https://pubchem.ncbi.nlm.nih.gov/compound/4-aminobenzoic_acid
101. NCIthesaurus. Aminobenzoic Acid (Code C61634) [Internet]. 2018. p. 1–2. Available from: https://ncim-stage.nci.nih.gov/ncimbrowser/ConceptReport.jsp?dictionary=NCI Metathesaurus&code=C0552314
102. Suryanarayan Cherukuvada; N. Jagadeesh Babu; Ashwini Nangia. Nitrofurantoin-Aminobenzoic Acid Cocrystal: Hydration Stability and Dissolution Rate Studies. J Pharm Sci. 2011;100(8):3233–44.
103. Sanphui P, Kumar SS, Nangia A. Pharmaceutical cocrystals of niclosamide. Cryst Growth Des [Internet]. 2012;12(9):4588–99. Available from: https://pubs.acs.org/doi/10.1021/cg300784v
104. Li Z, Matzger AJ. Influence of Coformer Stoichiometric Ratio on Pharmaceutical Cocrystal Dissolution: Three Cocrystals of Carbamazepine/4-Aminobenzoic Acid. Mol Pharm [Internet]. 2016;13(3):990–5. Available from: https://www.ncbi.nlm.nih.gov/pubmed/26837376

105. Kotbantao G, Charoenchaitrakool M. Processing of ketoconazole-4-aminobenzoic acid cocrystals using dense CO2as an antisolvent. J CO2 Util [Internet]. 2017;17:213–9. Available from: http://dx.doi.org/10.1016/j.jcou.2016.12.007
106. Sanphui P, Bolla G, Nangia A, Chernyshev V. Acemetacin cocrystals and salts: Structure solution from powder X-ray data and form selection of the piperazine salt. IUCrJ [Internet]. 2014;1(2):136–50. Available from: https://journals.iucr.org/m/issues/2014/02/00/bi5031/
107. Sanphui P, Devi VK, Clara D, Malviya N, Ganguly S, Desiraju GR. Cocrystals of hydrochlorothiazide: Solubility and diffusion/permeability enhancements through drug-coformer interactions. Mol Pharm [Internet]. 2015;12(5):1615–22. Available from: https://www.ncbi.nlm.nih.gov/pubmed/25800383
108. NCIthesaurus. Niacinamide (Code C2327) [Internet]. 2018. p. 1–2. Available from: https://ncit.nci.nih.gov/ncitbrowser/pages/home.jsf;jsessionid=C4D719385A9535A0A351385A54E82F9A
109. PubChem. Niacinamide [Internet]. 2018. p. 1–79. Available from: https://pubchem.ncbi.nlm.nih.gov/compound/nicotinamide
110. HMDB. Showing metabocard for Niacinamide [Internet]. 2018. p. 1–11. Available from: http://www.hmdb.ca/metabolites/HMDB0001406
111. Sodanapalli R, Nair R. Synthesis and Characterization of a Pharmaceutical Co-Crystal: (Aceclofenac: Nicotinamide). J Pharm [Internet]. 2011;3(6):1288–93. Available from: http://www.jpsr.pharmainfo.in/Documents/Volumes/Vol3Issue06/jpsr 03110606.pdf
112. Prawiro WS, Murtini G, Suprapti T, Cartika H. Enhancing Dissolution Rates of Gliclazide via Co- crystallization with Nicotinamide. 2016;4(4):899–905. Available from: https://www.ajouronline.com/index.php/AJAS/article/view/3820
113. Neurohr C, Marchivie M, Lecomte S, Cartigny Y, Couvrat N, Sanselme M, et al. Naproxen-Nicotinamide Cocrystals: Racemic and Conglomerate Structures Generated by CO2 Antisolvent Crystallization. Cryst Growth Des [Internet]. 2015;15(9):4616–26. Available from: https://pubs.acs.org/doi/10.1021/acs.cgd.5b00876
114. Ervasti T, Aaltonen J, Ketolainen J. Theophylline-nicotinamide cocrystal formation in physical mixture during storage. Int J Pharm [Internet]. 2015;486(1–2):121–30. Available from: http://dx.doi.org/10.1016/j.ijpharm.2015.03.012
115. Lin H-L, Zhang G-C, Huang Y-T, Lin S-Y. An Investigation of Indomethacin–Nicotinamide Cocrystal Formation Induced by Thermal Stress in the Solid or Liquid

State. J Pharm Sci [Internet]. 2014;103(8):2386–95. Available from: http://linkinghub.elsevier.com/retrieve/pii/S002235491530472X

116. Shewale S, Shete AS, Doijad RC, Kadam SS, Patil VA, Yadav A V. Formulation and Solid State Characterization of Nicotinamide-based Co-crystals of Fenofibrate. Indian J Pharm Sci [Internet]. 2015;77(3):328–34. Available from: http://www.ncbi.nlm.nih.gov/pubmed/26180279%0Ahttp://www.pubmedcentral.nih.gov/articlerender.fcgi?artid=PMC4502148

117. Qiao N. Investigation of Carbamazepine- Nicotinamide cocrystal solubility and dissolution by a UV imaging system. 2014.

118. PubChem. Malic Acid [Internet]. 2001. p. 153–95. Available from: http://linkinghub.elsevier.com/retrieve/pii/S1075628001280057

119. HMDB. Showing metabocard for Malic acid [Internet]. 2018. p. 1–8. Available from: http://www.hmdb.ca/metabolites/HMDB0000744

120. Leyssens T, Tumanova N, Robeyns K, Candoni N, Veesler S. Solution cocrystallization, an effective tool to explore the variety of cocrystal systems: caffeine/dicarboxylic acid cocrystals. CrystEngComm [Internet]. 2014;16(41):9603–11. Available from: http://xlink.rsc.org/?DOI=C4CE01495B

121. Imchalee R, Charoenchaitrakool M. Gas anti-solvent processing of a new sulfamethoxazole-l-malic acid cocrystal. J Ind Eng Chem [Internet]. 2015;25:12–5. Available from: http://dx.doi.org/10.1016/j.jiec.2014.11.009

122. NCIthesaurus. Adenine [Internet]. 2018. p. 1–2. Available from: https://ncit.nci.nih.gov/ncitbrowser/ConceptReport.jsp?dictionary=NCI_Thesaurus&version=18.08d&ns=ncit&code=C206&key=657820766&b=1&n=null

123. HMDB. Showing metabocard for Adenine [Internet]. 2018. p. 1–9. Available from: http://www.hmdb.ca/metabolites/HMDB0000034

124. Wang C, Song Z, Yu H, Liu K, Ma X. Adenine: An important drug scaffold for the design of antiviral agents. Acta Pharm Sin B [Internet]. 2015;5(5):431–41. Available from: https://www.ncbi.nlm.nih.gov/pubmed/26579473

125. Pharmawaldhof. Purines: Adenine (Grade I) [Internet]. 2018. p. 7–8. Available from: https://www.pharmawaldhof.de/product-groups/purines/

126. Du Y, Fang HX, Zhang Q, Zhang HL, Hong Z. Spectroscopic investigation on cocrystal formation between adenine and fumaric acid based on infrared and Raman techniques. Spectrochim Acta - Part A Mol Biomol Spectrosc [Internet]. 2016;153:580–5. Available from: http://dx.doi.org/10.1016/j.saa.2015.09.020

127. Thompson LJ, Elias N, Male L, Tremayne M. Supramolecular behavior of adenine with succinic, fumaric, and maleic acids: Tautomerism, cocrystallization, salt formation, and solvation. Cryst Growth Des [Internet]. 2013;13(4):1464–72.

Available from: https://pubs.acs.org/doi/abs/10.1021/cg301561j

128. HMDB. Showing metabocard for Mannitol [Internet]. 2018. p. 1–7. Available from: http://www.hmdb.ca/metabolites/HMDB0000765

129. NCIthesaurus. Mannitol [Internet]. 2018. p. 1–2. Available from: https://ncit.nci.nih.gov/ncitbrowser/ConceptReport.jsp?dictionary=NCI_Thesaurus&version=18.08d&ns=ncit&code=C625&key=n1572289370&b=1&n=null

130. PubChem. Mannitol [Internet]. 2018. p. 1–62. Available from: https://pubchem.ncbi.nlm.nih.gov/compound/D-mannitol

131. LGMpharma. Mannitol [Internet]. 2018. p. 6–9. Available from: https://www.lgmpharma.com/product/mannitol

132. PubChem. Tromethamine [Internet]. 2018. p. 1–2. Available from: https://pubchem.ncbi.nlm.nih.gov/compound/tromethamine

133. NCIthesaurus. Tromethamine [Internet]. 2016. p. 1–2. Available from: https://ncit.nci.nih.gov/ncitbrowser/ConceptReport.jsp?dictionary=NCI_Thesaurus&version=17.01e&ns=NCI_Thesaurus&code=C47775&key=n301926712&b=1&n=null

134. Bruni G, Berbenni V, Maggi L, Mustarelli P, Friuli V, Ferrara C, et al. Multicomponent crystals of gliclazide and tromethamine: preparation, physico-chemical, and pharmaceutical characterization. Drug Dev Ind Pharm [Internet]. 2018;44(2):243–50. Available from: https://www.tandfonline.com/doi/abs/10.1080/03639045.2017.1386208?src=recsys&journalCode=iddi20

135. Silva Filho SF, Pereira AC, Sarraguça JMG, Sarraguça MC, Lopes J, Façanha Filho P de F, et al. Synthesis of a Glibenclamide Cocrystal: Full Spectroscopic and Thermal Characterization. J Pharm Sci [Internet]. 2018;107(6):1597–604. Available from: https://www.ncbi.nlm.nih.gov/pubmed/29432762

136. Fisher Scientific. RETSCH PM 100 Planterary Ball Mill Grinding Jars [Internet]. 2018. p. 1. Available from: https://www.retsch.pt/pt/produtos/trituracao/moinhos-planetarios-e-de-bolas/pm-100/moinho-de-bolas-planetario-pm-100/

137. Retsch. Planetary Ball Mill PM 100 [Internet]. 2018. p. 1. Available from: https://www.retsch.pt/pt/produtos/trituracao/moinhos-planetarios-e-de-bolas/pm-100/moinho-de-bolas-planetario-pm-100/

138. Eilerman D, Rudman R. Polymorphism of crystalline poly(hydroxymethyl) compounds. III. The structures of crystalline and plastic tris(hydroxymethyl)aminomethane. J Chem Phys [Internet]. 1980;72(10):5656–66. Available from: https://aip.scitation.org/doi/10.1063/1.438982